

# Liquid Drop Breakup in Turbulent Flow

by

Cheng Zhong

A thesis submitted in partial fulfillment of the requirements for the degree of

**Master of Science**

Department of Mechanical Engineering  
University of Alberta

© Cheng Zhong, 2018

## Abstract

The focus of this study is to gain a fundamental understanding of liquid-liquid dispersion formation in homogeneous isotropic turbulence. This information is crucial to improve the reliability of existing models that describe drop breakup in turbulent flow. These models inherit numerous assumptions, simplifications, experimental constants and fitting parameters. Visualization and quantification of drop behavior in homogeneous turbulence will allow assessment of these models. Direct numerical simulations were used to investigate the dynamics of drop behavior. The free energy lattice Boltzmann method was used to perform simulations.

The homogeneous isotropic turbulence was generated in a three-dimensional fully-periodic domain of  $300^3$  lattice units in size using a forcing method. Three turbulent flow fields at different levels of energy input were investigated. Then, drops of different initial diameter were injected. The dispersed to continuous fluid viscosity ratios equal to 0.1, 1, and 10 were considered. The DNSs produce detailed description of the flow. The main goal of this study was to translate these data to the useful quantities that can be applied to assess the drop breakup models. This work specifically focused on understanding of drop interaction with turbulent structures. A normalized  $Q_n$  criterion was used to visualize the structures. Different combinations of a threshold value and a cutoff volume were studied to explore the effect of these two important parameters and to identify the best combination. The interaction between turbulent vortices and the drops was visualized by extracting coherent structures and tracking liquid-liquid interface in two phase turbulence. The three-dimensional

energy spectra of single phase and two-phase turbulence were also quantified. The statistical characteristics of liquid-liquid turbulence were investigated: the probability density function of vorticity, of normalized energy dissipation rate, and the eigenvalues of the strain tensor. By utilizing these tools, the guidelines are proposed for improvement of the breakup models.

## Preface

A part of work in this study was presented in an extended abstract for the 26th Annual Conference of the CFD Society of Canada that was hosted at the University of Manitoba, June 10 - 12, 2018. Dr. Komrakova was the supervisory author of the abstract and was involved in the analysis of the results as well as the composition of the abstract.

## Acknowledgements

I would like to appreciate my supervisor Dr. Alexandra Komrakova for her enthusiasm and professional guidance in my research. She encouraged me to jump out of the safe zone and explore more exciting things. Everytime I was struggling for a problem, she was always there with invaluable suggestion that helped me come up with new ideas. She also patiently gave me support on writing. Under her supervision, I can feel the improvement of my ability and extension of my knowledge.

I would also thanks to Dr. Carlos Lange who gave me invaluable advice not only on research but also on life.

My thanks to my friends: Feiyang Jiang, Muxi Li, Lei Li, Zhen Yang, Li Lei. I have a good time at University of Alberta with their help.

Financial support from the Natural Sciences and Engineering Research Council of Canada is greatly appreciated. I would also appreciate the computational resource provided by Compute Canada.

Finally, numerous thanks to my parents.

# Table of Contents

<b>Abstract</b>	<b>ii</b>
<b>Preface</b>	<b>iv</b>
<b>Acknowledgments</b>	<b>v</b>
<b>1 Introduction</b>	<b>1</b>
1.1 Applications of liquid-liquid systems . . . . .	1
1.2 Introduction to CFD-PBE numerical framework . . . . .	7
1.3 Assumptions made in breakup kernels . . . . .	11
1.4 Introduction to coherent structures . . . . .	12
1.5 Objectives and goal of the thesis . . . . .	18
<b>2 DNSs of liquid-liquid systems</b>	<b>20</b>
2.1 Literature review on DNSs of turbulent liquid-liquid systems .	21
2.2 Free energy lattice Boltzmann method with multiple-relaxation- time operator . . . . .	25
2.3 Turbulence generation. Single-phase flow simulations . . . . .	33
2.4 Three-dimensional energy spectrum . . . . .	35
2.5 Visualization method of coherent structures . . . . .	43

<b>3</b>	<b>Results and Discussion</b>	<b>48</b>
3.1	Simulation parameters . . . . .	49
3.2	Single phase flow . . . . .	50
3.2.1	Energy spectra . . . . .	50
3.2.2	Vorticity . . . . .	53
3.2.3	Local energy dissipation rate . . . . .	55
3.2.4	Eigenvalues of strain tensor . . . . .	56
3.3	Effect of dispersed phase volume fraction . . . . .	58
3.3.1	Energy spectra . . . . .	58
3.3.2	Vorticity . . . . .	59
3.3.3	Local energy dissipation rate . . . . .	59
3.3.4	Eigenvalues of strain tensor . . . . .	61
3.4	Effect of dispersed phase viscosity . . . . .	62
3.4.1	Energy spectra . . . . .	62
3.4.2	Vorticity . . . . .	63
3.4.3	Local energy dissipation rate . . . . .	63
3.4.4	Eigenvalues of strain tensor . . . . .	65
3.5	Coherent structures . . . . .	67
3.5.1	Single-phase flow . . . . .	67
3.5.2	Two-phase flow . . . . .	74
<b>4</b>	<b>Conclusions</b>	<b>76</b>
<b>5</b>	<b>Future work</b>	<b>80</b>
	<b>Appendix A MRT implementation</b>	<b>102</b>

Appendix B Procedure and script for 3D fft and energy spectrum	104
Appendix C Procedure and script for coherent structures	109

# List of Tables

3.1	Simulation parameters. Lattice units: [lu] - lattice units for length scale; [ts] - time step. . . . .	49
3.2	Turbulent kinetic energy and average energy dissipation rate calculated by different methods. . . . .	53
3.3	Parameters and results of coherent structures under effect of $Q_{th}$ . $N$ is the number of structures; $V_{max}$ is the volume of the maximum structure. . . . .	68
3.4	Parameters and results of coherent structures under effect of $V_{cr}$ . $N$ is the number of structures; $V_{max}$ is the volume of the maximum structure. . . . .	70
3.5	Parameters and results of coherent structures of different flow conditions. $N$ is the number of structures; $V_{max}$ is the volume of the maximum structure; $V_{cst}$ is the total volume of all structures; $V_t$ is the volume of the domain. . . . .	72

# List of Figures

2.1	D3Q19 lattice arrangement . . . . .	28
2.2	Three-dimensional shell ingestion . . . . .	38
2.3	A random two-dimensional structure . . . . .	47
3.1	Energy spectra of single phase turbulent flows at different energy inputs. (a) Energy spectra; (b) Compensated energy spectra; (c) Dissipated energy spectra. . . . .	51
3.2	PDF of vorticity in single phase turbulent flows of different energy inputs . . . . .	54
3.3	PDF of normalized energy dissipation rate in single phase turbulent flows of different energy inputs . . . . .	55
3.4	PDF of eigenvalues of strain tensor of single phase turbulent flows of different energy inputs . . . . .	57
3.5	Energy spectra of two-phase turbulent flows of different dispersed phase volume fraction in Case 2. (a) Energy spectra; (b) Dissipated energy spectra; (c) Compensated energy spectra. . . . .	60
3.6	PDF of vorticity in two phase turbulent flows of different dispersed phase volume fraction in Case 2 . . . . .	61

3.7	PDF of normalized energy dissipation rate in two phase turbulent flows of different dispersed phase volume fraction in Case 2 . . . . .	62
3.8	PDF of eigenvalues of strain tensor of single phase and two phase turbulent flows of different dispersed phase volume fraction in Case 2 . . . . .	63
3.9	Energy spectra of two-phase turbulent flows of different viscosity ratio at $\phi = 0.05\%$ in Case 2. (a) Energy spectra; (b) Dissipated energy spectra; (c) Compensated energy spectra. . . . .	64
3.10	PDF of vorticity in two phase turbulent flows of different viscosity ratio at $\phi = 0.05\%$ in Case 2 . . . . .	65
3.11	PDF of normalized energy dissipation rate in two phase turbulent flows of different viscosity ratio at $\phi = 0.05\%$ in Case 2 . . . . .	66
3.12	PDF of eigenvalues in two phase turbulent flows of different viscosity ratio at $\phi = 0.05\%$ in Case 2 . . . . .	67
3.13	Coherent structures of different threshold $Q_{th}$ extracted in Case 2. (a) $Q_{th} = 0.8, V_{cr}/V_{max} = 4\%$ ; (b) $Q_{th} = 0.85, V_{cr}/V_{max} = 4\%$ ; (c) $Q_{th} = 0.9, V_{cr}/V_{max} = 4\%$ . . . . .	69
3.14	Coherent structures of different volume criterion $V_{cr}$ . (a) $Q_{th} = 0.8, V_{cr}/V_{max} = 0\%$ ; (b) $Q_{th} = 0.8, V_{cr}/V_{max} = 2\%$ ; (c) $Q_{th} = 0.8, V_{cr}/V_{max} = 4\%$ . . . . .	71

3.15	Coherent structures and corresponding PDF of volume-equivalent diameter. $Q_{th} = 0.8, V_{cr}/V_{max} = 4\%$ . (a) Coherent structures of Case 1; (b) PDF of volume-equivalent diameter of Case 1; (c) Coherent structures of Case 2; (d) PDF of volume-equivalent diameter of Case 2; (e) Coherent structures of Case 3; (f) PDF of volume-equivalent diameter of Case 3. . . . .	73
3.16	Drop/coherent structures and corresponding PDF of volume-equivalent diameter in Case 2 at different time instants. $Q_{th} = 0.8, V_{cr}/V_{max} = 4\%$ . (a) Drop/coherent structures at $t/t_K = 10$ ; (b) PDF of volume-equivalent diameter at $t/t_K = 10$ ; (c) Drop/coherent structures at $t/t_K = 15$ ; (d) PDF of volume-equivalent diameter at $t/t_K = 15$ . . . . .	75

# Chapter 1

## Introduction

### 1.1 Applications of liquid-liquid systems

Emulsions and dispersions are of great interest in chemical industry [1, 2, 3], pharmacy [4, 5, 6, 7], electrochemistry [8, 9, 10], biology [11, 12, 13], petroleum industry [14, 15, 16], food [17, 18, 19], cosmetics [20, 21, 22], and agriculture [23, 24, 25]. In these systems, at least two immiscible liquids are agitated to generate a dispersed flow that ensures good contact between the phases and allows for the control of the interfacial area. The additional gases, liquids, or solids may also exist in these systems. When the liquids are agitated, multiple events occur in the system simultaneously: the breakup of drops, known as ‘dispersion’; the merging of drops, known as ‘coalescence’; and the suspension of drops [26]. These events results in the variance of drop size distribution (DSD) in the liquid-liquid system, thus, affects the final state of the system.

In an agitated vessel, for different operating conditions such as various impeller speed and agitation time, the different state of dispersed phase and phase contact will form. The variance of liquid-liquid interface or drop size distribu-

tion in the system results in the variance of mass transfer and heat transfer rates between the phases [11]. Due to various goals of industrial applications, the liquid-liquid systems are controlled to reach the different requirements on properties of flows such as the interfacial area, and, thus, drop size distributions. For example, a specific phase contact has to be formed in nitration reactions, because the reaction rate and temperature are mainly governed by the interfacial area; in suspension polymerization process, the generation of uniform beads is necessary [26], thus, a specific drop size distribution should be reached.

The thorough understanding of liquid-liquid system formation leads to improvement of industrial process, quantity and quality of products. For example, improvement of speed of liquid-liquid extraction in chemical industry fulfilled by interface control was provided in [2], in that study, the target analyte that exist in homogeneous aqueous phase was extracted into a water-immiscible sedimented phase. The interference that would have resulted from organic-aqueous phase contact disappears.

In the chemical and biochemical industries, the exploration of immiscible liquid-liquid dispersion in stirred vessels is important because it commonly exists in industrial processes such as liquid-liquid extraction [27], and suspension polymerization [28]. In solvent extraction problem, a large interfacial area between two liquid phases is necessary to keep the mass transfer between two phases, which results in a requirement of continuous agitation [29]. In food and pharmaceutical industries, the emulsification often occurs when small drops (for example,  $1\mu m$ ) are distributed in continuous phases [30, 31]. Usually, the emulsion is stable and viscous, the rheological characteristics are non-Newtonian.

The demand on environment protection boosts the development of renewable energy such as biofuels [32, 33]. The liquid-liquid equilibrium state is vital in the design of separation and purification process of crude bioethanol and biodiesel fuel [12]. However, it is also proposed in [12] that the equilibrium data that is used to predict liquid-liquid equilibrium state is not available from experiments. Thus, a UNIQUAC Functional-group Activity Coefficients is introduced to gain equilibrium data. To have a higher product yields and prevent unexpected repolymerization in biofuel upgrading reactions [30], the hydrophobic zeolites are introduced to stabilize water/oil emulsions and catalyse reactions at liquid-liquid interface.

In an optic study, liquid-liquid systems are used as the lens in sensing, medical diagnostics [34, 35]. For example, by electrowetting or giving pressure on a water-oil interface, the optic properties of a drop will change with its shape. Based on this control of liquid-liquid interface, an easy adjustable tunable liquid lens are created for optic experiments [35].

The water-oil emulsions are also common in dyes and pigments problem [31, 36]. Due to the carcinogenic and mutagenic effect of effluents from industries such as printing, dyestuff manufacturing, these pollutants have to be diminished. Thus, liquid surfactant membranes and emulsion liquid membranes are used to remove or recover dyes from effluents [31].

In chemical industry, antibiotics are usually produced in a liquid-liquid system, therefore, the separation of antibiotics is very important. The aqueous system often consists of water and a room temperature ionic liquid. Solvent extraction methods such as liquid-liquid partitioning are studied to fulfill this goal [37].

Liquid-liquid dispersions are common in industries, but at the same time

they are complex. The predictive tools that provides a guideline on how to agitate the liquids in a given vessel in order to produce the dispersion with known properties are needed [38, 39, 40]. The control of liquid-liquid dispersion can improve the products, suppress undesired by-products, and optimize industrial processes [41, 42, 43]. Therefore, the comprehension of behaviour of the system on a drop scale is of significant, as well as the quantification of the interaction of the drop with the surrounding flow. Experiments and simulations can be used for these purposes.

A large number of studies on liquid-liquid systems were carried out experimentally [44, 45, 46, 47]. Through these experiments, phenomena, such as drop breakup and coalescence, were observed. Various theories and assumptions were also introduced from the observation and analyses. Experiments are needed to get more data about drop breakup.

One of the recent studies of a single drop breakup in a rotor-stator mixer combines experiment and simulation [48]. Several findings were outlined: the breakup event mainly exist at downstream region of stator and the inside of jet (the dispersed phase was inject in the system by jet); a larger mother drop increases the time that drop interacts with vortex; the increase of Weber number results in the increase of breakup probability; the distance between current state to the equilibrium state drop size decides the number of fragments after breakup.

A summary of various experiments on a single drop breakup in turbulent flows was given in [49]. With the development of experimental system, facilities of high precision are utilized to capture drops behavior in liquid-liquid system at a smaller length and time scale [50, 51]. Particle image velocimetry (PIV) method with high precision charge-coupled device (CCD) camera is often used

in liquid-liquid systems study. For example, four Photron Fastcam Ultima APX cameras were set up to obtain velocity field at a frame rate of  $1000Hz$  [50]. The total time of coalescence is around  $600ms$ . An experimental study on how dispersed phase volume fraction affects liquid-liquid velocity field was carried out in a baffled cylindrical tank stirred with a six-bladed Rushton turbine [51]. The diameter and height of tank are  $0.14m$ . The tip speed is  $1.3m/s$ . The PIV system contains a Kodak Megaplug ES:1.0 CCD camera. However, they found that under this experimental setup, the dispersed phase volume fraction can only up to 10%.

Hasan [52] summarized experiments at different length and times scales in turbulent liquid-liquid systems. The breakup time, which is defined as the time taken from the start of deformation of mother drop to the occurrence of breakage, is an important parameter to predict the population of drops in the binary system. The experiments in his review have drop breakup time that varies from  $1ms$  to  $100ms$ , the diameter of mother drop varies from  $0.1mm$  to  $3mm$ , the breakup time will increase with the increase of drop size and vice versa. However, he pointed out that wide discrepancy exists in the measurement of breakup time because the start of deformation is usually not accurately recorded in experiments. Similar errors also occurs at the observation of occurrence of breakage: the resolution and frame rate limitation may result in the ignorance of infinitesimal satellite that is generated at first moments of breakup process. For the same reason, the record of drop size distribution in liquid-liquid system may be inaccurate, it will result in the inaccurate prediction of mass transfer and heat transfer.

Therefore, drawbacks and limitations still exist in the experimental study of liquid-liquid systems. With the development of computational technology,

the numerical study becomes a powerful tool that interacts with experimental study in the investigation of liquid-liquid systems.

As is denoted in Hasan's review [52], the breakup time decreases with the decrease of drop size. If the size of drop is decreased to much smaller scale, such as Kolmogorov length scale, the experimental facilities will not be able to capture the mother drop and daughters, as well as the breakup event because it will finish in a very short time. Thus, the experimental investigation at a very small length scale and time scale is not a good choice.

Besides, for a given experimental setup, the operating conditions are usually limited. For example, the dispersed phase volume fraction in the experimental setup given in [51] can only up to 10%. The modification of experiment is necessary if the investigation goes to a larger volume fraction.

In chemical industry, the study of mixing time in a liquid-liquid system is significant because it decides the performance of chemical reaction [53]. This is also a vital parameter that is taken into account for mixing system design, optimization, and scale-up from the laboratory scale to the industrial scale. It directly reflects the effectiveness of mixing system. Usually, it is challenging to investigate the mixing time in an industrial scale facility, experiments such as oil-water mixing were carried out in a laboratory size tank. The results obtained from the experiment were usually combined with laboratory scale empirical correlation, thus, problems may exist when extrapolating results to industrial scale agitated vessels [54]. Meanwhile, the experiment study didn't provide detailed localized information as well as the homogeneity degree at different locations [55, 56]. Therefore, the investigation on detail location is limited in experiments.

The disposal of material used in experiments is also a problem. Some

liquids in experiments such as liquid-liquid extraction are pollutants for environment [31]. The oil-water binary system is the common among these liquid-liquid systems, to dispose pollutions and clean the experimental facilities, methods such as oil skimmers, centrifuges, and depth filters are adopted, materials such as polyvinylidene fluoride membranes, boron nitride nanotubes-coated stainless steel meshes, and marshmallow-like gels are utilized, thus, extra budget and time are needed [57].

The demand of investigation on the bridge of local hydrodynamics of the flow and the breakup events boosts the development of multi-scale numerical frameworks.

## **1.2 Introduction to CFD-PBE numerical framework**

With the development of computational technology, the computational fluid dynamics (CFD) becomes a powerful tool. Attempts to better understand the dynamics of turbulent liquid-liquid systems resulted in the development of a numerical framework that involves CFD simulations of flow coupled with the solution of the population balance equation (PBE) that accounts for drop breakup and coalescence. Various modifications of this framework are implemented in commercial software [58, 59, 60]. The wide applications of CFD-PBE numerical framework are reported: investigate drop breakup and coalescence in a pulsed column [61]; simulate the fluidized bed spray granulation [62]; study local hydrodynamics for cell proliferation and protein synthesis in a stirred bioreactor [63].

The population balance plays a critical role in industrial applications [64, 65, 66]. For example, it can be used to predict the nanoparticle precipitation in production [67], forecast the granule growth behaviour [68], control crystal size [69], predict bubble/drop/aggregation breakup and coalescence [70, 38, 71] in agricultural chemicals, minerals, pharmaceuticals, etc. The application of population balance not only covers liquid-liquid systems [72] but also gas-liquid [73], solid-liquid [74] and gas-solid [75] systems. In the implementation of population balance, variables such as the number, mass or volume of particles of the dispersed phase are usually used to describe the population [76], the distributions of particles and the way it affects system behavior are of great interest in research.

The fundamental assumption of PBE is that there must be a number density of particles at each point, the equation is often coupled with conservation equations for entities in continuous phase [76]. In liquid-liquid systems, the breakup and coalescence of dispersed phases can be explained in terms of population balance because new particles can occur in breakup and coalescence processes.

The derivation process of PBE was provided in [76] in detail, it presented a general multi-dimensional form of the PBE:

$$\frac{\partial f}{\partial t} + \nabla_x \cdot \dot{X}f + \nabla_r \cdot \dot{R}f = h \quad (1.1)$$

where  $f$  denotes the number density function  $f(x, r, t)$  with external ( $x$ ) and internal ( $r$ ) coordinates;  $\dot{X}$  and  $\dot{R}$  are velocities for external and internal coordinates;  $h$  represents the resultant net generation rate of particles from birth and death.

In the liquid-liquid system, the continuity equation for the number density function  $f$  is provided by [77]:

$$\frac{\partial f(V)}{\partial t} + \nabla \cdot (\vec{u}f(V)) = S(V) \quad (1.2)$$

where  $V$  is the drop volume that is regarded as an internal coordinate;  $S(V)$  are source terms consist of breakage and coalescence of the drop [77]:

$$S(V) = B^c(V) - D^c(V) + B^b(V) - D^b(V) \quad (1.3)$$

where  $B^b$  and  $B^c$  are the birth rate due to breakage and coalescence;  $D^b$ , and  $D^c$  are the death rate due to breakage and coalescence.

In this study, the coalescence of drop is neglected. The source terms due to breakage are then replaced by [78]:

$$S(V) = \int_d^\infty \beta(V, V')g(V')f(V')dV' - g(V)f(V) \quad (1.4)$$

where  $\beta(V, V')$  is the daughter distribution function that illustrates the size distribution of daughter drops split out from a mother drop of size  $V'$ ;  $g(V')$  denotes breakup kernel (or frequency of breakup) of mother drop of size  $V'$ .

The persistent challenge of such multi-scale simulations lies in the fact that the results are highly dependent on the choice of the breakup and coalescence sub-models (or kernels) that require specification of breakup time, breakup frequency, number of fragments after the breakup, daughter size distribution, etc [79, 80]. For example, even for a simplified PBE (Equation (1.4)) in which only the breakup event in liquid-liquid flow is considered, the different choice of breakup kernel significantly affects the results of PBE. In recent years, many

breakup kernels were provided [81, 80, 82]. However, some obvious discrepancies exist in these kernels, they may result in the non-accurate probability of equal breakup, the dependence on energy dissipation rate, the ignorance of small break fraction [70, 83]. A complete breakup kernel must contain the breakup rate and daughter size distribution [83]. A common breakup kernel (CT kernel) that takes the energy dissipation rate  $\varepsilon$ , dispersed phase density  $\rho_c$ , and interfacial energy  $\sigma$  into account was proposed in [84]:

$$g(V) = C_1 \frac{\varepsilon^{1/3}}{V^{2/9}} \exp\left(-\frac{C_2 \sigma}{\rho_d \varepsilon^{2/3} V^{5/9}}\right) \quad (1.5)$$

where  $C_1$  and  $C_2$  are two constants. As another example, a multifractal (MF) kernel is proposed in [85]:

$$g(V) = \int_{\alpha_{min}}^{\alpha^x} g(V, \alpha) P(\alpha) d\alpha \quad (1.6)$$

where  $\alpha$  is singularity strength  $P(\alpha)$  is the probability density. The detail of expansion of each components were given in [85, 86, 87]. The comparison of two breakup kernels were reported in [78]: the CT breakup kernel only depends on the energy dissipation rate, other turbulent properties as well as the effect of viscous stress are not involved; the MF breakup kernel is a viscosity dependent kernel, it covers the effect of internal intermittency on breakup such as the large fluctuations on turbulent dissipation rate). The preassumption of both two breakup kernels is that drops breakup because of the pressure fluctuation.

It was also demonstrated that the breakup rate can be over or under predicted by an order of magnitude depending on the underlying assumption of drop/vortex interactions [88].

Considering that the CFD-PBE is becoming an indispensable tool to analysis liquid-liquid systems, therefore, fundamentally well-justified sub-models that can be used for CFD-PBE multi-scale simulations are highly needed. Before the development of sub-models, the major assumptions made in breakup kernels are identified.

### 1.3 Assumptions made in breakup kernels

Several assumptions in breakup kernels are summarized:

- The large-scale deformation in which the unstable oscillations result in drop break up is more frequent than the tearing mechanism that generates a small drop [89]. The observation of experiment revealed that the unequal size breakup had higher probability compared to the equal size breakup.
- In turbulent flow, only vortices of size equal to or smaller than the drop size leads to the drop breakup [90]. Vortices larger than drop size merely transport drops.
- With the kinetic energy  $E(\lambda)$  at vortex size  $\lambda$ , the daughter drop size is confined by the minimum and maximum breakup fraction  $f_{v,min}$  and  $f_{v,max}$  [83]. The dynamic pressure of vortex  $0.5\rho_c u_\lambda^2$  must be larger than the capillary pressure  $\sigma/r$ , it results in the minimum breakup fraction. The vortex kinetic energy must be larger than increment of surface energy in breakup process, it results in the maximum breakup fraction.
- If a drop has volume  $v$ , the probability of breaking up into two daughter

drops with volumes  $vf_v$  and  $(1-v)f_v$  also stay at the range between  $f_{v,min}(v, E(\lambda))$  and  $f_{v,max}(v, E(\lambda))$  [83].

- There is no mean relative velocity discrepancy between continuous phase and dispersed phase. Therefore, the breakup event is only resulted from turbulent velocity fluctuation [88].
- The relationship between daughter size distribution and the required energy for daughter drop formation is linear. [79]

Among these assumptions, the interaction between drop and vortices is of great interest. Attempts are made in finding relationship between breakup event and surrounding vortex.

## 1.4 Introduction to coherent structures

Drop/vortex interaction is important because it affects the breakup mechanism of assumption in breakup kernel, however, the data that are available for this analysis are limited. To understand the drop/vortex interaction, the visualization of coherent structures is used. The coherent structure is a region concentrated with high vorticity that makes fluid move around a core, it is coherent in space and temporally evolves vortical motions [91, 92]. Coherent structures are regarded as the elementary components where vortices cluster in turbulent flow [93].

Vortex is to be observed as an rotational region around a core. The concept of vorticity proposed to describe a vortex was defined as the curl of velocity ( $\omega = \nabla \times v$ ). The identification of coherent structures commonly relies on properties of vortices [94]. The turbulent coherent structures were

investigated to reveal the information of turbulence such as pressure, velocity, energy et al. Accurate, convenient and low cost methods were developed and preferred by investigators. Those commonly used methods for the extraction of coherent structures are Reynolds decomposition [95], Galilean (constant convection velocity) decomposition [95], large eddy simulation (LES) decomposition (low-pass filtering) [95], Q criterion [96, 97, 98, 99], Coherent Vortex Simulation (CVS) [100, 101, 102], and Lagrangian method [103, 104].

Adrian et al [95] used Galilean decomposition, Reynolds decomposition, and LES decomposition to visualize vortices in turbulent pipe flow when Reynolds number equals to 50000. Two-dimensional vorticity contours were given. The Reynolds decomposition was not good at vortices visualization because it extracted small-scale vortices well but missed large-scale properties. Besides, the LES decomposition was found to be the best for vorticity visualization due to the good presentation of eddies in all three layers of flow in the pipe.

Q criterion is the widely adopted method for coherent structures extraction due to its low computational cost. It is classified as a Eulerian method based on the principle. In Q criterion, Q is defined as the balance between rotation and strain rates. Thus, the region with positive Q indicates higher rotation. Using this method, Dubief and Delcayre [96] obtained worms shape vortex structures in isotropic free decaying turbulence. Furthermore, in a turbulent mixing layer simulation, they realized that the large-scale span-wise vortices together with stream-wise vortices were forcefully affected by two-dimensional initial perturbations. As for the channel flow with  $Re = 160$  and  $Ma = 0.3$ , they found that it is the coherent structures at the inner region that bolsters the turbulence flow. Besides, the second eigenvalues isosurfaces plots for these

simulations were given.  $Q$  isosurfaces and second eigenvalues isosurfaces plots were always near the same, but there was more noise in second eigenvalues isosurfaces plot.

Using  $Q$  criterion, Kareem et al. [97] extracted vortex structures from large, intermediate and fine scale homogeneous isotropic turbulent fields at Taylor microscale Reynolds number equal to 81. The threshold values for three flow fields are 5.406, 6.103 and 6.012 correspondingly. In order to generate clear plots, structures with the volume lower than 4% of the maximum structure volume were erased as noise. Vortex structures in fine scale flow were observed to be more sprier in stretching than those in larger scale flow. In large scale flow, structures were easier to stretch when the breakup of vortex occurs.

Ghasempour et al [98] studied structure properties in turbulent pipe flow using  $Q$  criterion, the Reynolds number was 20000. They introduced a vortex tracking method to capture single coherent vortices in turbulent flow through its lifetime. Repeating the vortex cross-section, boundary and volume tracking procedure, investigators can get lifetime tracking of a vortex, which helps to identify properties of coherent vortex such as TKE, volume and aspect ratio. They visualized the shape of a vortex from birth to break up. The variance of captured TKE with the variance of threshold values was also given.

Later, a normalized  $Q_n$  criterion was introduced [99]. The  $Q$  is normalized by rotation squared. The simulation was still performed in a pipe, the threshold value of  $Q_n$  was selected as 0.1 to capture as many structures as possible. Considering the fact that vortices can grow up after absorbing turbulent kinetic energy (TKE), they introduced morphological methods to simulate as well as track the growth process and Biot-Sawart law to avoid overgrowth. Properties of vortices and the probability distribution of TKE are found to be

insistent with the dynamic Smagorinsky-Lilly subgrid scale model.

The Lagrangian method is also a popular method which is used to extract coherent structures. Haller and Yuan [103] proposed that the vital difference between Lagrangian method and Eulerian method such as Q criterion is that the Lagrangian method focuses on the boundaries of structures instead of the transitory properties. They defined material lines to depict boundaries of structures. Moreover, a scrupulous structure extraction criterion was also provided. They performed this analytic criterion on a two-dimensional barotropic turbulence flow for validation. The structures gleaned by them were found to be in agreement with those derived from statistics.

Green et al [104] captured coherent structures using this Lagrangian method in an isolated hairpin vortex flow and a fully developed turbulent flow. The results were then compared to those obtained from Eulerian method - the Q criterion. The Reynolds number was 180. By calculating the direct Lyapunov exponent (DLE), they obtained Lagrangian coherent structures with better detail. Moreover, the extraction was found to be definitely independent by using Lagrangian method while the extraction procedure was determined by the threshold value using Eulerian method. However, the Lagrangian method needs more computational calculation due to the larger amount of data involved in.

Farge and Schneider [100] proposed Coherent Vortex Simulation (CVS) method based on Ha Minh's semi-deterministic model. The principle of CVS is computing the coherent structures, which is the organized part of a flow, and modeling the incoherent turbulent environment, which is the random part of a flow. The implementation of CVS method depends on the type of turbulent flow owing to the nonlinear filtering pass. They performed CVS method on

two-dimensional mixing layer flow and wavelet forced homogeneous isotropic turbulent flow, the results were in consonance with those obtained by DNS.

Farge et al [101] also extracted coherent structures from three dimensional homogeneous isotropic turbulent flow at  $Re_\lambda = 150$  using CVS method, the computational domain consists of  $256^3$  grids. They realized that the classical Richardson's scenario that the transmission of energy is accompanied by the breakup of eddies is not able to demonstrate the energy cascade. Thus, they claimed that the transfer of energy is the result of nonlinear vortex interactions. The coherent energy transfers through the whole of inertial range. As for the incoherent energy, it exists at the whole of inertial scales but dissipation just occurs at the smallest scales.

Schneider et al [102] implement CVS method in three dimensional forced and unforced turbulent mixing layers. The Taylor microscale Reynolds number was 150. The coherent structures gained by orthogonal wavelet basis was represented by 3.8% of the wavelets but includes more than 99% of turbulent kinetic energy in forced mixing layer. And in the unforced mixing layer simulation, the obtained coherent structures was represented by 4.2% of the wavelet. Moreover, the comparison of CVS filtering and LES filtering such as the low-pass Fourier cut-off filtering was given.

Turiel et al [105] studied extraction of vortex structures using CVS in an oceanic flow. They realized that the loss of energy in oceanic coherent flows is relatively high. Furthermore, the incoherent part obtained was not in Gaussian distribution, which made the wavelet decomposition unreal.

Other efforts on turbulent coherent structures were also made in last decades. In 2001, Miyauchi and Tanahashi [106] studied the generalization of scaling law of structure by comparing vortices in homogeneous isotropic turbulence, turbu-

lence mixing layer, turbulent channel flows and MHD homogeneous turbulence at the fine scale. Velocities such as azimuthal, axial and advection velocity as well as length scales such as Kolmogorov microscale, Taylor microscale, and integral length scale were analyzed as the characteristic indicators. The probability density function of the diameter of eddy and circulation were also given to analyzing properties.

Samanta et al [107] performed DNS in both viscoelastic and Newtonian fluids turbulent flow in a parallel-plate channel. The Reynolds number was 180. They used Karhunen-Loeve (K-L) analysis to study the time evolution of coherent structures.

Experimental studies were also performed to analyze coherent structures. Grulke et al [108] did an experimental study of coherent structures in turbulent fluctuations of a simple magnetized torus (SMT) device. They found that the physical properties of plasma can decide the shape of coherent structures.

Staplehurst et al [109] did an experimental study for large-scale columnar structures based on the structure formation theory proposed by Davidson et al [110]. The experiment was performed in a homogeneous freely decaying rotating turbulent flow with  $Ro \approx 1$ . They introduced two-point correlations in the axial direction to study columnar structures. The structure formation was found to be validated.

These references reveal that coherent structures are important in the study of drop behavior in liquid-liquid systems. To visualize coherent structures, the normalized  $Q_n$  criterion is the best method for this study due to its relatively low computational cost, meanwhile, it removes the limitation resulted from the order effect that occurs in the widely used method -  $Q$  criterion.

## 1.5 Objectives and goal of the thesis

The goal of this study is to develop various tools for analysis of data obtained from the direct numerical simulations (DNSs) of liquid-liquid dispersions in homogeneous isotropic turbulent flow. The results of such analysis will then be used to develop well-grounded sub-models for PBEs. The DNSs of liquid-liquid dispersions in a homogeneous isotropic turbulent flow field were performed using the diffuse interface free energy lattice Boltzmann method (LBM). The multi-relaxation-time (MRT) collision operator was used for the collision step. First, the fully-developed turbulence was generated in a three-dimensional fully-periodic cubic domain using a forcing method. Then, a drop of different size and viscosity ratio was injected into the turbulent flow field. The evolution of liquid-liquid interface and coherent structures was visualized. The statistical characteristics of turbulence were also presented.

The underlying objectives of the study are to

- Identify the fundamental assumption used to derive the drop breakup kernels that significantly affect the drop size distribution. For instance, most of the models preassume that drop breaks after interaction with a *single* turbulent vortex. There is no either experimental or numerical evidence for this. Another basic question is whether vortices of the size greater than the drop diameter lead to drop breakup. Most of the existing models are based on the assumption that only vortices of the size equal to or smaller control drop breakup.
- Analyze the statistical characteristics of turbulence. For example, the probability density distribution of vorticity.

- Derive the calculation of three-dimensional spectrum of turbulence and develop the tool for calculation.
- Implement the multi-relaxation-time collision operator for the lattice Boltzmann method to improve the stability of simulations.
- Find an evidence for or disprove the outlined assumptions by visualization and quantification of the results of high-resolution three-dimensional DNSs of liquid-liquid dispersion in homogeneous isotropic turbulence.

## Chapter 2

# DNSs of liquid-liquid systems

In Section 2.1, a literature review focused on direct numerical simulations of turbulent liquid-liquid systems is presented. In Section 2.2, the free energy lattice Boltzmann method is introduced, two different collision operators are compared. In Section 2.3, the generation of single phase turbulent flow is given. In Section 2.4, the calculation of three-dimensional energy spectra is presented. In Section 2.5, the normalized  $Q_n$  criterion and newly designed boundary identification method are introduced for the visualization of coherent structures.

## 2.1 Literature review on DNSs of turbulent liquid-liquid systems

Only studies of turbulent liquid-liquid systems using DNSs are reviewed here. Due to the limited number of studies in this area, it is important to discuss them in order to verify and validate the numerical methods that are used for complex systems.

Derksen and Akker [111] simulated liquid-liquid dispersion in stirred three-dimensional periodic domain. Two fluids with the same viscosity and density were set in the simulation. The turbulent flow was generated by the lattice Boltzmann method (LBM) in a  $256^3$  cells domain. The initial droplet diameter was 20 lattice units. The dispersed phase volume fraction was 16%. The fluid was turbulent at the beginning, its turbulent kinetic energy (TKE) decayed quickly after stepping into a short steady balance. They provided coalescence and breakup process of droplets in cross-section view. The drop size distributions (DSD) was also given. The DSD became wider with time, and more small droplets were generated. It revealed that the breakup process was dominant. To contrast, the coalescence process dominates if there was no turbulent force injected into the fluid.

Komrakova et al [112] explored drop deformation and breakup in liquid-liquid simple shear flow using LBM. Five dimensionless numbers, Reynolds number  $Re$ , capillary number  $Ca$ , viscosity ratio  $\lambda$ , Peclet number  $Pe$  and Cahn number  $Ch$ , were introduced to fully describe the liquid-liquid system. The impact of  $Pe$ ,  $Ch$  and mesh resolution on the mechanism of deformation was studied. In 2015, Komrakova et al [113] studied the effect of Kolmogorov scale resolution, energy input, viscosity ratio and dispersed phase volume frac-

tion on deformation of droplets in a three-dimensional periodic domain. The homogeneous isotropic turbulent flow was created by linear forcing. The comparison of kinetic energy spectrum in single-phase and two-phase was also given. The Introduction of the second phase changes the energy spectrum fiercely. They also highlighted the three drawbacks of the numerical method they used: the numerical dissolution of small drops, over-estimation of drop coalescence and the occurrence of spurious currents.

Hagiwara et al [114] investigated drop deformation in a turbulent channel flow domain which was meshed as  $64 \times 44 \times 32$  by DNSs. Classification of five different types of turbulent structures were provided: shear, convergence, eddy, donor eddies and streaming. They were classified using the zone classification method given in [115]. They found that the droplet was sharpened in the shear-dominant region while squeezed in the convergence-dominant region. The deformation in the eddy-dominant region was not obvious.

Scarbolo and Soldati [116] investigated drop dynamic in turbulent channel flow using DNS combined with interface tracking. The shear Reynolds number was  $Re_\tau = 100$  and Peclet number was  $Pe = 2.56 \times 10^5$ . The four different Weber numbers were  $We = 0.0053, 0.0106, 0.0212, 0.0424$ . The ratio between Kolmogorov length scale and drop diameter was from 0.06 to 0.13. The simulation domain was divided into  $256 \times 128 \times 129$  meshes. They found the existence of interface generated discrepancy of surrounding velocity field, which led to the vorticity generation. The figures that drop surrounded by coherent structures were also given, the drop with low deformability was surrounded by more coherent structures.

Roccon et al [117] studied viscosity effect on the breakup and coalescence of drops in a wall-bounded turbulent flow. The  $4\pi h \times 2\pi h \times 2h$  domain was

divided into  $512 \times 256 \times 257$  meshes. Turbulent flows with Weber number  $We = 0.75, 1.5, 3$  were generated, the viscosity ratio between dispersed phase and continuous phase were  $\lambda = 0.01, 0.1, 1, 10, 100$  for each Weber number. 256 drops with diameter  $d = 90$  meshes were injected into the turbulent flow at  $Re_\tau = 150$ . The two-phase flow was tracked by the phase field method (PFM). The average velocity of the mixture of two phases was observed always to be increased in time due to the absorption of turbulent kinetic energy by drops. Furthermore, the drop was not likely to deform at small Weber number  $We < 1$  because the surface tension, which prevents the drop breakage, was dominant, and the change of viscosity ratio didn't affect drop breakup or coalescence rate in this situation. In the contrast, drop tends to deform at larger Weber number  $We > 1$ , and the increment of viscosity ratio drastically decreased the breakup rate and increased the coalescence rate.

The DNS of drop/near-wall turbulence interaction was reported by Iwasaki [118] et al. The simulation was resolved in a rectangular domain. A drop of diameter equals to one-fourth of the wall distance was initially placed in the range of 20 - 60 wall units from one moving wall. To investigate effects of viscosity  $\mu_d/\mu_c$  and interfacial tension  $\sigma^* = \sigma/\rho U_W^2 h$  of drop (where  $U_W^2$  was the speed of moving wall,  $h$  was half of distance between two moving walls), three different cases were implemented: the fluid element  $\mu_d/\mu_c = 1, \sigma^* = 0$ ; the viscous drop without interfacial tension  $\mu_d/\mu_c = 40, \sigma^* = 0$ ; the viscous drop with interfacial tension  $\mu_d/\mu_c = 40, \sigma^* = 0.01$ . An equal density was set for dispersed and continuous phase. The Reynolds numbers  $Re^* = U_W h/\nu$  and  $Re^+ = u_\tau h/\nu$  were 1300 and 82.6 respectively (where  $u_\tau$  was the friction velocity). The liquid-liquid interface was tracked by VOF method. They found that the deformation of high-viscosity drop was smaller compared to

the deformation of fluid element; for the high-viscosity drop with interfacial tension, the deformation nearly did not occur. Thus, both the high-viscosity and interfacial tension suppress the deformation. They also extracted coherent structures at near-wall region, the existence of drop with interfacial tension was found to result in the attenuation of near-wall streamwise vortex. Besides, in the wake flow region of drop, the occurrence of small vortex was observed. Finally, in a wide region around the drop, the Reynolds-shear stress product was observed to be higher than that in other region. They attributed this phenomenon to the introduced translational flow by the drop.

Yuge and Hagiwara [119] studied non-isothermal turbulent upward channel flow by DNS. The hydrofluoroether-water binary system was used. The Reynolds number  $Re_\tau$  was 180. Four identical drops were placed at near-wall region and tracked by VOF method. Some conclusions were provided: several types of secondary flows introduced by drops resulted in the increase of Reynolds shear stress product, they were mitigated by the adjacent drops in streamwise direction; The near-wall drops deformed large streamwise vortices and mitigated small vortices; The drops increased heat transfer in binary system.

Combining with various liquid-liquid interface tracking methods, the implementation of DNS simulations helps exploring and explaining numerous fundamental behavior and phenomena in turbulent binary systems that contain multi-scales.

## 2.2 Free energy lattice Boltzmann method with multiple-relaxation-time operator

The diffuse interface free energy lattice Boltzmann method (LBM) proposed by Swift et al. [120] is used here. In diffuse interface methods [121, 122, 123], the interface is defined as a finite-thickness transition area where the variance of physical quantities is continuous. To describe composition of system, the order parameter  $\varphi$  is introduced [124, 125, 126]. It is regarded as the relative concentration of two components. The solution of continuity and momentum equations in conjunction with the Cahn-Hilliard convection-diffusion equation for the order parameter is adopted to simulate behavior of binary mixture [127]. Therefore, the continuity, momentum, convection-diffusion equations decide density, velocity and order parameter respectively [128].

$$\partial_t \rho + \partial_\alpha (\rho u_\alpha) = 0 \quad (2.1a)$$

$$\partial_t (\rho u_\alpha) + \partial_\beta (\rho u_\alpha u_\beta) = \quad (2.1b)$$

$$- \partial_\beta P_{\alpha\beta}^{th} + \partial_\beta \nu (\rho \partial_{\alpha\beta} u_\beta + \rho \partial_\beta u_\alpha) + \rho F_{t\alpha}$$

$$\partial_t \varphi + \partial_\alpha (\varphi u_\alpha) = M \partial_{\beta\beta}^2 \mu \quad (2.1c)$$

where  $u_\alpha$  is the velocity; the index  $\alpha$  stands for the Cartesian directions  $x$ ,  $y$ ,  $z$ ;  $\rho$  and  $\nu$  are the density and the kinematic viscosity of the mixture, respectively;  $M$  is the mobility;  $F_{t\alpha}$  is the forcing term to generate turbulence;  $P_{\alpha\beta}^{th}$  is the "thermodynamic" pressure tensor which includes an isotropic contribution  $P_{id} \delta_{\alpha\beta}$  that represents the ideal gas pressure and the "chemical" pressure tensor

$P_{\alpha\beta}^{chem}$  [128]:  $P_{\alpha\beta}^{th} = P_{id}\delta_{\alpha\beta} + P_{\alpha\beta}^{chem}$ . The ideal gas pressure is  $P_{id} = \frac{\rho}{c_s^2}$ , where  $c_s^2$  is sound speed. The  $P_{\alpha\beta}^{chem} = \left[ \frac{A}{2}\varphi^2 - \frac{3A}{4}\varphi^4 - K\varphi\partial_{\alpha\alpha}^2\varphi - \frac{1}{2}|\partial_{\alpha}\varphi|^2 \right] + K\partial_{\alpha}\varphi\partial_{\beta}\varphi$  is an active scalar and the set of Equation (2.1) is intimately coupled, because it is a function of order parameter  $\varphi$  [113].  $\mu(\varphi) = A\varphi - A\varphi^3 - K\partial_{\alpha\alpha}^2\varphi$  is the chemical potential. Here,  $A < 0$  and  $K$  are parameters of the free energy model that are related to the surface tension and interface thickness.

In LBM model, the macroscopic equations are solved in two steps: streaming and collision [129]. At each time step, particles stream to neighboring lattice points along fixed lattice links in streaming process, then the velocity distribution at each point relaxes towards equilibrium distribution in collision process. Two discrete single-particle density distribution functions  $f(\mathbf{r}, t)$  and  $g(\mathbf{r}, t)$  are used to describe the motion of fluid. The function  $f(\mathbf{r}, t)$  solves the continuity and momentum equations which are the Equation (2.1a) and (2.1b) respectively, the function  $g(\mathbf{r}, t)$  solves the convection-diffusion equation which is the Equation (2.1c).

Usually, the single-relaxation-time collision operator, also known as the Bhatnagar-Gross-Krook (BGK) operator [130], is adopted to solve the collision process. It is the simplest and widely used collision operator because distribution functions are relaxed by a single dimensionless relaxation parameter  $\tau$ . Under this scenario, the discrete lattice Boltzmann equations are given as [131]:

$$\begin{aligned} f_q(\mathbf{r}_{\alpha} + \mathbf{c}_{\alpha q}\Delta t, t + \Delta t) - f_q(\mathbf{r}_{\alpha}, t) &= \frac{-1}{\tau_f} (f_q - f_q^{eq}) + \mathbf{F}_q \\ g_q(\mathbf{r}_{\alpha} + \mathbf{c}_{\alpha q}\Delta t, t + \Delta t) - g_q(\mathbf{r}_{\alpha}, t) &= \frac{-1}{\tau_g} (g_q - g_q^{eq}) \end{aligned} \quad (2.2)$$

where index  $q$  represents the number of discrete velocity directions; index  $\alpha$

represents the Cartesian directions  $x$ ,  $y$  and  $z$ ;  $f_q^{eq}$  and  $g_q^{eq}$  are the discretized Maxwell-Boltzmann distribution functions (equilibrium distribution function);  $\tau_f$  and  $\tau_g$  are dimensionless relaxation parameters;  $\mathbf{c}_{\alpha q}$  is discrete velocity set and  $\mathbf{F}_q$  is the forcing term. The forcing term is incorporated as follows:

$$\mathbf{F}_q = w_q(\mathbf{c}_q \cdot \mathbf{F}_{t\alpha}) \quad (2.3)$$

The density  $\rho$ , local fluid momentum  $\rho u_\alpha$  and order parameter  $\varphi$  are defined as following:

$$\begin{aligned} \sum_q f_q &= \rho \\ \sum_q c_{\alpha q} f_q &= \rho u_\alpha + \frac{F_{t\alpha}}{2} \\ \sum_q g_q &= \varphi \end{aligned} \quad (2.4)$$

The calculation of equilibrium equations is given by [132]:

$$\begin{aligned} f_q^{eq} &= \frac{w_q}{c^2} \left( p_0 - K(\partial_{xx}^2 \varphi + \partial_{yy}^2 \varphi + \partial_{zz}^2 \varphi) + c_{\alpha q} \rho u_\alpha + \frac{3}{2c^2} \left[ c_{\alpha q} c_{\beta q} - \frac{c^2}{3} \delta_{\alpha\beta} \right] \rho u_\alpha u_\beta \right) \\ &\quad + \frac{K}{c^2} (w_q^{xx} \partial_x \varphi \partial_x \varphi + w_q^{yy} \partial_y \varphi \partial_y \varphi + w_q^{zz} \partial_z \varphi \partial_z \varphi \\ &\quad + w_q^{xy} \partial_x \varphi \partial_y \varphi + w_q^{xz} \partial_x \varphi \partial_z \varphi + w_q^{yz} \partial_y \varphi \partial_z \varphi) \end{aligned} \quad (2.5a)$$

$$g_q^{eq} = \frac{w_q}{c^2} \left( \Gamma \mu + c_{\alpha q} \varphi u_\alpha + \frac{3}{2c^2} \left[ c_{\alpha q} c_{\beta q} - \frac{c^2}{3} \delta_{\alpha\beta} \right] \varphi u_\alpha u_\beta \right) \quad (2.5b)$$

where  $w_q$  is weight corresponding to the norm of  $c_q$ ,  $c_s$  is the speed sound.  $p_0$  is the bulk pressure  $p_0 = c_s^2 \rho + \frac{A}{2} \varphi^2 + \frac{3B}{4} \varphi^4$ . The distributions for  $q = 0$  are

given by:

$$\begin{aligned}
 f_0^{eq} &= \rho - \sum_{q=1}^{18} f_q^{eq} \\
 g_0^{eq} &= \varphi - \sum_{q=1}^{18} g_q^{eq}
 \end{aligned}
 \tag{2.6}$$

In this study, the D3Q19 lattice arrangement (three dimensions and nineteen discrete velocity directions) is adopted. As is shown in Figure 2.1, the central point is connected with 6 central points in each face and 12 central points in each edge of the cube. Only uniform cubic lattices are used here, the mesh step  $\Delta x$  and time step  $\Delta t$  are taken as unity. Lattice Boltzmann method operates in lattice space in so-called lattice units (lu).

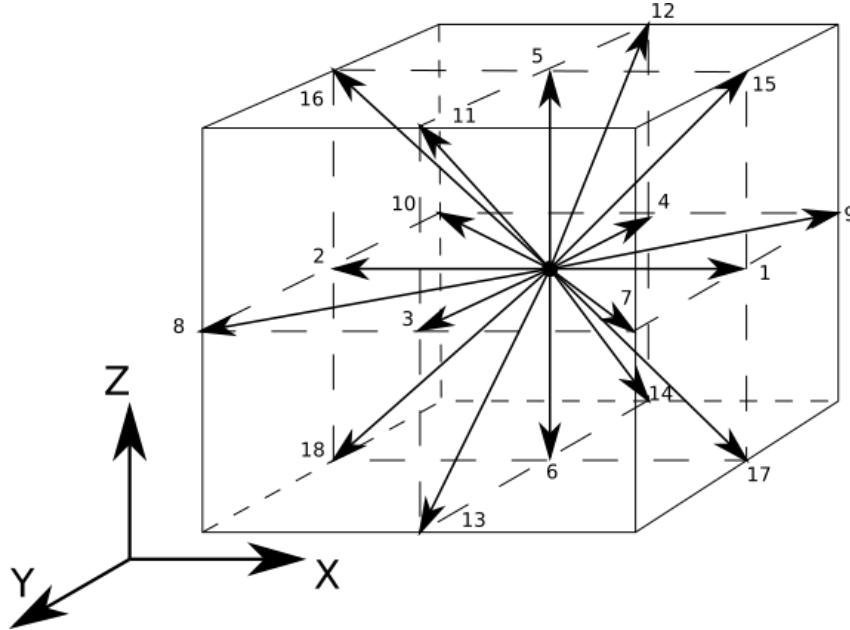


Figure 2.1: D3Q19 lattice arrangement

The discrete velocity sets and the weighting factors are defined as follows:

$$e_q = \begin{cases} (0, 0, 0) & q = 0 \\ (\pm 1, 0, 0), (0, \pm 1, 0), (0, 0, \pm 1) & q = 1, 2, \dots, 6 \\ (\pm 1, \pm 1, 0), (0, \pm 1, \pm 1), (\pm 1, 0, \pm 1) & q = 7, 8, \dots, 18 \end{cases} \quad (2.7)$$

and

$$w_q = \begin{cases} 1/3, & q = 0 \\ 1/18, & q = 1, 2, \dots, 6 \\ 1/36, & q = 7, 8, \dots, 18 \end{cases} \quad (2.8)$$

The multiple-relaxation-time (MRT) collision operator is implemented considering that multiple physical quantities in collision process may relax on different time scales [131]. It is used in this study to improve stability and accuracy of the simulations. Premnath et al. [133] analyzed advantageous of MRT operator by comparing with BGK operator. They proposed that numerical instability occurs in the relatively low viscosities fluids simulation. Due to computational constraints, the instability problems may be compounded in three-dimensional flows when physics may not be adequately resolved. The MRT operator is more stable than BGK operator because the different relaxation times can be individually relaxed to achieve stability. The MRT operator is also flexible enough to incorporate additional physics which cannot be naturally represented by BGK operator. In MRT operator, moments of distribution functions such as momentum and viscous stresses are solved directly, which provides a natural and convenient way to express various relaxation processes happened in various time scales due to collisions.

Therefore, the lattice Boltzmann equation which utilizes the MRT operator is given by:

$$f_q(\mathbf{r}_\alpha + \mathbf{c}_{\alpha q}\Delta t, t + \Delta t) - f_q(\mathbf{r}_\alpha, t) = -\mathbf{M}^{-1}\mathbf{S}(\mathbf{m}_q - \mathbf{m}_q^{eq}) + \mathbf{F}_q \quad (2.9)$$

where  $\mathbf{M}$  is a  $19 \times 19$  transformation matrix which transforms distribution functions  $f$  to velocity moments  $\mathbf{m}$ :

$$\mathbf{m} = \mathbf{M}f \quad (2.10)$$

Define collision matrix  $\hat{\mathbf{S}}$  as follow:

$$\hat{\mathbf{S}} = \mathbf{M}^{-1}\mathbf{S}\mathbf{M} \quad (2.11)$$

Therefore, the Equation (2.9) can be replaced by:

$$f_q(\mathbf{r}_\alpha + \mathbf{c}_{\alpha q}\Delta t, t + \Delta t) - f_q(\mathbf{r}_\alpha, t) = -\hat{\mathbf{S}}(f_q - f_q^{eq}) + \mathbf{F}_q \quad (2.12)$$

The eigenvalues of  $\mathbf{S}$  are all between 0 and 2 in order to maintain linear stability and the separation of scales [134]. It can be easily represented that BGK operator is a special case in which all relaxation times are equal, the collision matrix is  $\hat{\mathbf{S}} = \mathbf{M}^{-1}\frac{1}{\tau}\mathbf{I}\mathbf{M} = \frac{1}{\tau}\text{diag}(\mathbf{I})^T$ , where  $\tau > \frac{1}{2}$  is the single relaxation time of BGK.

The transformation matrix represents components of the 19 orthogonal basis column vectors:

$$\mathbf{M} = \left[ \varsigma_0, \varsigma_1, \dots, \varsigma_{18} \right]^T \quad (2.13)$$

The 19 orthogonal basis vectors  $\varsigma_{q\beta}$  and derived transformation matrix  $\mathbf{M}$  are listed in Appendix. The corresponding 19 velocity moments are given [135]:

$$\mathbf{m} = (\rho, e, e^2, j_x, q_x, j_y, q_y, j_z, q_z, 3p_{xx}, 3\pi_{xx}, p_{ww}, \pi_{ww}, p_{xy}, p_{yz}, p_{xz}, m_x, m_y, m_z)^T \quad (2.14)$$

where  $j_x, j_y, j_z$  are momentum or mass flux ( $\mathbf{j} = \rho\mathbf{u}$ );  $q_x, q_y, q_z$  are heat flux;  $p_{xx}, p_{ww}, p_{xy}, p_{yz}$ , and  $p_{xz}$  are components of the symmetric and traceless strain-rate tensor;  $\pi_{xx}$  and  $\pi_{ww}$  are fourth order moments which have the same symmetry as the diagonal part of the traceless tensor  $p_{ij}$ . The last three vectors are third order moments.

In MRT operator, the collision matrix (relaxation matrix)  $\hat{\mathbf{S}}$  is diagonal in moment space  $\mathbb{M}$ :

$$\hat{\mathbf{S}} = \text{diag}(s_0, s_1, s_2, s_3, s_4, s_5, s_6, s_7, s_8, s_9, s_{10}, s_{11}, s_{12}, s_{13}, s_{14}, s_{15}, s_{16}, s_{17}, s_{18})^T \quad (2.15)$$

where parameter  $s_q$  represent the inverse of the relaxation time ( $1/\tau$ ) of the various moments  $\mathbf{m}$  in reaching their equilibrium values  $\mathbf{m}^{eq}$ . Because the collision process conserves particular moments (density and components of momentum)  $s_0, s_3, s_5$  and  $s_7$ , the collision process values remain constant under variation of corresponding relaxation times. Thus, the relaxation parameters for these moments can be set to zero when there is no forcing term in the LBM. However, the collision matrix affects the forcing term in the effectively explicit in MRT LBM with forcing term, the relaxation times for these conserved moments should not be chosen as zero [133]. Therefore, they are set

as 1 for simplicity. The collision matrix then becomes:

$$\hat{\mathbf{S}} = \text{diag}(1, s_e, s_{e^2}, 1, s_q, 1, s_q, 1, s_q, s_\nu, s_\pi, s_\nu, s_\pi, s_\nu, s_\nu, s_m, s_m, s_m)^T \quad (2.16)$$

The equilibria of the non-conserved moments are given:

$$\begin{aligned} m_1^{eq} &= -11\rho + \frac{19}{\rho}(j_x^2 + j_y^2 + j_z^2) \\ m_2^{eq} &= \omega_\varepsilon + \frac{\omega_{\varepsilon j}}{\rho}(j_x^2 + j_y^2 + j_z^2) \\ m_{4,6,8}^{eq} &= -\frac{2}{3}j_{x,y,z} \\ m_9^{eq} &= \frac{1}{\rho}(2j_x^2 - j_y^2 - j_z^2) \\ m_{11}^{eq} &= \frac{1}{\rho}(j_y^2 - j_z^2) \\ m_{10}^{eq} &= \omega_{xx}m_9^{eq} \\ m_{12}^{eq} &= \omega_{xx}m_{11}^{eq} \\ m_{13}^{eq} &= \frac{1}{\rho}j_xj_y \\ m_{14}^{eq} &= \frac{1}{\rho}j_yj_z \\ m_{15}^{eq} &= \frac{1}{\rho}j_zj_x \\ m_{16}^{eq} &= m_{17}^{eq} = m_{18}^{eq} = 0 \end{aligned} \quad (2.17)$$

In order to optimize the linear stability of the model, the parameters are chosen as [136]:  $\omega_\varepsilon = \omega_{xx} = 0$ ,  $\omega_{\varepsilon j} = -475/63$ ,  $s_e = 1.19$ ,  $s_e^2 = s_\pi = 1.4$ ,  $s_q = 1.2$ ,  $s_m = 1.98$ . The speed sound is  $c_s = 1/\sqrt{3}$  in lattice units of

$\Delta x = \Delta t = 1$ . The kinematic viscosity  $\nu$  and bulk viscosity  $\xi$  are:

$$\nu = \frac{1}{3} \left( \frac{1}{s_\nu} - \frac{1}{2} \right) \quad (2.18)$$

$$\xi = \frac{2}{9} \left( \frac{1}{s_e} - \frac{1}{2} \right) \quad (2.19)$$

The continuous phase and injected dispersed phase are of different kinematic viscosity. Thus, the kinematic viscosity of the mixture is a function of order parameter [132]:

$$\nu(\varphi) = \nu_c \frac{\varphi_0 - \varphi}{2\varphi_0} + \nu_d \frac{\varphi_0 + \varphi}{2\varphi_0} \quad (2.20)$$

where  $\nu_c$  and  $\nu_d$  are the kinematic viscosities of continuous phase and dispersed phase, respectively.  $\varphi_0$  is set as 1.

## 2.3 Turbulence generation. Single-phase flow simulations

In this study, the statistically stationary homogeneous isotropic turbulence is generated in a three-dimension periodic domain. Due to the natural decay of turbulence, the energy input is the necessity for the maintenance of turbulence. Here, the energy input is organized by means of linear forcing that is proposed by Lundgren [137]. The local force imposed in the liquid is proportional to the local velocity

$$F_{t\alpha} = A_f u_\alpha \quad (2.21)$$

The parameter of force  $A_f$  is

$$A_f = \varepsilon / (3u_{rms}^2) \quad (2.22)$$

where  $\varepsilon$  is the volume-averaged energy dissipation rate per unit mass;  $u_{rms}$  is the volume-averaged root-mean-square fluid velocity. The dissipation rate  $\varepsilon$  is an input parameter in turbulence generation, if the resolution of the Kolmogorov length scale  $\eta_K$  is fixed, then these levels of dissipation can be set up by varying kinematic viscosity of the continuous phase  $\nu_c$  due to the relationship  $\eta_K = (\nu_c^3/\varepsilon)^{1/4}$ . The turbulence generation method does not allow to have the root-mean-square velocity  $u_{rms}$  as an input parameter. therefore, as the output parameter, the  $u_{rms}$  values were calculated every time step after the simulation was performed. Derksen [138], Valino et al. [139] successfully implemented this type of linear forcing in the environment of the LBM.

A non-zero velocity field is used to start with the turbulence generation. It was initialized at  $t = 0$  using the following relations

$$\begin{aligned} u_x &= u_{init} \sin\left(\frac{2\pi j}{\lambda_0}\right) \\ u_y &= u_{init} \sin\left(\frac{2\pi k}{\lambda_0}\right) \\ u_z &= u_{init} \sin\left(\frac{2\pi i}{\lambda_0}\right) \end{aligned} \quad (2.23)$$

where  $\lambda_0 = 1.01L_d/4$ ,  $i = j = k = (1 : L_d)$  (corresponding to  $x$ ,  $y$ , and  $z$ , respectively);  $u_{init} = 5u_K$  is the maximum velocity in the initial distribution;  $L_d$  is the domain edge size;  $u_K$  is the Kolmogorov velocity scale. This flow field is divergence free.

To achieve statistical stationary quantities, it is necessary to run simula-

tions for a longer period of time. Therefore, before injecting the dispersed phase, all simulations have to be conducted long enough to ensure time-invariant statistics. It ensures the full development of single phase turbulent flow [113].

## 2.4 Three-dimensional energy spectrum

According to Kolmogorov’s theory [140], the kinetic energy enters the turbulent flow at the largest scales of motion. With the breakup of eddies, the kinetic energy is continuously transferred to smaller scales until the Kolmogorov scale is reached. At this smallest length scale, the eddy motion is stable because the Reynolds number is sufficiently small, and the kinetic energy is dissipated due to viscous effect. This is also known as ‘energy cascade’. The energy cascade consists of two subranges: inertial subrange and dissipation subrange. In inertial subrange, the viscous effects are negligible, the inertial effect determines the dominant energy transfer from large to small eddies. The energy cascade in this subrange is described by:

$$E(\kappa) = C\varepsilon^{2/3}\kappa^{-5/3} \quad (2.24)$$

where  $C$  is a universal Kolmogorov constant,  $\varepsilon$  is the energy dissipation rate,  $\kappa$  is the wave number. This spectrum is also referred to as the Kolmogorov spectrum. In the dissipation subrange, the viscous effect is dominant, the energy is dissipated.

Here gives the derivation of calculation of three-dimensional energy spectrum. Considering two points  $i$  and  $j$  with distance  $\mathbf{r}$  in Cartesian coordinates,

where  $\mathbf{r}$  is the space vector between two points. The derivation of three dimensional energy spectra calculation presented below is based on [141, 142, 143]. In homogeneous isotropic turbulent flow, the correlation function between velocities of two measured points is given by [141]:

$$R_{ij}(\mathbf{r}) = \langle u_i(\mathbf{x})u_j(\mathbf{x} + \mathbf{r}) \rangle \quad (2.25)$$

where the angle brackets denote ensemble averaging,  $u_i$  and  $u_j$  are velocities at two points,  $\mathbf{x}$  is the location in Cartesian coordinates.

A spectrum is defined as the Fourier transforms of a correlation function. Thus, a pair of forward Fourier transform and inverse Fourier transform is [141]:

$$\tilde{f}(\kappa) = \frac{1}{2\pi} \int_{-\infty}^{\infty} f(r)e^{-i\kappa r} dr \quad (2.26)$$

$$f(r) = \int_{-\infty}^{\infty} \tilde{f}(\kappa)e^{i\kappa r} d\kappa \quad (2.27)$$

A three-dimensional spectrum is  $\Phi_{ij}(\boldsymbol{\kappa})$  calculated as [141]:

$$\Phi_{ij}(\boldsymbol{\kappa}) = \frac{1}{8\pi^3} \iiint_{-\infty}^{\infty} R_{ij}(\mathbf{r})e^{-i\boldsymbol{\kappa}\mathbf{r}} d\mathbf{r} \quad (2.28)$$

where  $\boldsymbol{\kappa} = (\kappa_1, \kappa_2, \kappa_3)$ , and  $\kappa = |\boldsymbol{\kappa}|$ .

Inversely:

$$R_{ij}(\mathbf{r}) = \iiint_{-\infty}^{\infty} e^{i\boldsymbol{\kappa}\mathbf{r}} \Phi_{ij}(\boldsymbol{\kappa}) d\boldsymbol{\kappa} \quad (2.29)$$

When  $i = j$ , we get:

$$R_{ii}(0) = \langle u_i^2 \rangle = \iiint_{-\infty}^{\infty} \Phi_{ii}(\boldsymbol{\kappa}) d\boldsymbol{\kappa} \quad (2.30)$$

The total turbulent kinetic energy  $E_{tke}$  is an integrity of energy spectrum  $E(\kappa)$ . For simplicity, the direction of the Fourier modes is often removed because it has no effect on the calculation. Thus, the length of of the wave number vector instead of the vector itself is used:  $\kappa = |\boldsymbol{\kappa}| = (\kappa_1^2 + \kappa_2^2 + \kappa_3^2)^{1/2}$ . This is obtained by integrating over the spherical shell  $S(\kappa)$ , where  $\kappa$  denotes the radius of the sphere. Figure 2.2 represents the shell of radius  $\kappa$ , the surface denotes the energy spectrum ( $\kappa$ ) of a specific radius  $\kappa$ . Therefore, the total turbulent kinetic energy  $E_{tke}$  is regarded as the sum of various ( $\kappa$ ) which are denoted by diferent surfaces of different radius  $\kappa$ .

Combining with the Equation (2.30), we get:

$$\begin{aligned} E_{tke} &= \int_0^{\infty} E(\kappa) d\kappa \\ &= \frac{1}{2} \langle u_i^2 \rangle \\ &= \iiint_{-\infty}^{\infty} \frac{1}{2} \Phi_{ii}(\boldsymbol{\kappa}) d\boldsymbol{\kappa} \\ &= \int_0^{\infty} \oint \frac{1}{2} \Phi_{ii}(\boldsymbol{\kappa}) dS(\kappa) d\kappa \end{aligned} \quad (2.31)$$

From Equation (2.31), the relationship is obtained:

$$\begin{aligned} E(\kappa) &= \oint \frac{1}{2} \Phi_{ii}(\boldsymbol{\kappa}) dS(\kappa) \\ &= \frac{1}{2} \Phi_{ii}(\boldsymbol{\kappa}) 4\pi\kappa^2 \\ &= 2\pi\kappa^2 \Phi_{ii}(\boldsymbol{\kappa}) \end{aligned} \quad (2.32)$$

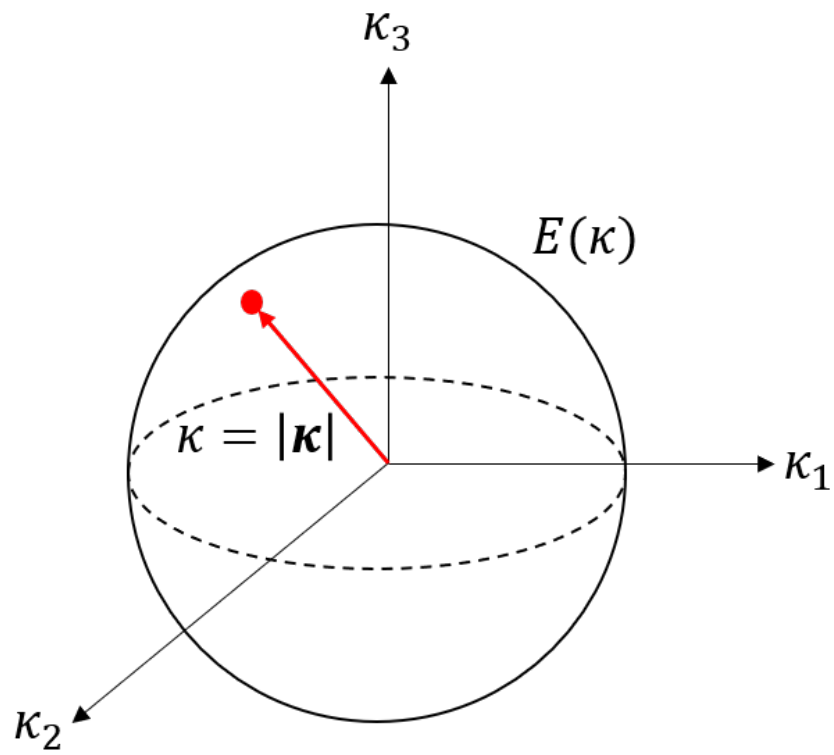


Figure 2.2: Three-dimensional shell ingestion

In Equation (2.31), we can also get:

$$\begin{aligned}
E_{tke} &= \iiint_{-\infty}^{\infty} \frac{1}{2} \Phi_{ii}(\boldsymbol{\kappa}) d\boldsymbol{\kappa} \\
&= \frac{1}{2} \sum_{\boldsymbol{\kappa}} \Phi_{ii}(\boldsymbol{\kappa}) \Delta\kappa_1 \Delta\kappa_2 \Delta\kappa_3
\end{aligned} \tag{2.33}$$

The total turbulent kinetic energy can be also calculated by:

$$\begin{aligned}
E_{tke} &= \sum_{\boldsymbol{\kappa}} E(\boldsymbol{\kappa}) \\
&= \frac{1}{2} \langle \tilde{u}^*(\boldsymbol{\kappa}) \tilde{u}(\boldsymbol{\kappa}) \rangle
\end{aligned} \tag{2.34}$$

Combining with the Equation (2.33) and (2.34), the calculation of  $\Phi_{ii}$  is given (in this study, the interval of wave number is the same):

$$\Phi_{ii} = \frac{\langle \tilde{u}^*(\boldsymbol{\kappa}) \tilde{u}(\boldsymbol{\kappa}) \rangle}{(\Delta\kappa)^3} \tag{2.35}$$

Substitute the Equation (2.35) into Equation (2.32):

$$\begin{aligned}
E(\boldsymbol{\kappa}) &= 2\pi\kappa^2 \Phi_{ii}(\boldsymbol{\kappa}) \\
&= 2\pi\kappa^2 \frac{\langle \tilde{u}^*(\boldsymbol{\kappa}) \tilde{u}(\boldsymbol{\kappa}) \rangle}{(\Delta\kappa)^3}
\end{aligned} \tag{2.36}$$

where  $\tilde{u}^*(\boldsymbol{\kappa})$  is the conjugate of  $\tilde{u}(\boldsymbol{\kappa})$ .

To implement the Equation (2.36) in computer code, a process of three-dimensional energy spectrum calculation is proposed:

1. Transfer the three physical space (in Cartesian coordinates) velocity fields  $u(x, y, z)$ ,  $v(x, y, z)$ ,  $w(x, y, z)$  to Fourier space velocity fields  $\tilde{u}_1(\kappa_1, \kappa_2, \kappa_3)$ ,  $\tilde{u}_2(\kappa_1, \kappa_2, \kappa_3)$ ,  $\tilde{u}_3(\kappa_1, \kappa_2, \kappa_3)$  using Fast Fourier Transfer (FFT), such as the MATLAB function ‘fftn’.

2. Calculate  $\langle \tilde{u}_i(\kappa_1, \kappa_2, \kappa_3) \tilde{u}_i^*(\kappa_1, \kappa_2, \kappa_3) \rangle$ , the angle brackets denote the ensemble average. The ensemble average of a random variable  $x$  is given as  $\langle x \rangle = \frac{1}{V} \sum_{n=1}^V x_n$ . Thus, the  $\langle \tilde{u}_i(\kappa_1, \kappa_2, \kappa_3) \tilde{u}_i^*(\kappa_1, \kappa_2, \kappa_3) \rangle$  of different components are:

$$\frac{\sum_{\kappa_1=1}^N \sum_{\kappa_2=1}^N \sum_{\kappa_3=1}^N \tilde{u}_1(\kappa_1, \kappa_2, \kappa_3) \tilde{u}_1^*(\kappa_1, \kappa_2, \kappa_3)}{(N \times N \times N)^2}$$

$$\frac{\sum_{\kappa_1=1}^N \sum_{\kappa_2=1}^N \sum_{\kappa_3=1}^N \tilde{u}_2(\kappa_1, \kappa_2, \kappa_3) \tilde{u}_2^*(\kappa_1, \kappa_2, \kappa_3)}{(N \times N \times N)^2}$$

$$\frac{\sum_{\kappa_1=1}^N \sum_{\kappa_2=1}^N \sum_{\kappa_3=1}^N \tilde{u}_3(\kappa_1, \kappa_2, \kappa_3) \tilde{u}_3^*(\kappa_1, \kappa_2, \kappa_3)}{(N \times N \times N)^2}$$

where  $N$  is the number of points along the edge of the domain ( $N = 300$  in our case).

3. Establish a Fourier space cube domain, the number allocated to each point along the edge is order in this array:  $R = [0, 1, \dots, N/2, -N/2 + 1, -N/2 + 2, \dots, -1]$ . This order is implemented to generate three dimensional coordinates defined by vectors  $X, Y, Z$  using MATLAB intrinsic function ‘meshgrid’:  $[X, Y, Z] = \text{meshgrid}(R, R, R)$ . Thus a Fourier space length tensor  $r(\kappa_1, \kappa_2, \kappa_3)$  of size  $N^3$  can be obtained in MATLAB, the code is:  $r = \sqrt{(X)^2 + (Y)^2 + (Z)^2}$ .
4. The length of wavenumber is divided into  $N/2$  bins from 1 to  $N/2$ . Therefore, the number of bins used in calculation is  $N/2$ .
5. The wavenumber is  $k_w = [1, N/2] \Delta x$ , where  $\Delta x = 2\pi/L$
6. For the  $p$ th bin, record all locations  $\mathcal{L}(\kappa_1, \kappa_2, \kappa_3)$  of points that satisfy the relationship:

$$r(\kappa_1, \kappa_2, \kappa_3)\Delta x \in \left( \frac{k_w(p-1) + k_w(p)}{2}, \frac{k_w(p) + k_w(p+1)}{2} \right].$$

The number of recorded points is  $\mathcal{N}$ .

7. The energy in each bin  $p$  is

$$E(p) = 2\pi k_w^2 \left( \frac{\sum \tilde{u}_1(\mathcal{L})\tilde{u}_1^*(\mathcal{L})}{N^2} + \frac{\sum \tilde{u}_2(\mathcal{L})\tilde{u}_2^*(\mathcal{L})}{N^2} + \frac{\sum \tilde{u}_3(\mathcal{L})\tilde{u}_3^*(\mathcal{L})}{N^2} \right) / (\mathcal{N}\Delta x^3),$$

where  $p \in [1, N/2]$

8. Plot energy spectrum  $E(p)$  as the function of  $k_w$ .

There are two ways to calculate the turbulent kinetic energy, the first one is calculated from Fourier space velocity field:

$$E_v = \frac{1}{2} \langle \tilde{u}_i(\kappa_1, \kappa_2, \kappa_3) \tilde{u}_i^*(\kappa_1, \kappa_2, \kappa_3) \rangle \quad (2.37)$$

The second one is calculated from the energy spectrum:

$$\begin{aligned} E_e &= \int_0^\infty E(\kappa) d\kappa \\ &= \sum E(\kappa) \Delta\kappa \end{aligned} \quad (2.38)$$

The energy dissipation rate is also calculated in two ways, the first one is the average of local energy dissipation rate of all points:

$$\varepsilon_v = \sum \varepsilon_p / L^3 \quad (2.39)$$

where  $\varepsilon_p$  is the local energy dissipation rate of each point, it is given by [144]:

$$\varepsilon_p = 2\nu \langle S_{ij} S_{ij} \rangle \quad (2.40)$$

where  $\nu$  is the kinematic viscosity of fluid,  $S_{ij}$  is the strain rate[144]:

$$S_{ij} = \frac{1}{2} \left( \frac{\partial u_i}{\partial x_j} + \frac{\partial u_j}{\partial x_i} \right) \quad (2.41)$$

where the velocity gradient tensor is[144]:

$$\frac{\partial u_i}{\partial x_j} = \begin{bmatrix} \frac{\partial u_1}{\partial x_1} & \frac{\partial u_1}{\partial x_2} & \frac{\partial u_1}{\partial x_3} \\ \frac{\partial u_2}{\partial x_1} & \frac{\partial u_2}{\partial x_2} & \frac{\partial u_2}{\partial x_3} \\ \frac{\partial u_3}{\partial x_1} & \frac{\partial u_3}{\partial x_2} & \frac{\partial u_3}{\partial x_3} \end{bmatrix} \quad (2.42)$$

The second way is based on the energy spectrum [140]:

$$\varepsilon_e = \int_0^\infty 2\nu\kappa^2 E(\kappa) d\kappa \quad (2.43)$$

The compensated energy spectrum is [140]:

$$E_c(\kappa) = E(\kappa)\kappa^{5/3}\varepsilon^{-2/3} \quad (2.44)$$

The Kolmogorov hypothesis predicts the  $-5/3$  spectrum in inertial sub-range. This power-law behavior is clearly visualized in the compensated energy spectrum because it is flattened.

The dissipated energy spectrum is [140]:

$$E_d(\kappa) = E(\kappa)\kappa^2\nu \quad (2.45)$$

## 2.5 Visualization method of coherent structures

The visualization and quantification of drop/vortices interaction is a primary source of information for developing the sub-models. The original  $Q$  criterion method transforms a velocity field (vector) to a  $Q$  field (scalar), which is then used to identify and visualize coherent structures. In this method,  $Q$  is defined as the balance between rotation and strain rate [98].

$$Q = \frac{1}{2} (\Omega^2 - S^2) \quad (2.46)$$

where  $\Omega_{ij} = \frac{1}{2} \left( \frac{\partial u_i}{\partial x_j} - \frac{\partial u_j}{\partial x_i} \right)$  is the rotation rate,  $S_{ij} = \frac{1}{2} \left( \frac{\partial u_i}{\partial x_j} + \frac{\partial u_j}{\partial x_i} \right)$  is the strain rate. These are the antisymmetric and symmetric parts of the velocity gradient tensor correspondingly.  $Q$  is defined as the balance between rotation and strain rates [98]. According to Equation (2.46), those areas with positive  $Q$  values have higher rotation rate.

However, sometimes the absolute maximum  $Q$  value is several orders of magnitude larger than the absolute minimum value. The wide range of  $Q$  values decreases the accuracy of visualization. The normalized  $Q_n$  criterion is an advanced method which solves this problem since it removes the effect of order resulted from the wide range of value  $Q$ . In this method,  $Q_n$  is obtained by normalizing  $Q$  with the rotation squared [99].

$$Q_n = \frac{\Omega^2 - S^2}{\Omega^2} \quad (2.47)$$

For a given time instant, the process of extraction of coherent structures

included following steps [97]:

1. Calculate  $Q_n$  values for the entire domain.
2. Set up a threshold value  $Q_{th}$  for the  $Q_n$  field. The selection of the threshold value affects the visualization results. The extracted coherent structures are small if the  $Q_{th}$  is high (close to the maximum  $Q_n$  value). However, a low threshold may make the coherent structures too dense to visualize.
3. Find the maximum  $Q_n$  value and its location. The point with the maximum  $Q_n$  value is regarded as the ‘starting point’ in a structure only if this maximum  $Q_n$  value is larger than the threshold  $Q_{th}$ .
4. Identify all neighboring points from the ‘starting point’, points whose  $Q_n$  values higher than the  $Q_{th}$  are sorted out as in the same structure.
5. Record all points in this structure in another group, then reset all  $Q_n$  values of these points to zero.
6. Repeat steps 3 to 5 until no more structure is extracted. Record the maximum volume of the structure.
7. Set up a volume criterion  $V_{cr}$ . To make the visualization clear, structures smaller than the volume criterion are regarded as noise and are removed. If the structure is larger than or equal to the  $V_{cr}$ , all  $Q_n$  values of the structure will be recorded. Usually, the volume criterion  $V_{cr}$  is set as less than the 4% of the maximum volume of coherent structures  $V_{cr} \leq 4\%V_{max}$  [97].

In Fig. 3.13, the coherent structures of single phase homogeneous isotropic turbulent flow are presented, they are colored by the vorticity magnitude. The maximum  $Q_n$  value of the entire domain is 1 while the maximum unnormalized  $Q$  value calculated by Equation (2.46) is  $1.745 \times 10^{-3}$ . The minimum meaningful  $Q_n$  and  $Q$  values are 0, because only areas with positive values have higher rotation rate.

In this study, a practical identification method is proposed to fulfill the step 4 of the process. The method is explained based on a two-dimensional structure. The three-dimensional structure identification can be achieved by adding one more dimension in the identification process. Before introducing the method, three operations have to be defined. Assume the  $Q_n$  value of point  $\mathcal{P}$  is higher than the threshold value, only the nearest four points surrounding  $\mathcal{P}$  are checked. If a point in the domain has  $Q_n$  value is lower than the threshold value, the point  $\mathcal{P}$  is then recorded as the ‘boundary point’. Assume a ‘moving block’ that only departures from the ‘starting point’ and moves on points one by one along with  $x$  and  $y$  directions; Assume a ‘flag’ on each point, set all ‘flags’ to zero at the beginning.

Fig. 2.3 covers a random complex two-dimensional coherent structure. The ‘starting point’ is marked with a star and with coordinate  $(0, 0)$ . Assume that this is the first structure. The process of two-dimensional structure identification includes the following steps:

1. Beginning from the ‘starting point’, the ‘moving block’ moves to each point one by one along with  $x$  and  $y$  directions. If the  $Q_n$  value on current ‘moving block’ is higher than the threshold value, then judge the value of flag, change the flag of this point to  $\mathcal{I}$  if the flag is zero,

where  $\mathcal{I}$  is the  $\mathcal{I}$ th structure that is under identification; If the flag is not zero, then jump it and moves on the next point. Keep moving until four ‘boundary points’ are recorded.

2. When ‘moving block’ moves on a point that is higher than the threshold and has ‘zero’ flag, check all points along with the direction which is perpendicular to the direction that the ‘moving block’ moves along currently. If the flags of points are zero, then change them to  $\mathcal{I}$ ; if they are not zero, then jump to the next point. This is called ‘perpendicular check’. Finish the ‘perpendicular check’ when two ‘boundary points’ are recorded. Only new ‘boundary points’ are recorded as the new generation ‘boundary points’. This step is regarded as the ‘second layer check’.

In Fig. 2.3, the ‘moving point’ is now at  $(-3, 0)$ . Check all points along  $y$  direction (marked by arrows) until two ‘boundary points’  $(-4, \pm 2)$  are recorded. Now all points between  $(-4, 2)$  and  $(-4, -2)$ ,  $(0, 0)$  and  $(-4, 0)$  have flag ‘1’ because this is the first structure. By the end of step 1 and 2, all ‘boundary points’ that can be recorded are marked as circles in Fig. 2.3, these points are classified as the first generation ‘boundary points’.

3. All this generation ‘boundary points’ are regarded as ‘starting point’, repeat these steps to get further generations of ‘boundary points’ until no more new ‘boundary points’ are found.

In Fig. 2.3, the second generation ‘boundary points’ are marked as triangles. All ‘boundary points’ are found and all flags in the structure are changed to ‘1’ till now. The structure is successfully identified.

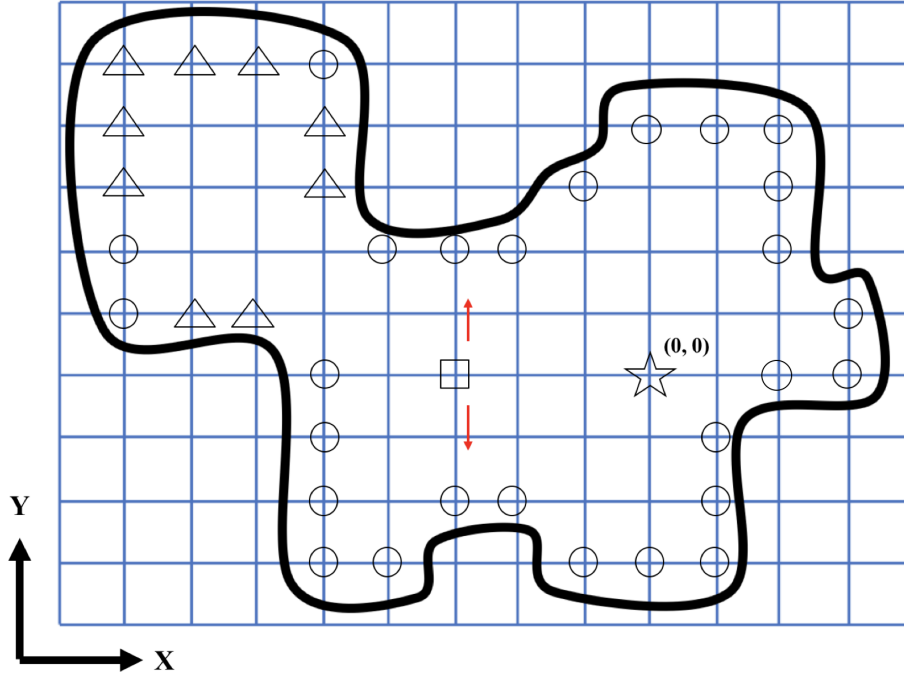


Figure 2.3: A random two-dimensional structure

To extend to the three-dimensional structures extraction, several modifications need to be implemented in the operation definition and identification process that were given above. The number of points which have to be checked to ensure a ‘boundary point’ becomes six; One more direction is added in the movement of ‘moving block’ and ‘perpendicular check’; The number of ‘boundary points’ in steps 1 and 2 are six and four; A further layer check - ‘third layer check’, which is similar to the ‘second layer check’ has to be added following the ‘second layer check’.

The normalized  $Q_n$  criterion extraction method coupled with the identification method described above can obtain coherent structures accurately despite the complexity of the vortices shape. With the unique ‘flag’ on each point, the raw data of exact positions and number of coherent structures are also obtained.

# Chapter 3

## Results and Discussion

In this chapter, results of multiple cases of single-phase and two-phase turbulent flow simulations are presented and discussed. The simulation cases and parameters are summarized in Section 3.1. To investigate statistical characteristics of liquid-liquid turbulent flow, the energy spectra, the probability distribution function (PDF) of vorticity, energy dissipation rate, and eigenvalues of strain tensor of the single-phase flow is discussed in Section 3.2. In Section 3.3, the effect of dispersed phase volume fraction on the energy spectra, PDF of vorticity, energy dissipation rate, and eigenvalues of strain tensor are presented. In Section 3.4, the effect of dispersed phase effect on the energy spectra, PDF of vorticity, energy dissipation rate, and eigenvalues of strain rate are shown. In Section 3.5, coherent structures of single-phase flow, and coherent structures together with the liquid-liquid interface of two-phase flow are given.

### 3.1 Simulation parameters

Three single-phase homogeneous isotropic turbulent flow fields were generated in a fully-periodic cubic domain of size  $L \times L \times L = 300 \times 300 \times 300$  lattice units [lu]. The Kolmogorov length scale  $\eta_K$  is set equal to 1 [lu] for all simulations.

The flow field in conventional mixing devices is very inhomogeneous. This means depending on location in the vessel, the drop will be exposed to different flow conditions. To investigate the behaviour of drop under different turbulent conditions, three cases characterized by different intensity of turbulent flow field were considered. To replicate these flow conditions, three values of relaxation time related to fluid viscosity were selected:  $\tau_c = 0.54, 0.525, 0.5$ . These relaxation times result in different values of viscosity of continuous phase  $\nu_c = c_s^2(\tau_c - 0.5)$ , they were then used in the Equation 2.20. The energy dissipation rate was calculated according to the Kolmogorov correlation [140]  $\varepsilon = \nu_c^3/\eta_K^4$ , where  $\eta_K = 1$  [lu]. The simulation parameters that characterize three turbulent flow fields are shown in Table 3.1.

The turbulent generation approach did not allow to set the volume-averaged root-mean-squared velocity  $u_{rms}$  a priori. For that reason, it was determined as a result of simulation. Based on obtained value, four parameters were calculated: Taylor micro-scale  $\lambda = (15\nu_c u_{rms}^2/\varepsilon)^{1/2}$  [140]; Taylor micro-scale

Table 3.1: Simulation parameters. Lattice units: [lu] - lattice units for length scale; [ts] - time step.

Case #	$\tau_c$	$\nu_c$	$\varepsilon$	$u_{rms}$	$t_K$ , [ts]	$t_{eddy}$ , [ts]	$\lambda$ , [lu]	$Re_\lambda$
Case 1	0.54	$13.3 \cdot 10^{-3}$	$2.4 \cdot 10^{-6}$	$5.1 \cdot 10^{-2}$	75	1102	14.85	56.91
Case 2	0.525	$8.3 \cdot 10^{-3}$	$5.8 \cdot 10^{-7}$	$3.2 \cdot 10^{-2}$	120	1770	14.87	57.07
Case 3	0.51	$3.3 \cdot 10^{-3}$	$3.7 \cdot 10^{-8}$	$1.3 \cdot 10^{-2}$	300	4424	14.91	57.41

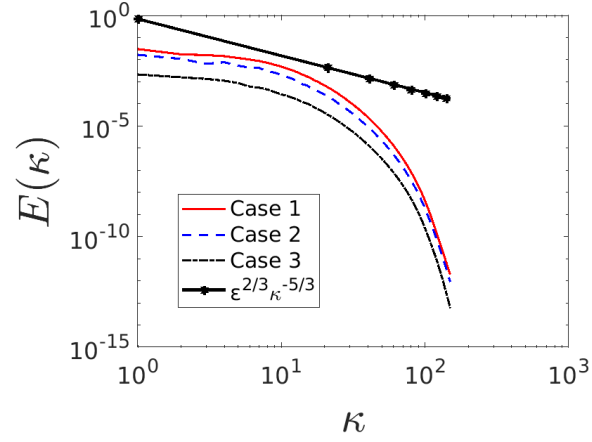
Reynolds number  $Re_\lambda = u_{rms}/\nu_c$ ; Kolmogorov time scale  $t_K = (\nu_c/\varepsilon)^{1/2}$ ; Eddy turnover time  $t_{eddy} = u_{rms}^2/\varepsilon$ . Therefore, for all considered cases,  $\lambda \approx 15$  and  $Re \approx 57$ . Thus parameters are also presented in Table 3.1.

First, a fully-developed turbulent flow field was generated. Then a spherical single mother drop was injected into the flow field of condition Case 2. The size of drop varies to make the dispersed phase volume fraction to be  $\phi = 0.02\%$ ,  $0.05\%$ ,  $3.35\%$ . Further, 382 spherical mother drops were injected into the same flow field, the diameter of each drop was 30 [lu], that makes the dispersed phase volume fraction to be 20%. The effect of dispersed phase viscosity was also investigated by setting the dispersed to continuous phase viscosity ratio to  $\mu_d/\mu_c = 0.1, 1, 10$ .

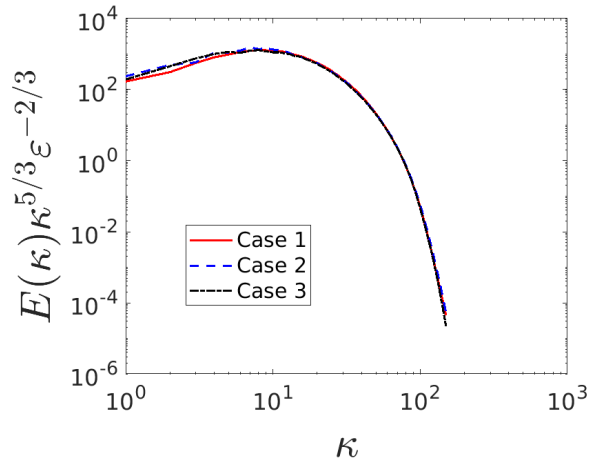
## 3.2 Single phase flow

### 3.2.1 Energy spectra

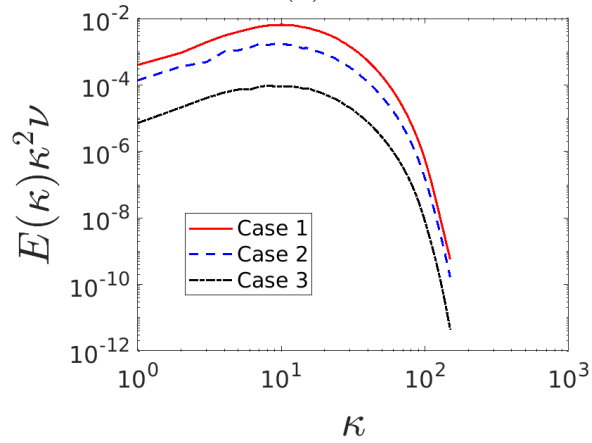
Fig. 3.1 presents the comparison of energy spectra, compensated energy spectra and dissipated energy spectra for Case 1, Case 2 and Case 3. As can be seen from Fig. 3.1(a), the simulation domain of edge length  $L = 300$  [lu] resolves the inertial sub-range in three cases. However, the resolved inertial sub-range in three cases are narrow. The Fig. 3.1(b) highlights this conclusion: by multiplying the energy spectrum by  $\kappa^{5/3}\varepsilon^{-2/3}$ , the curve that denotes inertial sub-range becomes a horizontal line in compensated energy spectra plot. The horizontal region only exists in a range  $8 < \kappa < 10$ . To resolve a wider inertial sub-range, it is necessary to extend the size of the simulation domain. In turn, this will increase the computational cost of DNSs.



(a)



(b)



(c)

Figure 3.1: Energy spectra of single phase turbulent flows at different energy inputs. (a) Energy spectra; (b) Compensated energy spectra; (c) Dissipated energy spectra.

In Fig. 3.1(a) the energy at low wave number (large length scale) is different in three cases. The energy entered turbulence is maximum in Case 1 while is minimum in Case 3. The discrepancy of energy between Case 1 and Case 2 is much smaller than that between Case 2 and Case 3. The energy entered in Case 2 is nearly the same as the energy entered in Case 1. This proves the parameter set in Table 3.1: the energy dissipation rate of Case 1 is 4.1 times larger than that of Case 2 while the energy dissipation rate of Case 2 is 15.7 times larger than that of Case 3. In Fig. 3.1(b), the dissipation  $\varepsilon$  and wave number  $\kappa$  have no effect on the plot, because by scaling with  $\kappa^{5/3}\varepsilon^{-2/3}$ , the relationship is obtained:  $E(\kappa)\kappa^{5/3}\varepsilon^{-2/3} \varepsilon^{2/3}\kappa^{-5/3} = \varepsilon^0\kappa^0$ . Thus, the three curves nearly overlap in the compensated energy spectrum.

In Fig. 3.1(c), the energy of Case 1 dissipated fast at high wave number, meaning that the higher energy input results in higher energy dissipation. By scaled with  $\kappa^2\nu$ , the relationship is obtained:  $E(\kappa)\kappa^2\nu \sim \varepsilon\kappa^{1/3} \sim \nu^3\kappa^{1/3}$ , the Kolmogorov  $-5/3$  law becomes  $1/3$ , the curve that represents the inertial sub-range in the log-log is parallel to the straight line of  $1/3$  slope. The viscosity in Case 1 is 1.6 times larger than that in Case 2, the viscosity in Case 2 is 2.5 times larger than that in Case 3. Due to the relationship of  $\nu^3$  in dissipated energy spectra, the discrepancy between Case 2 and Case 3 is far larger than that between Case 1 and Case 2. As can be seen, at large wave number, the higher energy input flow condition has higher energy dissipation. This supports the conclusion from Fig. 3.1.

It is also noticed that there is minor difference in these plots for a given time instant and the time-averaged data. Thus the energy spectra presented here are based on one time instant.

The turbulent kinetic energy calculated by Equation (2.37) and (2.38), as

Table 3.2: Turbulent kinetic energy and average energy dissipation rate calculated by different methods.

Case #	$E_v$	$E_e$	$\varepsilon_v$	$\varepsilon_e$	$\varepsilon$
Case 1	$3.5 \cdot 10^{-3}$	$3.1 \cdot 10^{-3}$	$1.6 \cdot 10^{-6}$	$2.3 \cdot 10^{-6}$	$2.4 \cdot 10^{-6}$
Case 2	$1.7 \cdot 10^{-3}$	$1.5 \cdot 10^{-3}$	$4.0 \cdot 10^{-7}$	$5.8 \cdot 10^{-7}$	$5.8 \cdot 10^{-7}$
Case 3	$2.5 \cdot 10^{-4}$	$2.2 \cdot 10^{-4}$	$2.4 \cdot 10^{-8}$	$3.5 \cdot 10^{-8}$	$3.7 \cdot 10^{-8}$

well as the average energy dissipation rate calculated by Equation (2.39) and (2.43) in three cases are given in Table. 3.2.  $E_v$  and  $E_e$  are the velocity-based and energy spectrum-based turbulent kinetic energy;  $\varepsilon_v$  and  $\varepsilon_e$  are the velocity-based and energy spectrum-based average energy dissipation rate.

As can be seen, the turbulent kinetic energy obtained from the velocity field and energy spectrum are not exactly the same, the one from velocity field is larger. For the average energy dissipation rate, the one obtained from energy spectrum is larger than that from velocity field. Compared to the energy dissipation rate  $\varepsilon$ , the results from energy spectrum are closer to these values.

### 3.2.2 Vorticity

Vortex is to be observed as an rotational region around a core. The concept of vorticity proposed to describe a vortex was defined as the curl of velocity ( $\omega = \nabla \times v$ ). The vorticity was calculated using the MATLAB intrinsic function ‘curl’. Fig. 3.2 represents the probability density function (PDF) of vorticity in single phase turbulent flows of three energy inputs. The calculation of vorticity was implemented for each lattice cube, thus, a three-dimensional vorticity magnitude field of  $300^3$  values was obtained. For a continuous variable  $X$ , the probability density function  $f(x)$  satisfies the relationship  $\int f(x)dx = 1$ .

Therefore, the probability density function for discrete random variable is  $p(x_i) = \frac{n_i}{N\delta x}$ , where  $n_i$  is the number of variable at  $x_i$ ,  $N$  is the total number of variable,  $\delta x$  is the step between  $x_i$  and  $x_{i+1}$ . The probability density function reveals the distribution of the variable.

As can be seen from the Fig. 3.2, the maximum density of vorticity in Case 1, Case 2, and Case 3 are 74, 120, and 305, respectively. Therefore, with the increase of energy input, the maximum density of vorticity decreases. The maximum density of vorticity in Case 3 is 2.5 times of that in Case 2, and the maximum density of vorticity in Case 2 is 1.6 times of that in Case 1.

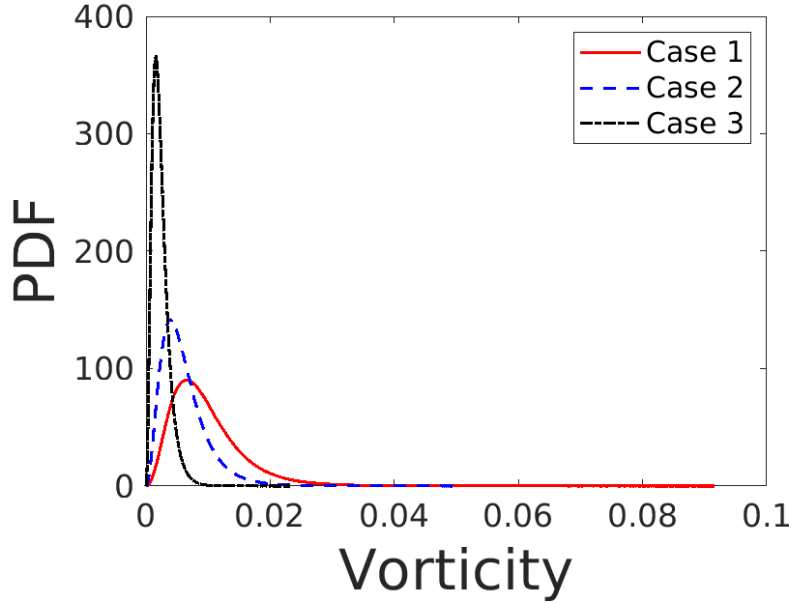


Figure 3.2: PDF of vorticity in single phase turbulent flows of different energy inputs

The increase of energy input also results in the increase of distribution of vorticity, i.e. the distribution of vorticity is wider. It validates the energy spectra in Fig. 3.1: for a given wave number (vortex of a given length scale), the vortex in larger energy input flow condition contains more energy because

the vorticity is higher.

### 3.2.3 Local energy dissipation rate

The energy dissipation rate reveals the rate at which the turbulent kinetic energy is transferred into thermal energy with the dissipation of small eddies [140]. The calculation is given from Equation (2.40) to (2.42). Fig. 3.3 represents the normalized PDF of energy dissipation rate in single phase turbulent flows of different energy inputs at one time instant. The energy dissipation rate of each lattice cube is calculated and normalized by the average dissipation rate of the corresponding case listed in Table. 3.1. For example, the curve that denotes flow condition of Case 1 is obtained by scaling with the average dissipation rate of Case 1 in Table. 3.1.

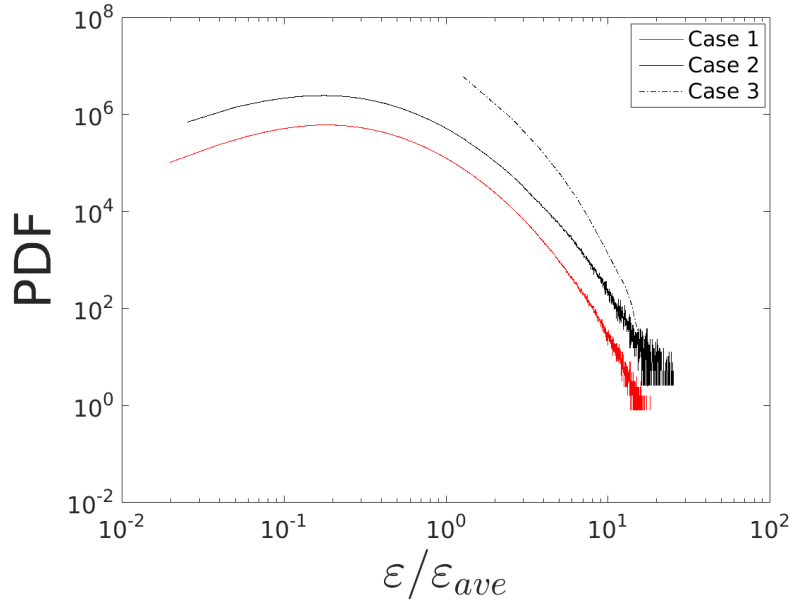


Figure 3.3: PDF of normalized energy dissipation rate in single phase turbulent flows of different energy inputs

As can be seen in the Fig. 3.3, in the Case 1 and Case 2, most of the

normalized energy dissipation rates in the region are smaller than the average energy dissipate rate  $\varepsilon_{ave}$ . The increase of energy input results in the decrease of PDF of normalized energy dissipation rate. Further, both the maximum and minimum values of normalized energy dissipation rate are smaller in the higher energy input case. The PDF of  $\varepsilon/\varepsilon_{ave}$  decreases at higher normalized dissipation rate, finally, the PDF oscillates at a specific state. For example, in Case 1, the PDF reaches the maximum value at  $\varepsilon/\varepsilon_{ave} = 0.18$ , then it decreases from  $5.98 \times 10^5$  to 1, finally, the PDF oscillates around 1. The distribution of  $\varepsilon/\varepsilon_{ave}$  is more discrete at higher value region.

### 3.2.4 Eigenvalues of strain tensor

The velocity gradient tensor given in the Equation (2.42) can be decomposed into a symmetric strain tensor and an antisymmetric rotation tensor. The vorticity in Section 3.2.2 describes the rotation rate of particles related to the rotation tensor. In this section, the eigenvalues of strain tensor are studied to reveal the compression and stretching. The strain tensor  $s_{ij}$  is given by:

$$s_{ij} = \frac{1}{2} \begin{bmatrix} \frac{\partial u_1}{\partial x_1} + \frac{\partial u_1}{\partial x_1} & \frac{\partial u_1}{\partial x_2} + \frac{\partial u_2}{\partial x_1} & \frac{\partial u_1}{\partial x_3} + \frac{\partial u_3}{\partial x_1} \\ \frac{\partial u_1}{\partial x_2} + \frac{\partial u_2}{\partial x_1} & \frac{\partial u_2}{\partial x_2} + \frac{\partial u_2}{\partial x_2} & \frac{\partial u_2}{\partial x_3} + \frac{\partial u_3}{\partial x_2} \\ \frac{\partial u_1}{\partial x_3} + \frac{\partial u_3}{\partial x_1} & \frac{\partial u_2}{\partial x_3} + \frac{\partial u_3}{\partial x_2} & \frac{\partial u_3}{\partial x_3} + \frac{\partial u_3}{\partial x_3} \end{bmatrix}$$

The eigenvalues of each strain tensor are calculated. The negative eigenvalue  $\lambda_1$  is most compressive while the positive eigenvalue  $\lambda_3$  is the most stretching, the eigenvalue  $\lambda_2$  between  $\lambda_1$  and  $\lambda_3$  is either compressive or stretching [145].

The eigenvalues of strain tensor are calculated using MATLAB 2017 in-

trinsic function ‘eig’ for each lattice cube. Fig. 3.4 represents the PDF of eigenvalues of strain tensor of single phase turbulent flows of different energy inputs, the red curves denote flow condition Case 1, blue curves denote flow condition Case 2, and black curves denote flow condition Case 3; the dashed curves represent eigenvalue  $\lambda_1$  (negative eigenvalue), solid curves represent eigenvalues  $\lambda_2$ , and dash-dot curves represent eigenvalues  $\lambda_3$  (positive eigenvalue),  $\lambda_1 < \lambda_2 < \lambda_3$ .

As can be seen, in higher energy input flow condition, the distribution of eigenvalues is wider. The increase of energy input results in the density decrease of  $\lambda_1$ , increase of  $\lambda_2$  and  $\lambda_3$ . Therefore, in higher energy input flow, the flow field is more stretching than compressive.

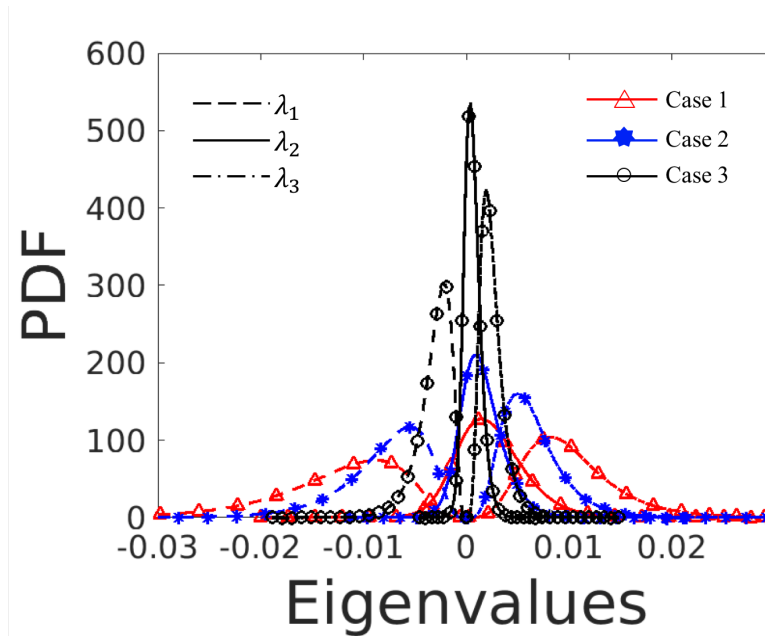


Figure 3.4: PDF of eigenvalues of strain tensor of single phase turbulent flows of different energy inputs

## 3.3 Effect of dispersed phase volume fraction

### 3.3.1 Energy spectra

In Fig. 3.5, the energy spectra for a single phase flow as well as for the cases with different values of dispersed phase volume fraction  $\phi$  in the flow condition Case 2 are shown. The spherical drop of different sizes are injected into the flow Case 2 to reach the different dispersed phase volume fraction  $\phi = 0.02\%$ ,  $0.05\%$ ,  $3.35\%$  and  $20\%$ . For the larger dispersed phase volume fraction, the energy at high wave number (small length scale) is larger. In Fig. 3.5(a), the energy of  $\phi = 20\%$  at high wave number is around  $10^5$  larger than the energy of single-phase flow. Therefore, the presence of deformable liquid-liquid interface promotes the energy dissipation. This is more clear in Fig. 3.5(b): the increase of dispersed phase volume fraction results in larger energy dissipation rate. The similar conclusion was found in [146], which was a study of solid-liquid dispersion: the larger dispersed phase volume fraction led to a higher turbulent energy at high wave number, it is accompanied by an increase of energy dissipation rate.

However, the slight decrease of energy in the inertial sub-range resulted by the increase of dispersed phase volume fraction is noticed. The energy of the condition  $\phi = 20\%$  around low wave number  $\kappa = 10$  is the minimum among different dispersed phase volume fraction cases. Therefore, in higher dispersed volume fraction case, the energy covered by different size eddies is distributed more uniformly. This conclusion is also supported by Fig. 3.5(c).

Another important finding of this work is that the implementation of MRT mitigated the artificial significant ( $10^{10} - 10^{12}$ ) energy gain at high wave numbers reported earlier [113]. This energy gain is obvious when the velocity at

the diffuse interface is of order equals to the spurious velocity that represents a numerical peculiarity of diffuse interface methods including LBM. Therefore, by implementing the MRT collision operator, the magnitude of physical velocity becomes larger than the spurious velocity.

### 3.3.2 Vorticity

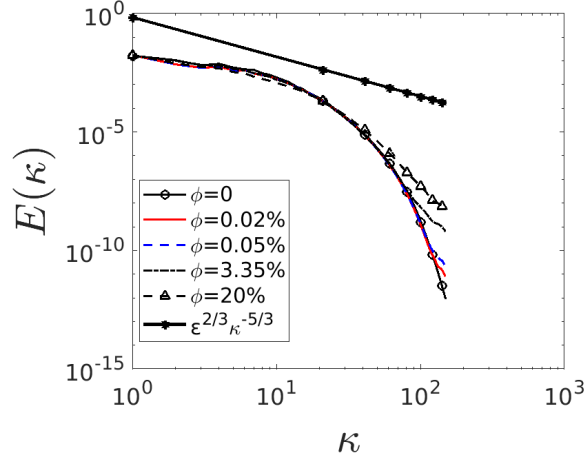
Fig. 3.6 represents the PDF of vorticity in two phase turbulent flows of different dispersed phase volume fraction. The increase of dispersed phase volume fraction results in the increase of density of distribution at lower vorticity (around 0) and decrease of density of distribution at higher vorticity (larger than  $3 \times 10^{-3}$ , smaller than  $-3 \times 10^{-3}$ ). Therefore, in high dispersed phase volume fraction case, the average vorticity magnitude of flow field is smaller.

### 3.3.3 Local energy dissipation rate

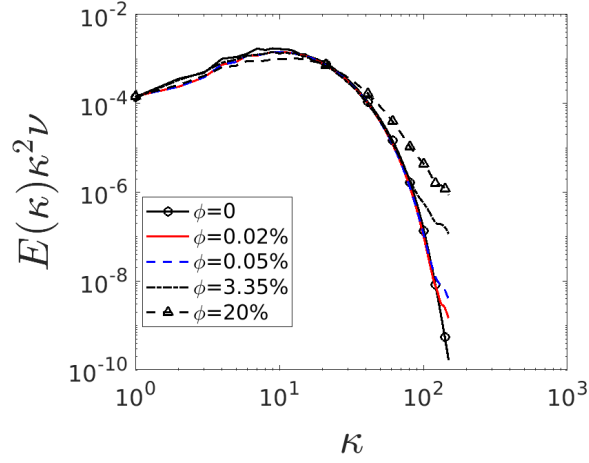
Fig. 3.7 gives the PDF of normalized energy dissipation rate in two phase turbulent flows of different dispersed phase volume, the energy dissipation rate for each lattice cube in domain is calculated and normalized by the average dissipation rate of Case 2 ( $\varepsilon_{ave} = 5.8 \times 10^{-7}$ ).

In the Fig. 3.7, the maximum PDF of  $\varepsilon/\varepsilon_{ave}$  is  $2.4 \times 10^6$  around  $\varepsilon/\varepsilon_{ave} = 0.18$  in drop-free turbulence, the maximum PDF of  $\varepsilon/\varepsilon_{ave}$  is  $3.5 \times 10^6$  around  $\varepsilon/\varepsilon_{ave} = 0.11$  in turbulence with  $\phi = 20\%$ . Therefore, the increase of liquid-liquid interface results in the increase of the maximum PDF of  $\varepsilon/\varepsilon_{ave}$ , and the decrease of value of  $\varepsilon/\varepsilon_{ave}$  that has the maximum PDF.

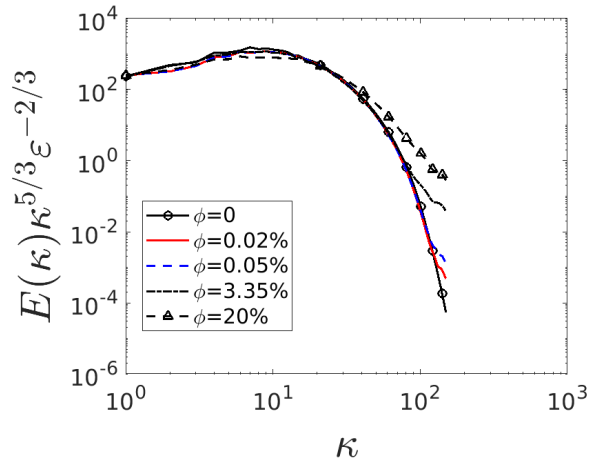
However, the increase of dispersed phase volume fraction results in the decrease of PDF at higher value of the normalized energy dissipation rate



(a)



(b)



(c)

Figure 3.5: Energy spectra of two-phase turbulent flows of different dispersed phase volume fraction in Case 2. (a) Energy spectra; (b) Dissipated energy spectra; (c) Compensated energy spectra.

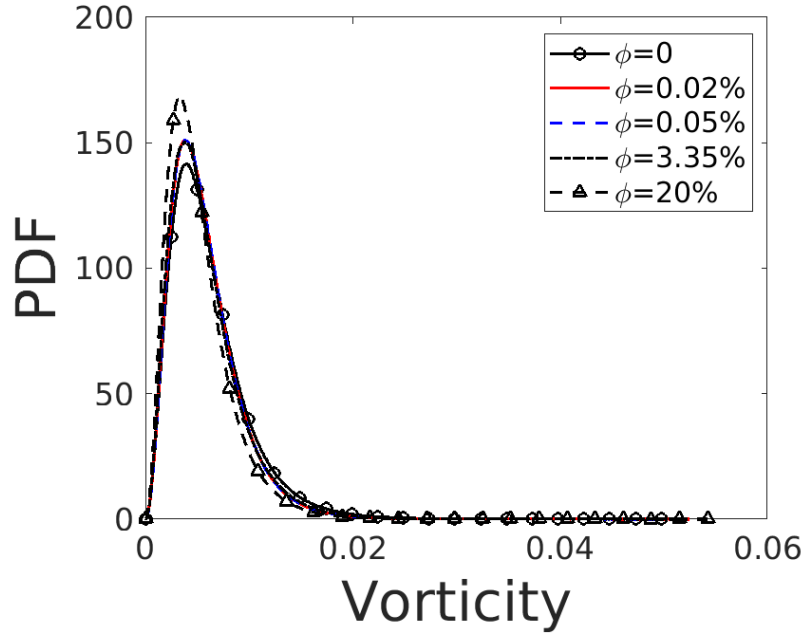


Figure 3.6: PDF of vorticity in two phase turbulent flows of different dispersed phase volume fraction in Case 2

( $\varepsilon/\varepsilon_{ave} > 0.38$ ). For example, at  $\varepsilon/\varepsilon_{ave} = 2$ , the PDF of  $\varepsilon/\varepsilon_{ave}$  equals to  $1.05 \times 10^5$  in  $\phi = 0$  while equals to  $5.73 \times 10^4$  in  $\phi = 0.20\%$ .

### 3.3.4 Eigenvalues of strain tensor

Fig. 3.8 represents the PDF of eigenvalues of strain tensor of single phase and two phase turbulent flows of different dispersed phase volume fraction, the black curves denote the case  $\phi = 0$  (single phase), red curves denote the case  $\phi = 0.02\%$ , blue curves denote the case  $\phi = 0.05\%$ , green curves denote the case  $\phi = 3.35\%$ , magenta curves denote the case  $\phi = 20\%$ ; the dashed curves represent eigenvalue  $\lambda_1$ , solid curves represent eigenvalues  $\lambda_2$ , and dash-dot curves represent eigenvalues  $\lambda_3$ ,  $\lambda_1 < \lambda_2 < \lambda_3$ .

As can be seen, the increase of dispersed phase volume fraction results

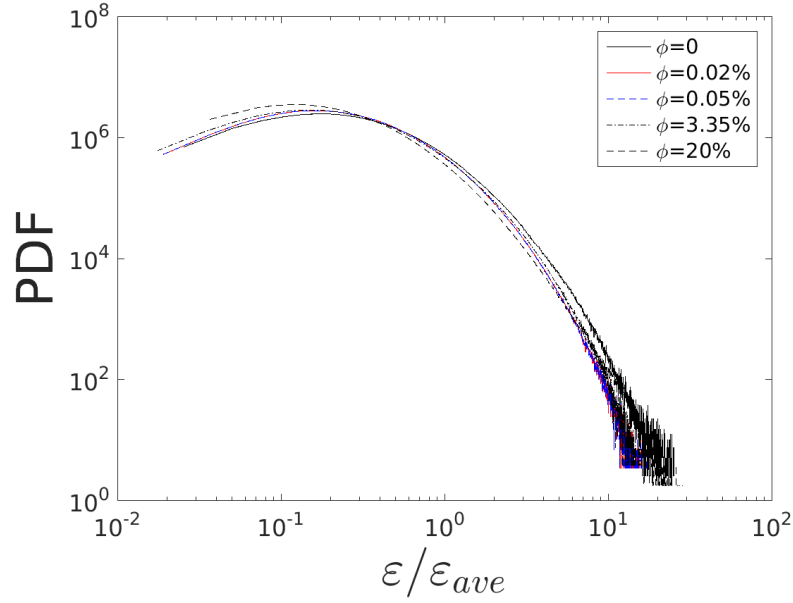


Figure 3.7: PDF of normalized energy dissipation rate in two phase turbulent flows of different dispersed phase volume fraction in Case 2

in the increase of the maximum probability density, and the increase of  $\lambda_1$ , decrease of  $\lambda_2$  as well as  $\lambda_3$ . This reveals that the increase of liquid-liquid interface boosts the compression.

## 3.4 Effect of dispersed phase viscosity

### 3.4.1 Energy spectra

The energy spectra in the flow condition Case 2 with different viscosity ratios  $\mu_d/\mu_c = 0.1, 1, 10$  at dispersed phase volume fraction  $\phi = 0.05\%$  are presented in Fig. 3.9. As is shown in Fig. 3.9(a) and (c), the change of viscosity ratio has no effect on the inertial sub-range. However, at high wave number, the small scale eddies in large viscosity ratio case contain less energy, the increase of dispersed phase viscosity suppresses dissipation rate.

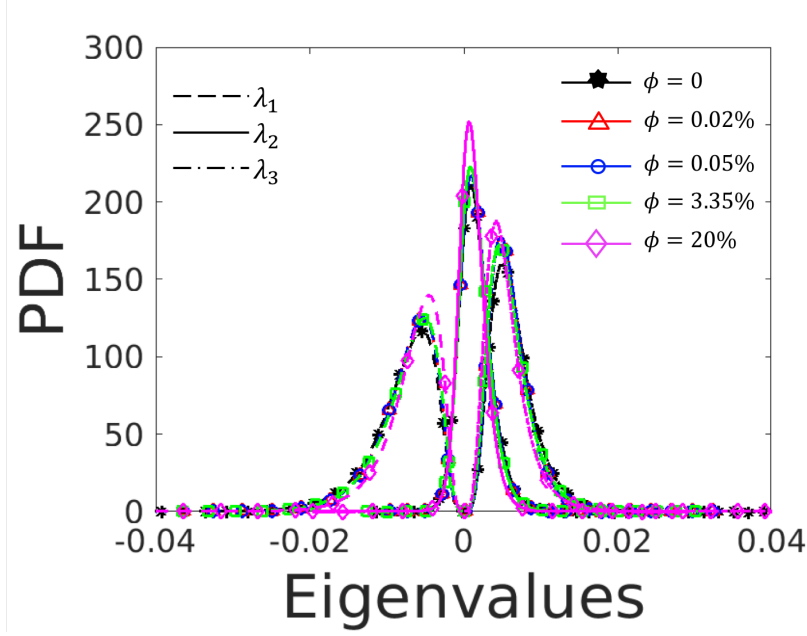


Figure 3.8: PDF of eigenvalues of strain tensor of single phase and two phase turbulent flows of different dispersed phase volume fraction in Case 2

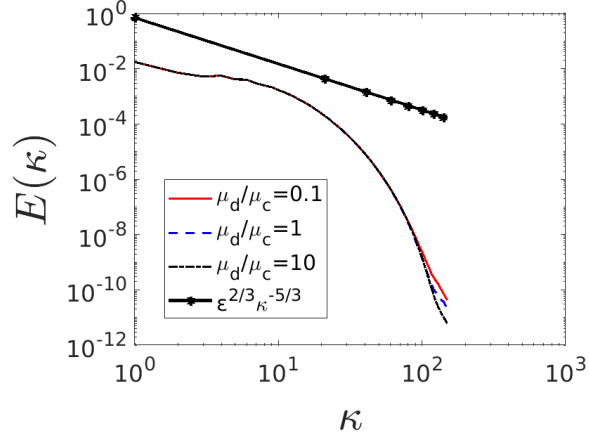
### 3.4.2 Vorticity

Fig. 3.10 represents the PDF of vorticity in two phase turbulent flows of different viscosity ratio, the viscosity ratio  $\mu_d/\mu_c$  is 0.1, 1, and 10. As can be seen, the change of viscosity nearly has no effect on the PDF of vorticity: the maximum is 125.5 in the case  $\mu_d/\mu_c = 1$ , 122.3 in the cases  $\mu_d/\mu_c = 0.1$  and  $\mu_d/\mu_c = 10$ .

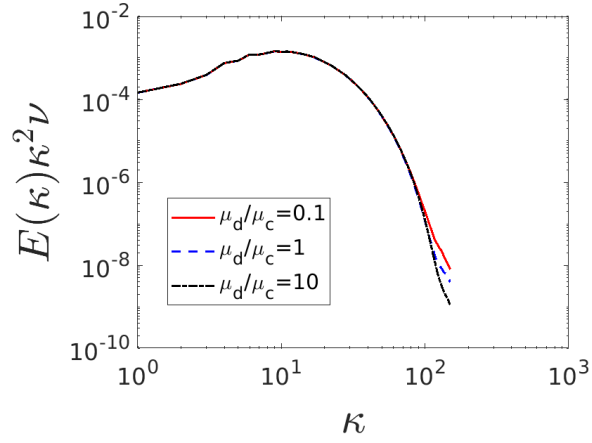
### 3.4.3 Local energy dissipation rate

Fig. 3.11 gives the PDF of normalized energy dissipation rate in two phase turbulent flows of different viscosity ratio, the energy dissipation rate of each lattice cube in domain is calculated and normalized by the average dissipation rate of Case 2 ( $\varepsilon_{ave} = 5.8 \times 10^{-7}$ ).

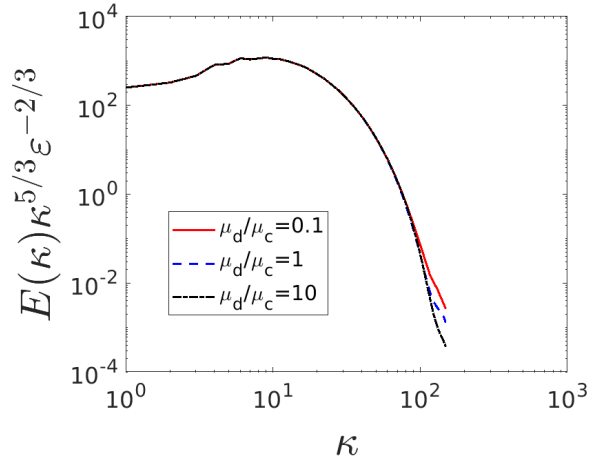
As can be seen, the maximum PDF is  $2.63 \times 10^6$ , it occurs around  $\varepsilon/\varepsilon_{ave} =$



(a)



(b)



(c)

Figure 3.9: Energy spectra of two-phase turbulent flows of different viscosity ratio at  $\phi = 0.05\%$  in Case 2. (a) Energy spectra; (b) Dissipated energy spectra; (c) Compensated energy spectra.

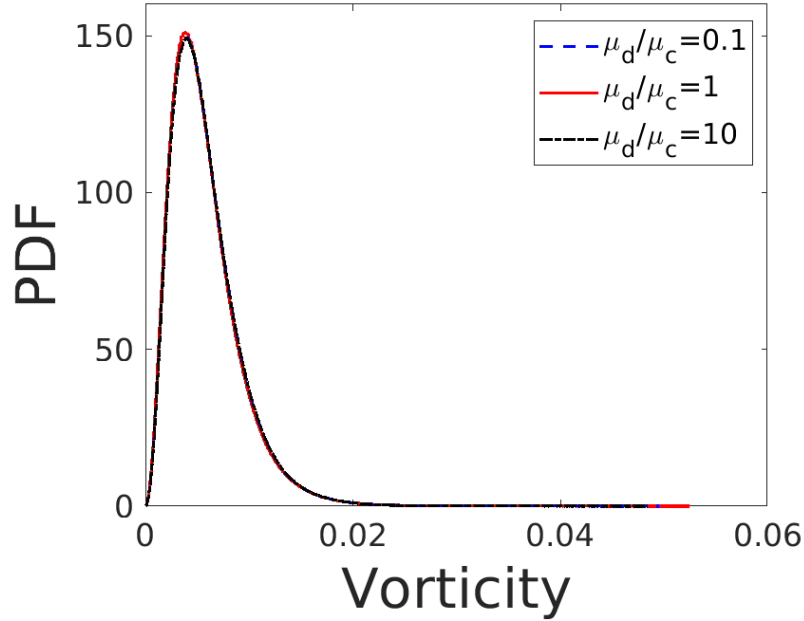


Figure 3.10: PDF of vorticity in two phase turbulent flows of different viscosity ratio at  $\phi = 0.05\%$  in Case 2

0.18 in three viscosity ratios cases. It is noticed that the variance of viscosity ratio  $\mu_d/\mu_c$  has no obviously influence on the PDF of normalized energy dissipation rate.

### 3.4.4 Eigenvalues of strain tensor

Fig. 3.12 represents the PDF of eigenvalues of strain tensor of two phase turbulent flows of different viscosity ratio  $\mu_d/\mu_c$ , the red curves denote the case  $\mu_d/\mu_c = 0.1$ , the blue curves denote the case  $\mu_d/\mu_c = 1$ , the black curves denote the case  $\mu_d/\mu_c = 10$ ; the dashed curves represent eigenvalue  $\lambda_1$ , solid curves represent eigenvalues  $\lambda_2$ , and dash-dot curves represent eigenvalues  $\lambda_3$ ,  $\lambda_1 < \lambda_2 < \lambda_3$ . As can be seen, the variance of viscosity ratio nearly results in no variance of PDF of eigenvalues. Thus, both the compression and stretching

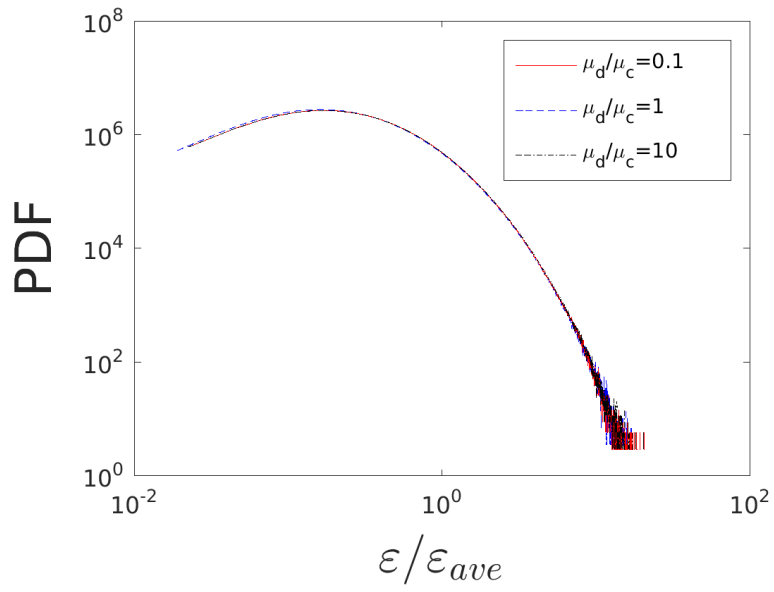


Figure 3.11: PDF of normalized energy dissipation rate in two phase turbulent flows of different viscosity ratio at  $\phi = 0.05\%$  in Case 2

are impervious from the variance of viscosity.

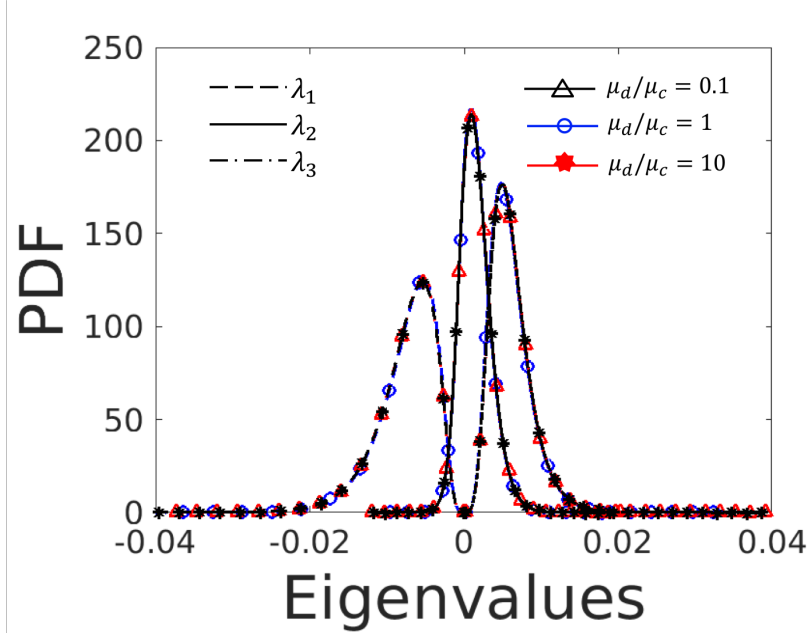


Figure 3.12: PDF of eigenvalues in two phase turbulent flows of different viscosity ratio at  $\phi = 0.05\%$  in Case 2

## 3.5 Coherent structures

### 3.5.1 Single-phase flow

In normalized  $Q_n$  criterion, the selection of threshold value  $Q_{th}$  and cutoff volume  $V_{cr}$  is important because it directly affects the extraction of coherent structures. Therefore, the effects of  $Q_{th}$  and  $V_{cr}$  are investigated on the flow condition of Case 2.

Fig. 3.13 presents coherent structures extracted under different  $Q_{th}$  in Case 2, the structures are colored by vorticity magnitude ( $\|\nabla \times u\|$ ). This figure reveals the effect of  $Q_{th}$ . In Table 3.3, the parameters and results of coherent structures under effect of  $Q_{th}$  were listed.

$V_{cr}$  is the cutoff volume,  $V_{max}$  is the volume of the maximum structure.  $N$  is the number of coherent structures in the domain. As can be seen, the increase

Table 3.3: Parameters and results of coherent structures under effect of  $Q_{th}$ .  $N$  is the number of structures;  $V_{max}$  is the volume of the maximum structure.

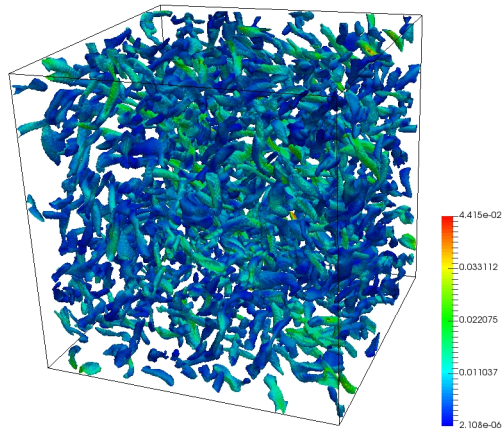
Figure #	$Q_{th}$	$V_{cr}/V_{max}$	$N$	$V_{max}$
Figure 3.13(a)	0.8		688	10162
Figure 3.13(b)	0.85	4%	778	5784
Figure 3.13(c)	0.9		879	2470

of  $Q_{th}$  results in the increase of the number of structures and decrease of the size of structures. The color remains the same in three sub-figures because the change of  $Q_{th}$  has no influence on the vorticity field.

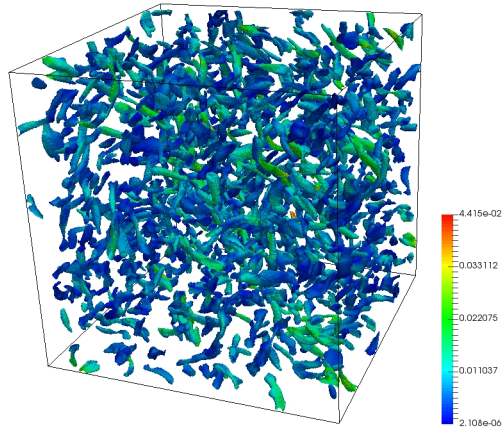
Therefore,  $Q_{th}$  should be carefully selected. If  $Q_{th}$  is large (close to 1), the size of structures will be small. It results in the lack of information in visualization, for example, part of important vortices maybe neglected; if  $Q_{th}$  is too small, the structures will be too dense to visualize. When  $Q_{th} = 0.8$ , the total volume of extracted coherent structures is 4.1% of the volume of the domain, it matches the published result [97]. Thus, in this study,  $Q_{th} = 0.8$  is regarded as a suitable threshold value for visualization.

Fig. 3.14 gives coherent structures extracted under the same  $Q_{th}$ , but the noises are removed under different  $V_{cr}$ . The structures are colored by vorticity magnitude ( $\|\nabla \times u\|$ ). In Table 3.4, the parameters and results of coherent structures under effect of  $V_{cr}$  were listed.

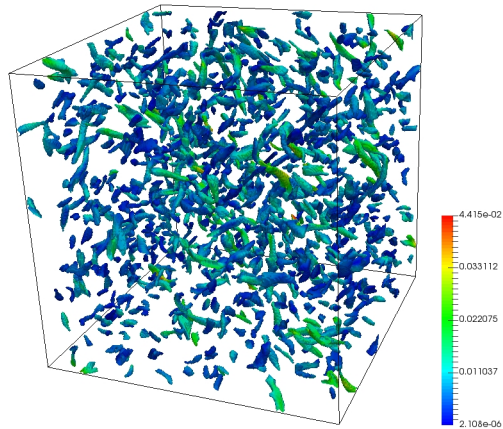
As can be seen, the increases of  $V_{cr}$  results in the decrease of the number of structures. Only 20% of number of structures remain when the  $V_{cr}$  is increased from 0 to 2% of the largest structure, but 62% of number of structures are left when the  $V_{cr}$  is increased from 2% to 4% of the largest structure. Therefore, the deduction of noise is more obvious at the beginning of increase of  $V_{cr}$ . With the increase of  $V_{cr}$ , the deduction of noise becomes weak. It is because the



(a)



(b)



(c)

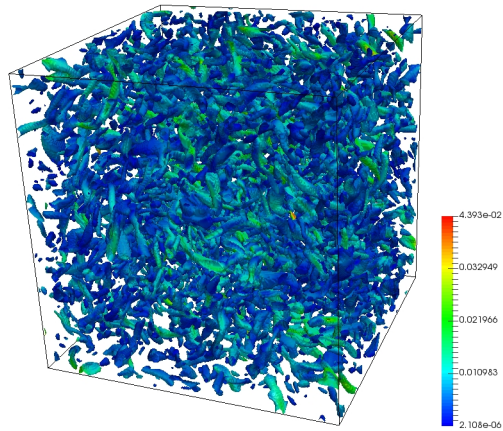
Figure 3.13: Coherent structures of different threshold  $Q_{th}$  extracted in Case 2. (a)  $Q_{th} = 0.8, V_{cr}/V_{max} = 4\%$ ; (b)  $Q_{th} = 0.85, V_{cr}/V_{max} = 4\%$ ; (c)  $Q_{th} = 0.9, V_{cr}/V_{max} = 4\%$ .

Table 3.4: Parameters and results of coherent structures under effect of  $V_{cr}$ .  $N$  is the number of structures;  $V_{max}$  is the volume of the maximum structure.

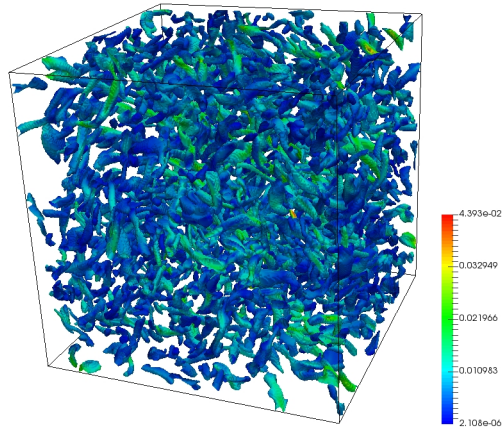
Figure #	$Q_{th}$	$V_{cr}/V_{max}$	$N$	$V_{max}$
Figure 3.14(a)		0	5521	
Figure 3.14(b)	0.8	2%	1114	10162
Figure 3.14(c)		4%	688	

noises are successfully removed. The cutoff volume  $V_{cr} = 4\%V_{max}$  is regarded as a suitable value.

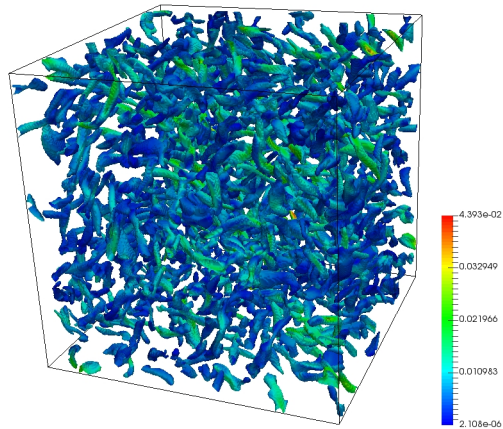
In Fig. 3.15, coherent structures of different cases and the corresponding probability distribution function (PDF) of volume-equivalent diameters are presented. In Table 3.5, the parameters and results of coherent structures of different flow conditions were listed.  $V_{cst}$  is the total volume of all coherent structures,  $V_t$  is the volume of domain. The volume-equivalent diameter of each structure is calculated by  $d_e = \left(\frac{6V_{cs}}{\pi}\right)^{1/3}$ , where  $V_{cs}$  is the volume of the structure. In Fig. 3.15(a), (c), (e), the coherent structures are colored by the vorticity magnitude ( $\|\nabla \times u\|$ ). As can be seen, the decrease of energy input results in the decrease of vorticity magnitude. It can be also concluded that in Case 1 and Case 2, the number of structures and the volume of the largest structure are respectively the same. It is attributed to the little difference in energy input in Case 1 and Case 2 represented in Fig. 3.1(a). In Fig. 3.15(b), (d), (f), all bins are of the same width. The volume-equivalent diameter of structures in Case 3 is larger than that in Case 1 and 2. Therefore, the lower energy input results in the decrease of the number structures and increase of the size of structures. The assumption is that in a lower energy input flow condition, the flow is less turbulent, from Fig. 3.1(c) the dissipation rate is less, the vortices remain large size, thus the number of structures is small. To



(a)



(b)



(c)

Figure 3.14: Coherent structures of different volume criterion  $V_{cr}$ . (a)  $Q_{th} = 0.8, V_{cr}/V_{max} = 0\%$ ; (b)  $Q_{th} = 0.8, V_{cr}/V_{max} = 2\%$ ; (c)  $Q_{th} = 0.8, V_{cr}/V_{max} = 4\%$ .

Table 3.5: Parameters and results of coherent structures of different flow conditions.  $N$  is the number of structures;  $V_{max}$  is the volume of the maximum structure;  $V_{cst}$  is the total volume of all structures;  $V_t$  is the volume of the domain.

Figure #	$Q_{th}$	$V_{cr}/V_{max}$	$N$	$V_{max}$	$V_{cst}/V_t$
Figure 3.15(a)	0.8	4%	686	13882	4.1%
Figure 3.15(c)			688	10162	4.3%
Figure 3.15(e)			363	25937	3.4%

the contrary, a flow field with larger energy input is more turbulent, from Fig. 3.1(c) we know the dissipation rate is larger, the vortices in flow field tend to break up into smaller vortices, it leads to the large number and small size of structures.

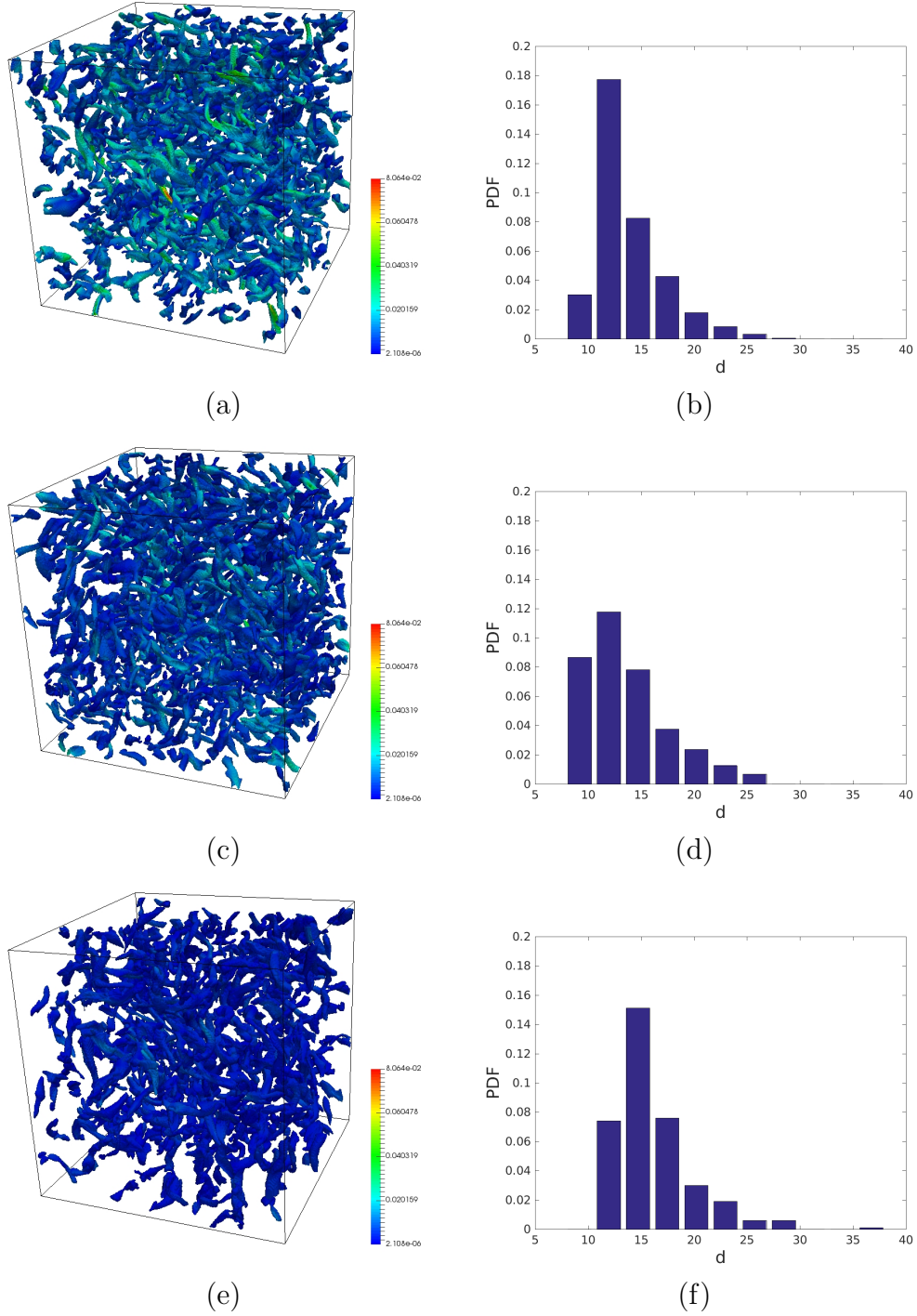


Figure 3.15: Coherent structures and corresponding PDF of volume-equivalent diameter.  $Q_{th} = 0.8, V_{cr}/V_{max} = 4\%$ . (a) Coherent structures of Case 1; (b) PDF of volume-equivalent diameter of Case 1; (c) Coherent structures of Case 2; (d) PDF of volume-equivalent diameter of Case 2; (e) Coherent structures of Case 3; (f) PDF of volume-equivalent diameter of Case 3.

### 3.5.2 Two-phase flow

Visualization of turbulent flow field together with the liquid-liquid interface provides valuable information on how drop/vortices interaction occurs. The most commonly used assumption in breakup models is that only vortices of the size equal to or less than the drop size are responsible for drop breakup.

In Fig. 3.16, drop/coherent structures and the corresponding PDF of the volume-equivalent diameter of structures are presented. The results are presented for two time instances: the first one  $t = 10t_K$  stands for the state just before the breakup, and the second state  $t = 15t_k$  is after drop disintegration, where  $t_K$  is the Kolmogorov time scale. The liquid-liquid interface is colored by a solid color (gray), and coherent structures are colored by vorticity magnitude. The threshold value  $Q_{th} = 0.8$  together with the cutoff volume  $V_{cr} = 4\%V_{max}$  makes the total volume of extracted coherent structures to be 4.3% of the simulation domain. This volume of structures ensures the clearance of visualization.

The number of coherent structures in Fig. 3.16(a) and (c) are 714 and 700, respectively. Thus, there is no obvious difference in numbers of structures. The PDF of volume-equivalent diameter of structures is calculated by  $d_e = \left(\frac{6V_{cs}}{\pi}\right)^{1/3}$ , where  $V_{cs}$  is the volume of the structure. As can be seen from Fig. 3.16(b) and (d), the size of structures slightly decreases after the breakup of a drop. The turbulent kinetic energy of extracted coherent structures is 4.07% and 4.05% of the total kinetic energy in Fig. 3.16(a) and (c). This phenomenon is explained by the Kolmogorov hypothesis that energy transforms to a smaller scale with the breakup of vortices. The most volume-equivalent diameter of coherent structures is equal to or smaller than 15 [lu], which is also close to

the Taylor micro-scale given in Table 3.1. The injected mother drop had a diameter of 30 [lu], which was larger than the vortices. After the breakup, the daughter drops that did not drop again were smaller than the vortices. Therefore, this result validates the general assumption that only vortices of size equal to or smaller than drop size are responsible for the breakup event.

Our results also indicate that not a single but multiple vortices interact with the drop at the same time. This interaction was revealed when a mother drop was injected into turbulent flows: a breakup of the drop took place.

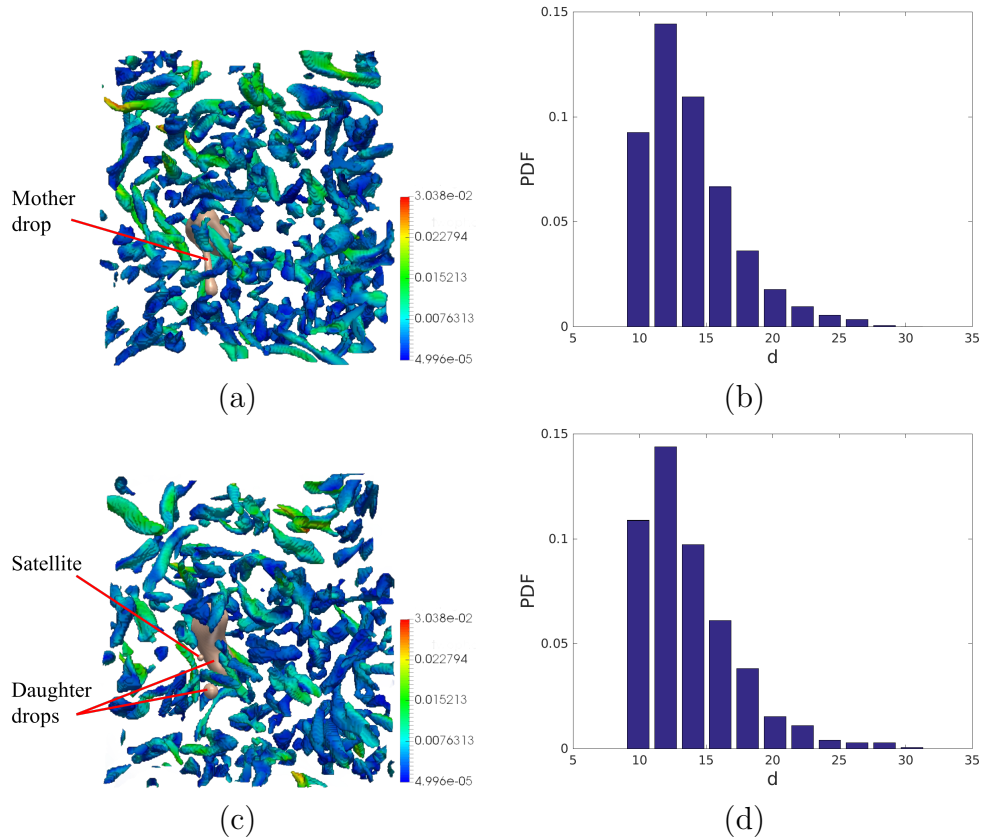


Figure 3.16: Drop/coherent structures and corresponding PDF of volume-equivalent diameter in Case 2 at different time instants.  $Q_{th} = 0.8$ ,  $V_{cr}/V_{max} = 4\%$ . (a) Drop/coherent structures at  $t/t_K = 10$ ; (b) PDF of volume-equivalent diameter at  $t/t_K = 10$ ; (c) Drop/coherent structures at  $t/t_K = 15$ ; (d) PDF of volume-equivalent diameter at  $t/t_K = 15$ .

# Chapter 4

## Conclusions

Liquid-liquid dispersions generated by the agitation of two immiscible liquids are of great importance in chemical and petroleum industries, pharmacy, biology, food, and cosmetics. In these multi-phase systems, the drop size distribution (DSD) of the dispersed phase defines dispersion properties. For that reason, the ability to predict and control the DSD is crucial. One of the modeling approaches used to estimate the DSD is based on the solution of population balance equations (PBEs). The persistent limitation of this approach is that the results heavily rely on the choice of breakup and coalescence models (kernels). In this study, direct numerical simulations (DNSs) are used to study a single drop behavior in homogeneous isotropic turbulence to understand the mechanisms of drop breakup. The results are necessary to develop well-grounded sub-models that can be incorporated into PBE modeling and improve its reliability.

In this study, three single phase flow conditions of different energy input were investigated in a three-dimensional cubic domain of size  $300^3$  [lu]. Then a spherical drop of different sizes was injected into the flow of con-

dition Case 2 to reach the different dispersed phase volume fraction  $\phi = 0, 0.02\%, 0.05\%, 3.35\%, 20\%$ . This is fulfilled to study the effect of dispersed phase volume fraction. the density and viscosity of drop are set to be the same with density and viscosity of continuous phase. Further, the dispersed phase to continuous phase viscosity ratio  $\mu_d/\mu_c$  is set as 0.1, 1, and 10 to explore the effect of viscosity ratio under condition  $\phi = 0.05\%$  in Case 2.

In the energy spectra of these single phase and two phase turbulent flow conditions, the inertial sub-range is observed to be resolved in the simulation domain. The increase of energy input, the increase dispersed phase volume fraction, as well as the decrease of viscosity ratio can promote the energy dissipation rate at high wave number. The increase of dispersed phase volume fraction can also makes the distribution of energy contained by eddies more uniform.

In the PDF of vorticity, as can be seen, the increase of energy input results in the increase of vorticity magnitude in flow field, the increase of dispersed phase volume fraction results in the decrease of vorticity magnitude, the variance of viscosity does not change the PDF of vorticity. Combined with the conclusion about energy dissipation rate at high wave number, it is assumed that the variance of ability at which the turbulent kinetic energy is transferred into thermal energy has no relevance on the variance of PDF of vorticity.

In the PDF of normalized energy dissipation rate, the increase of energy input results in the decrease of the probability density of normalized dissipation rate. The introduction of drop increases the PDF of normalized dissipation rate at low rate region: the maximum probability density increases from  $2.4 \times 10^6$  to  $3.5 \times 10^6$  with the increase of  $\phi$  from 0 to 20%. At high rate region, the probability density in high dispersed phase volume fraction is smaller. As for

the viscosity ratio, the effect on PDF of normalized energy dissipation rate is not obvious.

In the PDF of eigenvalues of strain tensor, both the increase of energy input, and the decrease of dispersed phase volume fraction can result in the decrease of the negative eigenvalue  $\lambda_1$ , as well as the increase of middle eigenvalue  $\lambda_2$  and positive eigenvalue  $\lambda_3$ , they promote the stretching. The variance of viscosity ratio does not change the PDF of eigenvalues.

Coherent structures are extracted by the normalized  $Q_n$  criterion. The effect of threshold value  $Q_{th}$  and the cutoff volume  $V_{cr}$  were investigated. It is found that the increase of  $Q_{th}$  results in the increase of number of structures and decrease of size of structures, the increase of  $V_{cr}$  results in the decrease of the small structures, the deduction of noise is obvious at the beginning of the increase of  $V_{cr}$ , the deduction effect is recessionary with the continuous increase of  $V_{cr}$ . The combination of  $Q_{th} = 0.8$  and  $V_{cr}/V_{max} = 4\%$  is found to be a suitable group for extraction of all cases in this study. This combination of parameter ensures that the extracted volume of structures is enough for visualization, and prevents a overcrowd visualization.

The coherent structures in three cases of different energy input are extracted, the corresponding PDF of volume-equivalent diameter reveals that the lower energy input results in the larger size of structures.

A general assumption in breakup models is that only vortices of size equal to or smaller than the drop size are responsible for breakup event. To verify the assumption, the liquid-liquid interface together with coherent structures at the time instants right before and after breakup are tracked and extracted, the corresponding PDF of volume-equivalent diameter is also given. The simulation results reveal that the coherent structures are all of size equal to or

smaller than the drop size, the assumption is validated in this study.

The development of tools for this study is based on Fortran 90 and MATLAB 2017. In Fortran 90, the MRT collision operator is implemented for the lattice Boltzmann method. In MATLAB 2017, the program of the normalized  $Q_n$  criterion coupled with the newly designed boundary identification method is created; the calculation of three-dimensional energy spectra is also fulfilled in MATLAB 2017. Besides, other analysis tools of statistical characteristics of liquid-liquid turbulent flow are developed relying on the interaction of Fortran 90 and MATLAB 2017. The visualization is finished in Paraview. These tools improve the stability of generation of turbulence, provide analysis and visualization of drop/vortex interaction as well as the statistical characteristics of turbulence. They are significant for the later use in the breakup kernel development for PBE.

# Chapter 5

## Future work

In this study, several numerical tools to analyze large-scale sets of data were developed. Together with the DNSs approach, this framework is a strong foundation to study fundamentals of drop breakup in turbulent flow and extraction of information relevant for breakup models.

Further comprehension of interaction between vortices and drop is needed. In this study, coherent structures of the entire flow field and liquid-liquid interface are presented for the preliminary understanding of interaction between vortices. In the future, more attention can be paid to coherent structures that close to the drop. Further, the time evolution of important coherent structures close to the drop also deserves an observation.

Deeper investigation of statistical characteristics of liquid-liquid turbulent flow is necessary. Besides the visualization of breakup event and vortices/drop interaction, the analysis of statistical characteristics such as the correlation of transversal and longitudinal velocity provides a quantitative description and comprehension of the binary system.

Finally, the development of more efficient analysis tools is recommended.

For example, it takes hours to extract coherent structures for only one case in this study. Due the large amount of data generated by DNS, the program for analysis and visualization has to work faster in order to investigate more cases from different aspects.

# Bibliography

- [1] K Bäumlér, M Wegener, AR Paschedag, and E Bänsch. Drop rise velocities and fluid dynamic behavior in standard test systems for liquid/liquid extraction—experimental and numerical investigations. *Chem. Eng. Sci.*, 66(3):426–439, 2011.
- [2] MA Farajzadeh, M Bahram, S Zorita, and BG Mehr. Optimization and application of homogeneous liquid–liquid extraction in preconcentration of copper (II) in a ternary solvent system. *J. Hazard. Mater.*, 161(2-3): 1535–1543, 2009.
- [3] F Pena-Pereira, I Lavilla, and C Bendicho. Miniaturized preconcentration methods based on liquid–liquid extraction and their application in inorganic ultratrace analysis and speciation: A review. *Spectrochim. Acta, Part B*, 64(1):1–15, 2009.
- [4] D Attwood. *Surfactant systems: their chemistry, pharmacy and biology*. Springer Science & Business Media, 2012.
- [5] PG Mazzola, AM Lopes, FA Hasmann, AF Jozala, TCV Penna, PO Magalhaes, CO Rangel-Yagui, and JA Pessoa. Liquid–liquid extraction of

- biomolecules: an overview and update of the main techniques. *J. Chem. Technol. Biotechnol.*, 83(2):143–157, 2008.
- [6] SC Cunha and JO Fernandes. Quantification of free and total bisphenol A and bisphenol B in human urine by dispersive liquid–liquid microextraction (DLLME) and heart-cutting multidimensional gas chromatography–mass spectrometry (MD–GC/MS). *Talanta*, 83(1): 117–125, 2010.
- [7] Gh Bahrami, SH Mirzaeei, and A Kiani. Determination of acyclovir in human serum by high-performance liquid chromatography using liquid–liquid extraction and its application in pharmacokinetic studies. *J. Chromatogr. B*, 816(1-2):327–331, 2005.
- [8] S Liu, Q Li, and Y Shao. Electrochemistry at micro-and nanoscopic liquid/liquid interfaces. *Chem. Soc. Rev.*, 40(5):2236–2253, 2011.
- [9] C Bora and SK Dolui. Fabrication of polypyrrole/graphene oxide nanocomposites by liquid/liquid interfacial polymerization and evaluation of their optical, electrical and electrochemical properties. *Comput. Theor. Polym. Sci.*, 53(4):923–932, 2012.
- [10] G Herzog, V Kam, and DWM Arrigan. Electrochemical behaviour of haemoglobin at the liquid/liquid interface. *Electrochim. Acta*, 53(24): 7204–7209, 2008.
- [11] AG Volkov. *Liquid interfaces in chemical, biological and pharmaceutical applications*. CRC Press, 2001.
- [12] H Kuramochi, K Maeda, S Kato, M Osako, K Nakamura, and S Sakai.

Application of UNIFAC models for prediction of vapor-liquid and liquid-liquid equilibria relevant to separation and purification processes of crude biodiesel fuel. *Fuel*, 88(8):1472–1477, 2009.

- [13] AA Hyman, CA Weber, and F Jülicher. Liquid-liquid phase separation in biology. *Annu. Rev. Cell Dev. Biol.*, 30:39–58, 2014.
- [14] KAP Colati, GP Dalmaschio, EVR de Castro, AO Gomes, BG Vaz, and W Romão. Monitoring the liquid/liquid extraction of naphthenic acids in brazilian crude oil using electrospray ionization FT-ICR mass spectrometry (ESI FT-ICR MS). *Fuel*, 108:647–655, 2013.
- [15] L Yang, BJ Azzopardi, A Belghazi, and S Nakanishi. Phase separation of liquid-liquid two-phase flow at a T-junction. *AIChE J.*, 52(1):141–149, 2006.
- [16] AZ Hezave, S Dorostkar, S Ayatollahi, M Nabipour, and B Hemmateenejad. Investigating the effect of ionic liquid (1-dodecyl-3-methylimidazolium chloride ([C12mim][Cl])) on the water/oil interfacial tension as a novel surfactant. *Colloids Surf., A*, 421:63–71, 2013.
- [17] X Wen, Q Yang, Z Yan, and Q Deng. Determination of cadmium and copper in water and food samples by dispersive liquid-liquid microextraction combined with UV-vis spectrophotometry. *Microchem. J.*, 97(2):249–254, 2011.
- [18] H Abdolmohammad-Zadeh and GH Sadeghi. Combination of ionic liquid-based dispersive liquid-liquid micro-extraction with stopped-flow spectrofluorometry for the pre-concentration and determination of alu-

- minum in natural waters, fruit juice and food samples. *Talanta*, 81(3): 778–785, 2010.
- [19] P Viñas, N Campillo, I López-García, and M Hernández-Córdoba. Dispersive liquid–liquid microextraction in food analysis. a critical review. *Anal. Bioanal. Chem.*, 406(8):2067–2099, 2014.
- [20] X Jia, Y Han, C Wei, T Duan, and H Chen. Speciation of mercury in liquid cosmetic samples by ionic liquid based dispersive liquid–liquid microextraction combined with high-performance liquid chromatography-inductively coupled plasma mass spectrometry. *J. Anal. At. Spectrom.*, 26(7):1380–1386, 2011.
- [21] N Cabaleiro, I De La Calle, C Bendicho, and I Lavilla. Current trends in liquid–liquid and solid–liquid extraction for cosmetic analysis: a review. *Anal. Methods*, 5(2):323–340, 2013.
- [22] N Memon, MI Bhangar, and MY Khuhawer. Determination of preservatives in cosmetics and food samples by micellar liquid chromatography. *J. Sep. Sci.*, 28(7):635–638, 2005.
- [23] B Khan, X Qiao, and LS Lee. Stereoselective sorption by agricultural soils and liquid–liquid partitioning of trenbolone ( $17\alpha$  and  $17\beta$ ) and tren-dione. *Environ. Sci. Technol.*, 43(23):8827–8833, 2009.
- [24] A Bidari, MR Ganjali, P Norouzi, MRM Hosseini, and Y Assadi. Sample preparation method for the analysis of some organophosphorus pesticides residues in tomato by ultrasound-assisted solvent extraction followed by dispersive liquid–liquid microextraction. *Food Chem.*, 126(4):1840–1844, 2011.

- [25] Q Wu, X Zhou, Y Li, X Zang, C Wang, and Z Wang. Application of dispersive liquid–liquid microextraction combined with high-performance liquid chromatography to the determination of carbamate pesticides in water samples. *Anal. Bioanal. Chem.*, 393(6-7):1755–1761, 2009.
- [26] VA Atiemo-Obeng, SM Kresta, and EL Paul. *Handbook of Industrial Mixing*. John Wiley & Sons, Incorporated, 2004.
- [27] F Valenzuela, C Fonseca, C Basualto, O Correa, C Tapia, and J Sapag. Removal of copper ions from a waste mine water by a liquid emulsion membrane method. *Miner. Eng.*, 18(1):33–40, 2005.
- [28] D Maggioris, A Goulas, AH Alexopoulos, EG Chatzi, and C Kiparissides. Prediction of particle size distribution in suspension polymerization reactors: effect of turbulence nonhomogeneity. *Chem. Eng. Sci.*, 55(20):4611–4627, 2000.
- [29] AW Nienow, MF Edwards, and N Harnby. *Mixing in the process industries*. Butterworth-Heinemann, 1997.
- [30] PA Zapata, J Faria, MP Ruiz, RE Jentoft, and DE Resasco. Hydrophobic zeolites for biofuel upgrading reactions at the liquid–liquid interface in water/oil emulsions. *JACS*, 134(20):8570–8578, 2012.
- [31] M Djenouhat, O Hamdaoui, M Chiha, and MH Samar. Ultrasonication-assisted preparation of water-in-oil emulsions and application to the removal of cationic dyes from water by emulsion liquid membrane: Part 1: Membrane stability. *Sep. Purif. Technol.*, 62(3):636–641, 2008.
- [32] S Crossley, J Faria, M Shen, and DE Resasco. Solid nanoparticles that

- catalyze biofuel upgrade reactions at the water/oil interface. *Science*, 327(5961):68–72, 2010.
- [33] PS Nigam and A Singh. Production of liquid biofuels from renewable resources. *Prog. Energy Combust. Sci.*, 37(1):52–68, 2011.
- [34] B Berge. Liquid lens technology: principle of electrowetting based lenses and applications to imaging. In *Micro Electro Mechanical Systems, 2005. MEMS 2005. 18th IEEE International Conference on*, pages 227–230. IEEE, 2005.
- [35] L Dong, AK Agarwal, DJ Beebe, and H Jiang. Adaptive liquid microlenses activated by stimuli-responsive hydrogels. *Nature*, 442(7102):551, 2006.
- [36] M Gharehbaghi and F Shemirani. A novel method for dye removal: ionic liquid-based dispersive liquid-liquid extraction (IL-DLLE). *CLEAN–Soil, Air, Water*, 40(3):290–297, 2012.
- [37] A Soto, A Arce, and MK Khoshkbarchi. Partitioning of antibiotics in a two-liquid phase system formed by water and a room temperature ionic liquid. *Sep. Purif. Technol.*, 44(3):242–246, 2005.
- [38] NB Raikar, SR Bhatia, MF Malone, and MA Henson. Experimental studies and population balance equation models for breakage prediction of emulsion drop size distributions. *Chem. Eng. Sci.*, 64(10):2433–2447, 2009.
- [39] J Lovick, AA Mouza, SV Paras, GJ Lye, and P Angeli. Drop size distribution in highly concentrated liquid–liquid dispersions using a light

- back scattering method. *J. Chem. Technol. Biotechnol.*, 80(5):483–601, 2005.
- [40] S Maaß, F Metz, T Rehm, and M Kraume. Prediction of drop sizes for liquid-liquid systems in stirred slim reactors-Part I: Single stage impellers. *Open Chem. Eng. J. Open*, 162(2):792–801, 2010.
- [41] CW Angle and HA Hamza. Predicting the sizes of toluene-diluted heavy oil emulsions in turbulent flow Part 2: Hinze-Kolmogorov based model adapted for increased oil fractions and energy dissipation in a stirred tank. *Chem. Eng. Sci.*, 61(22):7325–7335, 2006.
- [42] SN Maindarkar, H Hoogland, and MA Henson. Predicting the combined effects of oil and surfactant concentrations on the drop size distributions of homogenized emulsions. *Colloids Surf., A*, 467:18–30, 2015.
- [43] S Maaß, N Paul, and M Kraume. Influence of the dispersed phase fraction on experimental and predicted drop size distributions in breakage dominated stirred systems. *Chem. Eng. Sci.*, 76:140–153, 2012.
- [44] JO Hinze. Fundamentals of the hydrodynamic mechanism of splitting in dispersion processes. *AIChE J.*, 1(3):289–295, 1955.
- [45] GI Taylor. The formation of emulsions in definable fields of flow. *Proc. R. Soc. London, Ser. A, Containing Papers of a Mathematical and Physical Character*, 146(858):501–523, 1934.
- [46] GE Charles and SG Mason. The coalescence of liquid drops with flat liquid/liquid interfaces. *Journal of Colloid Science*, 15(3):236–267, 1960.

- [47] AE Handlos and T Baron. Mass and heat transfer from drops in liquid-liquid extraction. *AIChE J.*, 3(1):127–136, 1957.
- [48] M Ashar, D Arlov, F Carlsson, F Innings, and R Andersson. Single droplet breakup in a rotor-stator mixer. *Chem. Eng. Sci.*, 181:186–198, 2018.
- [49] S Maaß and M Kraume. Determination of breakage rates using single drop experiments. *Chem. Eng. Sci.*, 70:146–164, 2012.
- [50] C Ortiz-Dueñas, J Kim, and EK Longmire. Investigation of liquid-liquid drop coalescence using tomographic PIV. *Exp. Fluids*, 49(1):111–129, 2010.
- [51] FJE Svensson and A Rasmuson. PIV measurements in a liquid-liquid system at volume percentages up to 10% dispersed phase. *Exp. Fluids*, 41(6):917–931, 2006.
- [52] BO Hasan. Breakage of drops and bubbles in a stirred tank: A review of experimental studies. *Chin. J. Chem. Eng.*, 25(6):698–711, 2017.
- [53] D Cheng, X Feng, J Cheng, and C Yang. Numerical simulation of macro-mixing in liquid–liquid stirred tanks. *Chem. Eng. Sci.*, 101:272–282, 2013.
- [54] Y Zhao, X Li, J Cheng, C Yang, and Z Mao. Experimental study on liquid–liquid macromixing in a stirred tank. *Ind. Eng. Chem. Res.*, 50(10):5952–5958, 2011.
- [55] M Jahoda, M Moštěk, A Kukuková, and V Machoň. CFD modelling of

- liquid homogenization in stirred tanks with one and two impellers using large eddy simulation. *Chem. Eng. Res. Des.*, 85(5):616–625, 2007.
- [56] Feng Wang and Zai-Sha Mao. Numerical and experimental investigation of liquid- liquid two-phase flow in stirred tanks. *Industrial & engineering chemistry research*, 44(15):5776–5787, 2005.
- [57] Y Yu, H Chen, Y Liu, VSJ Craig, C Wang, LH Li, and Y Chen. Superhydrophobic and superoleophilic porous boron nitride nanosheet/polyvinylidene fluoride composite material for oil-polluted water cleanup. *Adv. Mater. Interfaces*, 2(1):1400267, 2015.
- [58] BV Balakin, AC Hoffmann, and P Kosinski. Coupling STAR-CD with a population-balance technique based on the classes method. *Powder Technol.*, 257:47–54, 2014.
- [59] A Vikhansky and A Splawski. Adaptive multiply size group method for CFD-population balance modelling of polydisperse flows. *Can. J. Chem. Eng.*, 93(8):1327–1334, 2015.
- [60] A Buffo, M Vanni, DL Marchisio, and RO Fox. Multivariate quadrature-based moments methods for turbulent polydisperse gas–liquid systems. *Int. J. Multiphase Flow*, 50:41–57, 2013.
- [61] A Amokrane, S Charton, N Sheibat-Othman, J Becker, JP Klein, and F Puel. Development of a CFD-PBE coupled model for the simulation of the drops behaviour in a pulsed column. *Can. J. Chem. Eng.*, 92(2): 220–233, 2014.

- [62] Z Li, J Kessel, G Grünewald, and M Kind. Coupled CFD-PBE simulation of nucleation in fluidized bed spray granulation. *Drying Technol.*, 31(15):1888–1896, 2013.
- [63] H Zhang, K Zhang, and S Fan. CFD simulation coupled with population balance equations for aerated stirred bioreactors. *Eng. Life Sci.*, 9(6): 421–430, 2009.
- [64] DL Wright, R McGraw, and DE Rosner. Bivariate extension of the quadrature method of moments for modeling simultaneous coagulation and sintering of particle populations. *J. Colloid Interface Sci.*, 236(2): 242–251, 2001.
- [65] IT Cameron, FY Wang, CD Immanuel, and F Stepanek. Process systems modelling and applications in granulation: A review. *Chem. Eng. Sci.*, 60(14):3723–3750, 2005.
- [66] DD Eberl, DE Kile, and VA Drits. On geological interpretations of crystal size distributions: Constant vs. proportionate growth. *Am. Mineral.*, 87(8-9):1235–1241, 2002.
- [67] HC Schwarzer, F Schwertfirm, M Manhart, HJ Schmid, and W Peukert. Predictive simulation of nanoparticle precipitation based on the population balance equation. *Chem. Eng. Sci.*, 61(1):167–181, 2006.
- [68] SM Iveson. Limitations of one-dimensional population balance models of wet granulation processes. *Powder Technol.*, 124(3):219–229, 2002.
- [69] H Briesen. Simulation of crystal size and shape by means of a reduced

- two-dimensional population balance model. *Chem. Eng. Sci.*, 61(1):104–112, 2006.
- [70] T Wang, J Wang, and Y Jin. Population balance model for gas- liquid flows: Influence of bubble coalescence and breakup models. *Ind. Eng. Chem. Res.*, 44(19):7540–7549, 2005.
- [71] M Vanni. Approximate population balance equations for aggregation–breakage processes. *J. Colloid Interface Sci.*, 221(2):143–160, 2000.
- [72] MM Attarakih, HJ Bart, and NM Faqir. Numerical solution of the bivariate population balance equation for the interacting hydrodynamics and mass transfer in liquid–liquid extraction columns. *Chem. Eng. Sci.*, 61(1):113–123, 2006.
- [73] T Wang, J Wang, and Y Jin. A CFD-PBM coupled model for gas-liquid flows. *AIChE J.*, 52(1):125–140, 2006.
- [74] CD Immanuel and FJ Doyle III. Solution technique for a multi-dimensional population balance model describing granulation processes. *Powder Technol.*, 156(2-3):213–225, 2005.
- [75] Cs Mihálykó, BG Lakatos, A Matejdesz, and T Blicke. Population balance model for particle-to-particle heat transfer in gas–solid systems. *Int. J. Heat Mass Transfer*, 47(6-7):1325–1334, 2004.
- [76] D Ramkrishna. *Population balances: Theory and applications to particulate systems in engineering*. Elsevier, 2000.
- [77] C Drumm. Coupling of computational fluid dynamics and population balance modelling for liquid-liquid extraction. 2010.

- [78] Z Gao, D Li, A Buffo, W Podgórska, and DL Marchisio. Simulation of droplet breakage in turbulent liquid-liquid dispersions with CFD-PBM: comparison of breakage kernels. *Chem. Eng. Sci.*, 142:277–288, 2016.
- [79] C Tsouris and LL Tavlarides. Breakage and coalescence models for drops in turbulent dispersions. *AIChE J.*, 40(3):395–406, 1994.
- [80] H Luo and HF Svendsen. Theoretical model for drop and bubble breakup in turbulent dispersions. *AIChE J.*, 42(5):1225–1233, 1996.
- [81] CH Lee, LE Erickson, and LA Glasgow. Bubble breakup and coalescence in turbulent gas-liquid dispersions. *Chem. Eng. Commun.*, 59(1-6):65–84, 1987.
- [82] L Hagesaether, HA Jakobsen, and HF Svendsen. A model for turbulent binary breakup of dispersed fluid particles. *Chem. Eng. Sci.*, 57(16):3251–3267, 2002.
- [83] T Wang, J Wang, and Y Jin. A novel theoretical breakup kernel function for bubbles/droplets in a turbulent flow. *Chem. Eng. Sci.*, 58(20):4629–4637, 2003.
- [84] CA Coualoglou and LL Tavlarides. Description of interaction processes in agitated liquid-liquid dispersions. *Chem. Eng. Sci.*, 32(11):1289–1297, 1977.
- [85] J Baldyga and W Podgórska. Drop break-up in intermittent turbulence: Maximum stable and transient sizes of drops. *Can. J. Chem. Eng.*, 76(3):456–470, 1998.

- [86] W Podgórska and J Bałdyga. Drop break-up and coalescence in a stirred tank. *Task Quarterly*, 7(3):409–424, 2003.
- [87] C Meneveau and KR Sreenivasan. The multifractal nature of turbulent energy dissipation. *J. Fluid Mech.*, 224:429–484, 1991.
- [88] R Andersson and B Andersson. Modeling the breakup of fluid particles in turbulent flows. *AIChE J.*, 52(6):2031–2038, 2006.
- [89] RP Hesketh, AW Etchells, and TWF Russell. Experimental observations of bubble breakage in turbulent flow. *Ind. Eng. Chem. Res.*, 30(5):835–841, 1991.
- [90] F Lehr and D Mewes. A transport equation for the interfacial area density applied to bubble columns. *Chem. Eng. Sci.*, 56(3):1159–1166, 2001.
- [91] M Lesieur. *Turbulence in fluids*, volume 40. Springer Science & Business Media, 2012.
- [92] J Jeong and F Hussain. On the identification of a vortex. *J. Fluid Mech.*, 285:69–94, 1995.
- [93] HE Fiedler. Coherent structures in turbulent flows. *Prog. Aerosp. Sci.*, 25(3):231–269, 1988.
- [94] AKMF Hussain. Coherent structures—reality and myth. *Phys. Fluids*, 26(10):2816–2850, 1983.
- [95] RJ Adrian, KT Christensen, and Z-C Liu. Analysis and interpretation of instantaneous turbulent velocity fields. *Exp. Fluids*, 29(3):275–290, 2000.

- [96] Y Dubief and F Delcayre. On coherent-vortex identification in turbulence. *J. Turbul.*, 1(1):011–011, 2000.
- [97] WA Kareem, S Izawa, AK Xiong, and Y Fukunishi. Extraction and tracking of multi-scaled vortices from a homogeneous isotropic turbulent field. *J. Turbul.*, (8):N12, 2007.
- [98] F Ghasempour, R Andersson, N Kevlahan, and B Andersson. Multidimensional turbulence spectra—identifying properties of turbulent structures. In *J. Phys. Conf. Ser.*, volume 318, page 042022. IOP Publishing, 2011.
- [99] F Ghasempour, R Andersson, and B Andersson. Identification and characterization of three-dimensional turbulent flow structures. *AIChE J.*, 62(4):1265–1277, 2016.
- [100] M Farge and K Schneider. Coherent vortex simulation (CVS), a semi-deterministic turbulence model using wavelets. *Flow, Turbulence and Combustion*, 66(4):393–426, 2001.
- [101] M Farge, G Pellegrino, and K Schneider. Coherent vortex extraction in 3D turbulent flows using orthogonal wavelets. *Phys. Rev. Lett.*, 87(5):054501, 2001.
- [102] K Schneider, M Farge, G Pellegrino, and MM Rogers. Coherent vortex simulation of three-dimensional turbulent mixing layers using orthogonal wavelets. *J. Fluid Mech.*, 534:39–66, 2005.
- [103] G Haller and G Yuan. Lagrangian coherent structures and mixing in two-dimensional turbulence. *Physica D*, 147(3-4):352–370, 2000.

- [104] MA Green, CW Rowley, and G Haller. Detection of Lagrangian coherent structures in three-dimensional turbulence. *J. Fluid Mech.*, 572:111–120, 2007.
- [105] A Turiel, J Isern-Fontanet, and E García-Ladona. Wavelet filtering to extract coherent vortices from altimetric data. *J. Atmos. Oceanic Technol.*, 24(12):2103–2119, 2007.
- [106] T Miyauchi and M Tanahashi. Coherent fine scale structure in turbulence. In *IUTAM Symposium on Geometry and Statistics of Turbulence*, pages 67–76. Springer, 2001.
- [107] G Samanta, GM Oxberry, AN Beris, RA Handler, and KD Housiadas. Time-evolution K-L analysis of coherent structures based on DNS of turbulent Newtonian and viscoelastic flows. *J. Turbul.*, (9):N41, 2008.
- [108] O Grulke, F Greiner, T Klinger, and A Piel. Comparative experimental study of coherent structures in a simple magnetized torus. *Plasma Phys. Controlled Fusion*, 43(4):525, 2001.
- [109] PJ Staplehurst, PA Davidson, and SB Dalziel. Structure formation in homogeneous freely decaying rotating turbulence. *J. Fluid Mech.*, 598:81–105, 2008.
- [110] PA Davidson, PJ Staplehurst, and SB Dalziel. On the evolution of eddies in a rapidly rotating system. *J. Fluid Mech.*, 557:135–144, 2006.
- [111] JJ Derksen and HEA Van Den Akker. Multi-scale simulations of stirred liquid–liquid dispersions. *Chem. Eng. Res. Des.*, 85(5):697–702, 2007.

- [112] AE Komrakova, Orest Shardt, D Eskin, and JJ Derksen. Lattice Boltzmann simulations of drop deformation and breakup in shear flow. *International Journal of Multiphase Flow*, 59:24–43, 2014.
- [113] AE Komrakova, D Eskin, and JJ Derksen. Numerical study of turbulent liquid-liquid dispersions. *AIChE J.*, 61(8):2618–2633, 2015.
- [114] Y Hagiwara, Y Takashina, and M Tanaka. Direct numerical simulation of the basic phase-interactions in liquid turbulent channel flow with immiscible droplets. *Nucl. Eng. Des.*, 175(1-2):49–57, 1997.
- [115] NK-R Kevlahan. Rapid distortion of turbulent structures. In *Advances in Turbulence IV*, pages 411–415. Springer, 1993.
- [116] L Scarbolo and A Soldati. Turbulence modulation across the interface of a large deformable drop. *J. Turbul.*, 14(11):27–43, 2013.
- [117] A Roccon, M De Paoli, F Zonta, and A Soldati. Viscosity-modulated breakup and coalescence of large drops in bounded turbulence. *Phys. Rev. Fluids*, 2(8):083603, 2017.
- [118] T Iwasaki, K Nishimura, M Tanaka, and Y Hagiwara. Direct numerical simulation of turbulent couette flow with immiscible droplets. *Int. J. Heat Fluid Flow*, 22(3):332–342, 2001.
- [119] T Yuge and Y Hagiwara. The modifications of near-wall turbulence structure and heat transfer by immiscible droplets in turbulent liquid-liquid two-phase flow. *Int. J. Heat Fluid Flow*, 25(3):471–480, 2004.
- [120] MR Swift, E Orlandini, WR Osborn, and JM Yeomans. Lattice Boltz-

- mann simulations of liquid-gas and binary fluid systems. *Phys. Rev. E*, 54(5):5041, 1996.
- [121] D Jacqmin. Calculation of two-phase Navier-Stokes flows using phase-field modeling. *J. Comput. Phys.*, 155(1):96–127, 1999.
- [122] F Magaletti, F Picano, M Chinappi, L Marino, and CM Casciola. The sharp-interface limit of the Cahn-Hilliard/Navier-Stokes model for binary fluids. *J. Fluid Mech.*, 714:95–126, 2013.
- [123] P Yue, JJ Feng, C Liu, and J Shen. A diffuse-interface method for simulating two-phase flows of complex fluids. *J. Fluid Mech.*, 515:293–317, 2004.
- [124] VE Badalassi, HD Cenicerros, and S Banerjee. Computation of multiphase systems with phase field models. *J. Comput. Phys.*, 190(2):371–397, 2003.
- [125] JW Cahn and JE Hilliard. Free energy of a nonuniform system. I. Interfacial free energy. *J. Chem. Phys.*, 28(2):258–267, 1958.
- [126] O Penrose and PC Fife. Thermodynamically consistent models of phase-field type for the kinetic of phase transitions. *Physica D*, 43(1):44–62, 1990.
- [127] AJ Bray. Theory of phase-ordering kinetics. *Adv. Phys.*, 51(2):481–587, 2002.
- [128] VM Kendon, ME Cates, I Pagonabarraga, J-C Desplat, and P Bladon. Inertial effects in three-dimensional spinodal decomposition of a sym-

- metric binary fluid mixture: a lattice Boltzmann study. *J. Fluid Mech.*, 440:147–203, 2001.
- [129] *Lattice Boltzmann method: fundamentals and engineering applications with computer codes*, author=Mohamad, AA. Springer Science & Business Media, 2011.
- [130] PL Bhatnagar, EP Gross, and M Krook. A model for collision processes in gases. I. Small amplitude processes in charged and neutral one-component systems. *Phys. Rev.*, 94(3):511, 1954.
- [131] D Zhang, K Papadikis, and S Gu. Three-dimensional multi-relaxation time lattice-Boltzmann model for the drop impact on a dry surface at large density ratio. *Int. J. Multiphase Flow*, 64:11–18, 2014.
- [132] AE Komrakova, D Eskin, and JJ Derksen. Lattice Boltzmann simulations of a single n-butanol drop rising in water. *Phys. Fluids*, 25(4):042102, 2013.
- [133] KN Premnath and J Abraham. Three-dimensional multi-relaxation time (MRT) lattice-Boltzmann models for multiphase flow. *J. Comput. Phys.*, 224(2):539–559, 2007.
- [134] D d’Humières. Multiple-relaxation-time lattice Boltzmann models in three dimensions. *Philos. Trans. R. Soc. London, Ser. A*, 360(1792):437–451, 2002.
- [135] H Yu, LS Luo, and SS Girimaji. LES of turbulent square jet flow using an MRT lattice Boltzmann model. *Comput. Fluids*, 35(8-9):957–965, 2006.

- [136] P Lallemand and LS Luo. Theory of the lattice Boltzmann method: Dispersion, dissipation, isotropy, Galilean invariance, and stability. *Phys. Rev. E*, 61(6):6546, 2000.
- [137] TS Lundgren. Linearly forces isotropic turbulence. Technical report, Minnesota Univ Minneapolis, 2003.
- [138] JJ Derksen. Flow-induced forces in sphere doublets. *J. Fluid Mech.*, 608:337–356, 2008.
- [139] L Valiño, J Martín, and G Házi. Dynamics of isotropic homogeneous turbulence with linear forcing using a lattice Boltzmann method. *Flow, turbulence and combustion*, 84(2):219, 2010.
- [140] SB Pope. Turbulent flows, 2001.
- [141] DK Wilson. Three-dimensional correlation and spectral functions for turbulent velocities in homogeneous and surface-blocked boundary layers. Technical report, Army Research Lab Adelphi MD, 1997.
- [142] PG Saffman. The large-scale structure of homogeneous turbulence. *J. Fluid Mech.*, 27(3):581–593, 1967.
- [143] T Tatsumi. The theory of decay process of incompressible isotropic turbulence. *Proc. R. Soc. Lond. A*, 239(1216):16–45, 1957.
- [144] D Xu and J Chen. Accurate estimate of turbulent dissipation rate using PIV data. *Exp. Therm Fluid Sci.*, 44:662–672, 2013.
- [145] D Saha, M Soos, B Luthi, M Holzner, A Liberzon, MU Babler, and W Kinzelbach. Experimental characterization of breakage rate of col-

loidal aggregates in axisymmetric extensional flow. *Langmuir*, 30(48): 14385–14395, 2014.

- [146] S Elghobashi and GC Truesdell. On the two-way interaction between homogeneous turbulence and dispersed solid particles. I: Turbulence modification. *Phys. Fluids A*, 5(7):1790–1801, 1993.

# Appendix A

## MRT implementation

The transformation matrix  $M$  is derived as:

$$\begin{pmatrix} 1 & 1 & 1 & 1 & 1 & 1 & 1 & 1 & 1 & 1 & 1 & 1 & 1 & 1 & 1 & 1 & 1 & 1 & 1 \\ -30 & -11 & -11 & -11 & -11 & -11 & -11 & 8 & 8 & 8 & 8 & 8 & 8 & 8 & 8 & 8 & 8 & 8 & 8 \\ 12 & -4 & -4 & -4 & -4 & -4 & -4 & 1 & 1 & 1 & 1 & 1 & 1 & 1 & 1 & 1 & 1 & 1 & 1 \\ 0 & 1 & -1 & 0 & 0 & 0 & 0 & 1 & -1 & 1 & -1 & 0 & 0 & 0 & 0 & 1 & -1 & 1 & -1 \\ 0 & -4 & 4 & 0 & 0 & 0 & 0 & 1 & -1 & 1 & -1 & 0 & 0 & 0 & 0 & 1 & -1 & 1 & -1 \\ 0 & 0 & 0 & 1 & -1 & 0 & 0 & 1 & 1 & -1 & -1 & 1 & -1 & 1 & -1 & 0 & 0 & 0 & 0 \\ 0 & 0 & 0 & -4 & 4 & 0 & 0 & 1 & 1 & -1 & -1 & 1 & -1 & 1 & -1 & 0 & 0 & 0 & 0 \\ 0 & 0 & 0 & 0 & 0 & 1 & -1 & 0 & 0 & 0 & 0 & 1 & 1 & -1 & -1 & 1 & 1 & -1 & -1 \\ 0 & 0 & 0 & 0 & 0 & -4 & 4 & 0 & 0 & 0 & 0 & 1 & 1 & -1 & -1 & 1 & 1 & -1 & -1 \\ 0 & 2 & 2 & -1 & -1 & -1 & -1 & 1 & 1 & 1 & 1 & -2 & -2 & -2 & -2 & 1 & 1 & 1 & 1 \\ 0 & -4 & -4 & 2 & 2 & 2 & 2 & 1 & 1 & 1 & 1 & -2 & -2 & -2 & -2 & 1 & 1 & 1 & 1 \\ 0 & 0 & 0 & 1 & 1 & -1 & -1 & 1 & 1 & 1 & 1 & 0 & 0 & 0 & 0 & -1 & -1 & -1 & -1 \\ 0 & 0 & 0 & -2 & -2 & 2 & 2 & 1 & 1 & 1 & 1 & 0 & 0 & 0 & 0 & -1 & -1 & -1 & -1 \\ 0 & 0 & 0 & 0 & 0 & 0 & 0 & 0 & 1 & -1 & -1 & 1 & 0 & 0 & 0 & 0 & 0 & 0 & 0 \\ 0 & 0 & 0 & 0 & 0 & 0 & 0 & 0 & 0 & 0 & 0 & 1 & -1 & -1 & 1 & 0 & 0 & 0 & 0 \\ 0 & 0 & 0 & 0 & 0 & 0 & 0 & 0 & 0 & 0 & 0 & 0 & 0 & 0 & 0 & 1 & -1 & -1 & 1 \\ 0 & 0 & 0 & 0 & 0 & 0 & 0 & 1 & -1 & 1 & -1 & 0 & 0 & 0 & 0 & -1 & 1 & -1 & 1 \\ 0 & 0 & 0 & 0 & 0 & 0 & 0 & -1 & -1 & 1 & 1 & 1 & -1 & 1 & -1 & 0 & 0 & 0 & 0 \\ 0 & 0 & 0 & 0 & 0 & 0 & 0 & 0 & 0 & 0 & 0 & -1 & -1 & 1 & 1 & 1 & 1 & -1 & -1 \end{pmatrix}$$

The 19 orthogonal basis vectors  $\varsigma_{q\beta}$  are given:

$$\begin{aligned}
\varsigma_{0\beta} &= \| e_\beta \| \\
\varsigma_{1\beta} &= 19 \| e_\beta \|^2 - 30 \\
\varsigma_{2\beta} &= (21 \| e_\beta \|^4 - 53 \| e_\beta \|^2 + 24)/2 \\
\varsigma_{3\beta} &= e_{\beta x} \\
\varsigma_{5\beta} &= e_{\beta y} \\
\varsigma_{7\beta} &= e_{\beta z} \\
\varsigma_{4\beta} &= (5 \| e_\beta \|^2 - 9)e_{\beta x} \\
\varsigma_{6\beta} &= (5 \| e_\beta \|^2 - 9)e_{\beta y} \\
\varsigma_{8\beta} &= (5 \| e_\beta \|^2 - 9)e_{\beta z} \\
\varsigma_{9\beta} &= 3e_{\beta x}^2 - \| e_\beta \|^2 \\
\varsigma_{11\beta} &= e_{\beta y}^2 - e_{\beta z}^2 [0] \\
\varsigma_{13\beta} &= e_{\beta x}e_{\beta y} \\
\varsigma_{14\beta} &= e_{\beta y}e_{\beta z} \\
\varsigma_{15\beta} &= e_{\beta z}e_{\beta x} \\
\varsigma_{10\beta} &= (3 \| e_\beta \|^2 - 5)(3e_{\beta x}^2 - \| e_\beta \|^2) \\
\varsigma_{12\beta} &= (3 \| e_\beta \|^2 - 5)(e_{\beta y}^2 - e_{\beta z}^2) \\
\varsigma_{16\beta} &= (e_{\beta y}^2 - e_{\beta z}^2)e_{\beta x} \\
\varsigma_{17\beta} &= (e_{\beta z}^2 - e_{\beta x}^2)e_{\beta y} \\
\varsigma_{18\beta} &= (e_{\beta x}^2 - e_{\beta y}^2)e_{\beta z}
\end{aligned} \tag{1.1}$$

where  $\beta \in \{0, 1, \dots, 18\}$ .

# Appendix B

## Procedure and script for 3D fft and energy spectrum

The three dimensional velocity fields  $u$ ,  $v$ ,  $w$  are inputs, the calculation is in MATLAB. Part of code is referred from the GitHub user 'fdietzsc' , the link is: <https://github.com/fdietzsc/hita>.

```
1 clc
2 clear
3 filepath1='/home/grad1/cheng/CZ Jan ...
    16/twophase/d300c6_case3/velx/';
4 filepath2='/home/grad1/cheng/CZ Jan ...
    16/twophase/d300c6_case3/vely/';
5 filepath3='/home/grad1/cheng/CZ Jan ...
    16/twophase/d300c6_case3/velz/';
6 filepath4='/home/grad1/cheng/CZ Jan ...
    16/twophase/d300c6_case3/energy spectrum/';
7 etak=1; %Kolmogrov scale
```

```

8 nu=(0.0005*0.1+1-0.0005)*8.3E-003;
9 epsilon=5.8E-007; %energy dissipation rate
10 dim=300;
11 avespectrum=0;
12 counter=0;
13 for t=12:1:12
14 u=reshape(load([filepath1,'velx',num2str(t,'%04i'),'dat']),&...
15 [dim,dim,dim]);
16 v=reshape(load([filepath2,'vely',num2str(t,'%04i'),'dat']),&...
17 [dim,dim,dim]);
18 w=reshape(load([filepath3,'velz',num2str(t,'%04i'),'dat']),&...
19 [dim,dim,dim]);
20 uu_fft=fftn(u);
21 vv_fft=fftn(v);
22 ww_fft=fftn(w);
23
24 muu = abs(uu_fft)/length(u)^3;
25 mvv = abs(vv_fft)/length(v)^3;
26 mww = abs(ww_fft)/length(w)^3;
27
28 muu = muu.^2;
29 mvv = mvv.^2;
30 mww = mww.^2;
31
32 k_end = (dim)/2;
33
34 rx=[0:1:dim-1] - (dim)/2+1;
35 ry=[0:1:dim-1] - (dim)/2+1;
36 rz=[0:1:dim-1] - (dim)/2+1;
37
38 R_x=circshift(rx',[ (dim)/2+1 1]);

```

```

39 R_y=circshift(ry',[ (dim)/2+1 1]);
40 R_z=circshift(rz',[ (dim)/2+1 1]);
41
42 [X,Y,Z]= meshgrid(R_x,R_y,R_z);
43 r=(sqrt(X.^2+Y.^2+Z.^2));
44
45 dx=2*pi/dim;
46 k=[1:k_end].*dx;
47 kll=[1:k_end];
48
49 spectrum=zeros(size(k,2),1);
50 bin_counter=zeros(size(k,2),1);
51 for N=2:k_end-1
52     picker = (r(:, :, :) * dx <= (k(N+1) + k(N))/2) & ...
53             (r(:, :, :) * dx > (k(N) + k(N-1))/2);
54     spectrum(N) = sum(muu(picker))+...
55                 sum(mvv(picker))+...
56                 sum(mww(picker));
57     bin_counter(N) = size(find(picker==1),1);
58 end
59
60 picker = (r(:, :, :) * dx <= (k(2) + k(1))/2);
61 spectrum(1) = sum(muu(picker))+...
62             sum(mvv(picker))+...
63             sum(mww(picker));
64 bin_counter(1) = size(find(picker==1),1);
65
66 picker = (r(:, :, :) * dx > (k(end) + k(end-1))/2) & ...
67         r(:, :, :) * dx <= k(end));
68 spectrum(end) = sum(muu(picker))+...
69               sum(mvv(picker))+...

```

```

70         sum(mww(picker));
71     bin_counter(end) = size(find(picker==1),1);
72
73     spectrum = spectrum*2*pi.*k'.^2./(bin_counter.*dx.^3);
74
75     avespectrum=avespectrum+spectrum;
76     counter=counter+1;
77 end
78 avespectrum=avespectrum/counter;
79
80     y = [kll; avespectrum'];
81     fid = fopen([filepath4,'average_spectrum.dat'], 'w');
82     fprintf(fid, '%15.8E %15.8E\n', y);
83     fclose(fid);
84
85     compk=kll;
86     kll=kll/(2*pi/etak); %scale kll
87     energy=avespectrum/(epsilon^(2/3)*etak^(5/3));
88
89     slopel=epsilon^(2/3)*kll.^(-5/3);
90
91     scaled=[kll;energy';slopel];
92     fid = fopen([filepath4,'average_spectrum_scaled.dat'], 'w');
93     fprintf(fid, '%15.8E %15.8E %15.8E\n', scaled);
94     fclose(fid);
95
96 %-----compensated energy spectrum-----
97     compspectrum = avespectrum.*compk'.^(5/3)*epsilon^(-2/3);
98     compk=compk*etak;
99     compensated = [compk;compspectrum'];
100    fid = fopen([filepath4,'average_spectrum_compensated.dat'], ...

```

```

        'w');
101     fprintf(fid, '%15.8E %15.8E\n', compensated);
102     fclose(fid);
103
104     %-----Dissipation energy spectrum-----
105     dissspectrum = avespectrum.*compk'.^2*nu;
106     dissk=compk*etak;
107     dissipated = [dissk;dissspectrum'];
108     fid = fopen([filepath4,'average_spectrum_dissipated.dat'], ...
        'w');
109     fprintf(fid, '%15.8E %15.8E\n', dissipated);
110     fclose(fid);

```

# Appendix C

## Procedure and script for coherent structures

The simulation parameters are set in the ‘simparam’ module in FORTRAN 90. In the main program, two subroutines are called: getvelocity.f90 and getq.f90. The getvelocity.f90 extract velocity data from original data file, the getq.f90 generated  $Q_n$  field from velocity. The main program is:

```
1  !-----  
2  !-----  
3  !----- Simulation parameters  
4  !-----  
5  !-----  
6  
7  module simparam  
8  !  
9  ! Simulation domain  
10 !
```

```

11  integer,parameter::ni=300,nj=300,nk=300
12  real(kind=8),parameter::dx=1.0d0,dy=1.0d0,dz=1.0d0
13  !
14  ! Liquid parameter
15  real(kind=8),parameter::nu=8.296E-003 !viscosity
16  !
17  end module simparam
18  !-----
19  !-----
20  !----- Main program
21  !-----
22  !-----
23  program main
24  use simparam
25  implicit none
26  !-----
27  integer::ifld
28  real(kind=8),dimension(:, :, :),allocatable::vx,vy,vz
29  allocate( vx(ni,nj,nk) )
30  allocate( vy(ni,nj,nk) )
31  allocate( vz(ni,nj,nk) )
32  do ifld=12,12,1
33  !-----
34  ! Get velocity from VTK file
35  !-----
36  call getvelocity(ifld,vx,vy,vz)
37  !-----
38  ! Calculate q values
39  !-----
40  call getq(ifld,vx,vy,vz)
41  enddo

```

```
42 deallocate(vx)
43 deallocate(vy)
44 deallocate(vz)
45 end program main
```

The getvelocity.f90 subroutine is:

```
1 subroutine getvelocity(ifld,vx,vy,vz)
2 use simparam
3 implicit none
4 integer,intent(inout)::ifld
5 real(kind=8),intent(inout)::vx(ni,nj,nk),vy(ni,nj,nk)
6 real(kind=8),intent(inout)::vz(ni,nj,nk)
7 integer ::jump,i,j,k,p,temp,d0,d1,d2,d3
8 character ::store
9 real(kind=8),dimension(1:ni*nj*nk)::q
10 character(len=71) datfile1
11 character(len=67) datfile2,datfile3,datfile4
12 datfile1(1:63)='/home/grad1/cheng/CZ Jan ...
    16/twophase/d300c6_case3/paraviewv/vlc' !50+
13 datfile1(68:71)='.vtk'
14 datfile2(1:59)='/home/grad1/cheng/CZ Jan ...
    16/twophase/d300c6_case3/velx/velx'
15 datfile2(64:67)='.dat'
16 datfile3(1:59)='/home/grad1/cheng/CZ Jan ...
    16/twophase/d300c6_case3/vely/vely'
17 datfile3(64:67)='.dat'
18 datfile4(1:59)='/home/grad1/cheng/CZ Jan ...
    16/twophase/d300c6_case3/velz/velz'
19 datfile4(64:67)='.dat'
20
21 102 format (e15.8,1X,e15.8,1X,e15.8)
22 103 format (A)
23 104 format (A,1X,I4,1X,I4,1X,I4)
24 105 format (A,1X,I1,1X,I1,1X,I1)
```

```

25 106 format (A,1X,I8)
26 107 format (f6.3)
27 108 format (f6.3,1X,f6.3,1X,f6.3)
28
29 if (ifld .lt. 10) then
30     d0=0
31     d1=0
32     d2=0
33     d3=ifld
34 endif
35 !-----
36 if ((ifld .ge. 10) .and. (ifld .lt. 100)) then
37     d0=0
38     d1=0
39     d2=inT(ifld/10)
40     d3=ifld-d2*10
41 endif
42 !-----
43 if ((ifld .ge. 100) .and. (ifld .lt. 1000)) then
44     d0=0
45     d1=inT(ifld/100)
46     d2=ifld-d1*100
47     d2=inT(d2/10)
48     d3=ifld-d1*100-d2*10
49 endif
50 !-----
51 if (ifld .ge. 1000) then
52     d0=inT(ifld/1000)
53     d1=ifld-d0*1000
54     d1=inT(d1/100)
55     d2=ifld-d0*1000-d1*100

```

```

56     d2=inT(d2/10)
57     d3=ifld-d0*1000-d1*100-d2*10
58 endif
59 datfile1(64:64)=char(d0+48)
60 datfile1(65:65)=char(d1+48)
61 datfile1(66:66)=char(d2+48)
62 datfile1(67:67)=char(d3+48)
63 !-----
64 datfile2(60:60)=char(d0+48)
65 datfile2(61:61)=char(d1+48)
66 datfile2(62:62)=char(d2+48)
67 datfile2(63:63)=char(d3+48)
68 !-----
69 datfile3(60:60)=char(d0+48)
70 datfile3(61:61)=char(d1+48)
71 datfile3(62:62)=char(d2+48)
72 datfile3(63:63)=char(d3+48)
73 !-----
74 datfile4(60:60)=char(d0+48)
75 datfile4(61:61)=char(d1+48)
76 datfile4(62:62)=char(d2+48)
77 datfile4(63:63)=char(d3+48)
78
79 open(unit=133,file=datfile1,form='formatted',status='unknown')
80 open(unit=212,file=datfile2,form='formatted',status='unknown')
81 open(unit=213,file=datfile3,form='formatted',status='unknown')
82 open(unit=214,file=datfile4,form='formatted',status='unknown')
83
84 do jump=1,9
85     read(133,'(A13)') store
86 enddo

```

```
87
88 do k=1,nk
89 do j=1,nj
90 do i=1,ni
91 read(133,102)vx(i,j,k),vy(i,j,k),vz(i,j,k)
92 write(212,102)vx(i,j,k)
93 write(213,102)vy(i,j,k)
94 write(214,102)vz(i,j,k)
95 enddo
96 enddo
97 enddo
98 close(unit=133)
99 close(unit=212)
100 close(unit=213)
101 close(unit=214)
102
103 end subroutine getvelocity
```

The getq.f90 subroutine is:

```
1  subroutine getq(ifld,vx,vy,vz)
2  use simparam
3  IMPLICIT NONE
4  integer,intent(inout)::ifld
5  real(kind=8),intent(in)::vx(ni,nj,nk),vy(ni,nj,nk),vz(ni,nj,nk)
6  integer ::jump,i,j,k,p,temp,ip,jp,kp,d0,d1,d2,d3
7  character ::store
8  real(kind=8),dimension(1:ni*nj*nk)::q,qq
9  real(kind=8)::omega2,s2,numerator,denominator
10 character(len=67) datfile10,datfile11
11
12 datfile10(1:59)='/home/grad1/cheng/CZ Jan ...
    16/onephase/d300b1_case3/qval/qval'
13 datfile10(64:67)='.dat'
14 datfile11(1:59)='/home/grad1/cheng/CZ Jan ...
    16/onephase/d300b1_case3/qval/qori'
15 datfile11(64:67)='.dat'
16
17 101 format (e15.6,1X,e15.6,1X,e15.6)
18 102 format (E11.3)
19 103 format (A)
20 104 format (A,1X,I4,1X,I4,1X,I4)
21 105 format (A,1X,I1,1X,I1,1X,I1)
22 106 format (A,1X,I8)
23 107 format (f6.3)
24 108 format (f6.3,1X,f6.3,1X,f6.3)
25 109 format (f12.3)
26
```

```

27  if (ifld .lt. 10) then
28      d0=0
29      d1=0
30      d2=0
31      d3=ifld
32  endif
33  !-----
34  if ((ifld .ge. 10) .and. (ifld .lt. 100)) then
35      d0=0
36      d1=0
37      d2=inT(ifld/10)
38      d3=ifld-d2*10
39  endif
40  !-----
41  if ((ifld .ge. 100) .and. (ifld .lt. 1000)) then
42      d0=0
43      d1=inT(ifld/100)
44      d2=ifld-d1*100
45      d2=inT(d2/10)
46      d3=ifld-d1*100-d2*10
47  endif
48  !-----
49  if (ifld .ge. 1000) then
50      d0=inT(ifld/1000)
51      d1=ifld-d0*1000
52      d1=inT(d1/100)
53      d2=ifld-d0*1000-d1*100
54      d2=inT(d2/10)
55      d3=ifld-d0*1000-d1*100-d2*10
56  endif
57  !-----

```

```

58  datfile10(60:60)=char(d0+48)
59  datfile10(61:61)=char(d1+48)
60  datfile10(62:62)=char(d2+48)
61  datfile10(63:63)=char(d3+48)
62  !-----
63  datfile11(60:60)=char(d0+48)
64  datfile11(61:61)=char(d1+48)
65  datfile11(62:62)=char(d2+48)
66  datfile11(63:63)=char(d3+48)
67  !-----
68  open(unit=216,file=datfile10,form='formatted',status='unknown')
69  open(unit=217,file=datfile11,form='formatted',status='unknown')
70
71  p=0
72  do k=1,nk
73    kp=k+1
74    if (kp.gt.nk) kp=kp-nk
75  do j=1,nj
76    jp=j+1
77    if (jp.gt.nj) jp=jp-nj
78  do i=1,ni
79    ip=i+1
80    if (ip.gt.ni) ip=ip-ni
81
82  p=p+1
83  numerator=-2.0d0*(vx(ip,j,k)-vx(i,j,k))*(vx(ip,j,k)-vx(i,j,k))&
84            &/(dx*dx)&
85            &-4.0d0*(vx(i,jp,k)-vx(i,j,k))*(vy(ip,j,k)-vy(i,j,k))&
86            &/(dy*dx)&
87            &-2.0d0*(vy(i,jp,k)-vy(i,j,k))*(vy(i,jp,k)-vy(i,j,k))&
88            &/(dy*dy)&

```

```

89      &-4.0d0*(vx(i,j,kp)-vx(i,j,k))*(vz(ip,j,k)-vz(i,j,k))&
90      &/ (dz*dx) &
91      &-2.0d0*(vz(i,j,kp)-vz(i,j,k))*(vz(i,j,kp)-vz(i,j,k))&
92      &/ (dz*dz) &
93      &-4.0d0*(vy(i,j,kp)-vy(i,j,k))*(vz(i,jp,k)-vz(i,j,k))&
94      &/ (dz*dy)
95
96  denominator= ...
          1.0d0*(vx(i,jp,k)-vx(i,j,k))*(vx(i,jp,k)-vx(i,j,k))&
97          &/ (dy*dy) &
98          &+1.0d0*(vy(ip,j,k)-vy(i,j,k))*(vy(ip,j,k)-vy(i,j,k))&
99          &/ (dx*dx) &
100         &-2.0d0*(vx(i,jp,k)-vx(i,j,k))*(vy(ip,j,k)-vy(i,j,k))&
101         &/ (dy*dx) &
102         &+1.0d0*(vx(i,j,kp)-vx(i,j,k))*(vx(i,j,kp)-vx(i,j,k))&
103         &/ (dz*dz) &
104         &+1.0d0*(vz(ip,j,k)-vz(i,j,k))*(vz(ip,j,k)-vz(i,j,k))&
105         &/ (dx*dx) &
106         &-2.0d0*(vx(i,j,kp)-vx(i,j,k))*(vz(ip,j,k)-vz(i,j,k))&
107         &/ (dz*dx) &
108         &+1.0d0*(vy(i,j,kp)-vy(i,j,k))*(vy(i,j,kp)-vy(i,j,k))&
109         &/ (dz*dz) &
110         &+1.0d0*(vz(i,jp,k)-vz(i,j,k))*(vz(i,jp,k)-vz(i,j,k))&
111         &/ (dz*dz) &
112         &-2.0d0*(vy(i,j,kp)-vy(i,j,k))*(vz(i,jp,k)-vz(i,j,k))&
113         &/ (dz*dy)
114
115  q(p)=numerator/denominator
116  qq(p)=0.5d0*numerator
117  enddo
118  enddo

```

```
119 enddo
120
121 do p=1,ni*nj*nk
122 write(216,*)q(p)
123 write(217,*)qq(p)
124 enddo
125
126 close(unit=216)
127 close(unit=217)
128
129 end subroutine getq
```

With the  $Q_n$  field, the MATLAB code is then used to extract coherent structures:

```
1 clc
2 clear
3 tic
4 filepath1='/home/grad1/cheng/CZ Jan ...
      16/twophase/d300a6_case3/qval/';
5 filepath2='/home/grad1/cheng/CZ Jan ...
      16/twophase/d300a6_case3/qnum/';
6 dim=300;
7 hh=waitbar(0,'calculating...');
8 aa1=22;
9 aa2=22;
10 interv=1;
11 for t=aa1:interv:aa2
12 q=reshape(load([filepath1,'qval',num2str(t,'%04i'),'.dat'])...
13     ,[dim,dim,dim]);    %original q 3d matrix
14 qcheck=q;
15 qcheck(qcheck>100)=NaN;
16 qqq=max(qcheck(:))
17 % threshold=0.8*qqq;
18 threshold=0.8;
19 qboundx(1)=0;
20 qboundy(1)=0;
21 qboundz(1)=0;
22
23 qboundx(:)=[];
24 qboundy(:)=[];
25 qboundz(:)=[];
```

```

26 qnum=zeros(dim,dim,dim);
27 qfinal=zeros(dim,dim,dim);
28 n=1;
29 cutoffvolume=507;
30 q(q<threshold)=0;
31 qchange=q; %changeable q 3d ...
    matrix
32
33 qmax=max(max(max(qchange)));
34 while qmax >= threshold
35     [r,c,v]=ind2sub(size(qchange),find(qchange==qmax));
36     for i=1:length(r)
37         %-----the max q is at point (x,y,z)-----
38         x=r(i);
39         y=c(i);
40         z=v(i);
41         %-----
42         xloc=x;
43         yloc=y;
44         zloc=z;
45         if qchange(xloc,yloc,zloc)>= threshold
46             thismaxpoint=true;
47             %-----large ...
                loop-----
48             while qchange(xloc,yloc,zloc) >= threshold ...
                %move to +x direction
49                 qnum(xloc,yloc,zloc)=n; %marked ...
                    this point in "nth" vortex
50                 xx=xloc; %point ...
                    (xloc,yloc,zloc) is regarded as a temporary ...
                    origin

```

```

51     yy=yloc;
52     zz=zloc;
53     %-----litte loop-----
54     while qchange(xx,yy,zz) >= threshold
55         qnum(xx,yy,zz)=n;
56         xxx=xx;
57         yyy=yy;
58         zzz=zz;
59         %-----very little loope-----
60         while qchange(xxx,yyy,zzz) >= threshold
61             qnum(xxx,yyy,zzz)=n;
62             zzz=zzz+1; %move to +zzz direction
63             if zzz>dim
64                 zzz=zzz-dim;
65             end
66         end
67         qboundx(end+1)=xxx;
68         qboundy(end+1)=yyy;
69         if zzz==1
70             qboundz(end+1)=dim;
71         else
72             qboundz(end+1)=zzz-1;
73         end
74         zzz=zz;
75
76         while qchange(xxx,yyy,zzz) >= threshold
77             qnum(xxx,yyy,zzz)=n;
78             zzz=zzz-1; %move to -zzz
79             if zzz<1
80                 zzz=zzz+dim;
81             end

```

```

82         end
83         qboundx (end+1)=xxx;
84         qboundy (end+1)=yyy;
85         if zzz==dim;
86             qboundz (end+1)=1;
87         else
88             qboundz (end+1)=zzz+1;
89         end
90         zzz=zz;
91         %-----end very little loop-----
92
93         yy=yy+1;           %move to +yy direction
94         if yy>dim
95             yy=yy-dim;
96         end
97     end
98     qboundx (end+1)=xx;
99     if yy==1
100         qboundy (end+1)=dim;
101     else
102         qboundy (end+1)=yy-1;
103     end
104     qboundz (end+1)=zz;
105     yy=yloc;
106
107     while qchange (xx,yy,zz) >= threshold
108         qnum (xx,yy,zz)=n;
109         %-----very little loope-----
110         while qchange (xxx,yyy,zzz) >= threshold
111             qnum (xxx,yyy,zzz)=n;
112             zzz=zzz+1; %move to +zzz direction

```

```

113         if zzz>dim
114             zzz=zzz-dim;
115         end
116     end
117     qboundx(end+1)=xxx;
118     qboundy(end+1)=yyy;
119     if zzz==1
120         qboundz(end+1)=dim;
121     else
122         qboundz(end+1)=zzz-1;
123     end
124     zzz=zz;
125
126     while qchange(xxx,yyy,zzz) >= threshold
127         qnum(xxx,yyy,zzz)=n;
128         zzz=zzz-1; %move to -zzz
129         if zzz<1
130             zzz=zzz+dim;
131         end
132     end
133     qboundx(end+1)=xxx;
134     qboundy(end+1)=yyy;
135     if zzz==dim;
136         qboundz(end+1)=1;
137     else
138         qboundz(end+1)=zzz+1;
139     end
140     zzz=zz;
141     %-----end very little loop-----
142     yy=yy-1; %move to -yy direction
143     if yy<1

```

```

144         yy=yy+dim;
145     end
146 end
147 qboundx (end+1)=xx;
148 if yy==dim
149     qboundy (end+1)=1;
150 else
151     qboundy (end+1)=yy+1;
152 end
153 qboundz (end+1)=zz;
154 yy=yloc;
155
156 while qchange(xx,yy,zz) >= threshold
157     qnum(xx,yy,zz)=n;
158     %-----very little loope-----
159     while qchange(xxx,yyy,zzz) >= threshold
160         qnum(xxx,yyy,zzz)=n;
161         yyy=yyy+1; %move to +yyy direction
162         if yyy>dim
163             yyy=yyy-dim;
164         end
165     end
166     qboundx (end+1)=xxx;
167     if yyy==1
168         qboundy (end+1)=dim;
169     else
170         qboundy (end+1)=yyy-1;
171     end
172     qboundz (end+1)=zzz;
173     yyy=yy;
174

```

```

175         while qchange(xxx,yyy,zzz) >= threshold
176             qnum(xxx,yyy,zzz)=n;
177             yyy=yyy-1; %move to -yyy
178             if yyy<1
179                 yyy=yyy+dim;
180             end
181         end
182         qboundx(end+1)=xxx;
183         if yyy==dim
184             qboundy(end+1)=1;
185         else
186             qboundy(end+1)=yyy+1;
187         end
188         qboundz(end+1)=zzz;
189         YYY=YY;
190         %-----end very little loop-----
191         zz=zz+1; %move to +zz direction
192         if zz>dim
193             zz=zz-dim;
194         end
195     end
196     qboundx(end+1)=xx;
197     qboundy(end+1)=yy;
198     if zz==1
199         qboundz(end+1)=dim;
200     else
201         qboundz(end+1)=zz-1;
202     end
203     zz=zloc;
204
205     while qchange(xx,yy,zz) >= threshold

```

```

206     qnum(xx,yy,zz)=n;
207     %-----very little loope-----
208     while qchange(xxx,yyy,zzz) >= threshold
209         qnum(xxx,yyy,zzz)=n;
210         yyy=yyy+1; %move to +yyy direction
211         if yyy>dim
212             yyy=yyy-dim;
213         end
214     end
215     qboundx(end+1)=xxx;
216     if yyy==1
217         qboundy(end+1)=dim;
218     else
219         qboundy(end+1)=yyy-1;
220     end
221     qboundz(end+1)=zzz;
222     yyy=yy;
223
224     while qchange(xxx,yyy,zzz) >= threshold
225         qnum(xxx,yyy,zzz)=n;
226         yyy=yyy-1; %move to -yyy
227         if yyy<1
228             yyy=yyy+dim;
229         end
230     end
231     qboundx(end+1)=xxx;
232     if yyy==dim
233         qboundy(end+1)=1;
234     else
235         qboundy(end+1)=yyy+1;
236     end

```

```

237         qboundz (end+1)=zzz;
238         yyy=yy;
239         %-----end very little loop-----
240         zz=zz-1;           %move to -zz direction
241         if zz<1
242             zz=zz+dim;
243         end
244     end
245     qboundx (end+1)=xx;
246     qboundy (end+1)=yy;
247     if zz==dim;
248         qboundz (end+1)=1;
249     else
250         qboundz (end+1)=zz+1;
251     end
252     zz=zloc;
253     %-----end little loop-----
254     xloc=xloc+1;
255     if xloc>dim
256         xloc=xloc-dim;
257     end
258 end
259 if xloc==1
260     qboundx (end+1)=dim;
261 else
262     qboundx (end+1)=xloc-1;
263 end
264 qboundy (end+1)=yloc;
265 qboundz (end+1)=zloc;
266 xloc=x;           ...
                %reset xloc to original x (where max q exists)

```

```

267      %-----end large ...
          loop-----
268
269      %-----large ...
          loop-----
270      while qchange(xloc,yloc,zloc) >= threshold      ...
          %move to -x direction
271          qnum(xloc,yloc,zloc)=n;
272          %----litte loop-----
273          while qchange(xx,yy,zz) >= threshold
274              qnum(xx,yy,zz)=n;
275              %-----very little loope-----
276              while qchange(xxx,yyy,zzz) >= threshold
277                  qnum(xxx,yyy,zzz)=n;
278                  zzz=zzz+1;  %move to +zzz direction
279                  if zzz>dim
280                      zzz=zzz-dim;
281                  end
282              end
283              qboundx(end+1)=xxx;
284              qboundy(end+1)=yyy;
285              if zzz==1
286                  qboundz(end+1)=dim;
287              else
288                  qboundz(end+1)=zzz-1;
289              end
290              zzz=zz;
291
292              while qchange(xxx,yyy,zzz) >= threshold
293                  qnum(xxx,yyy,zzz)=n;
294                  zzz=zzz-1;  %move to -zzz

```

```

295         if zzz<1
296             zzz=zzz+dim;
297         end
298     end
299     qboundx(end+1)=xxx;
300     qboundy(end+1)=yyy;
301     if zzz==dim
302         qboundz(end+1)=1;
303     else
304         qboundz(end+1)=zzz+1;
305     end
306     zzz=zz;
307     %-----end very little loop-----
308     yy=yy+1;           %move to +yy direction
309     if yy>dim
310         yy=yy-dim;
311     end
312 end
313 qboundx(end+1)=xx;
314 if yy==1
315     qboundy(end+1)=dim;
316 else
317     qboundy(end+1)=yy-1;
318 end
319 qboundz(end+1)=zz;
320 yy=yloc;
321
322 while qchange(xx,yy,zz) >= threshold
323     qnum(xx,yy,zz)=n;
324     %-----very little loope-----
325     while qchange(xxx,yyy,zzz) >= threshold

```

```

326         qnum(xxx,yyy,zzz)=n;
327         zzz=zzz+1; %move to +zzz direction
328         if zzz>dim
329             zzz=zzz-dim;
330         end
331     end
332     qboundx(end+1)=xxx;
333     qboundy(end+1)=yyy;
334     if zzz==1
335         qboundz(end+1)=dim;
336     else
337         qboundz(end+1)=zzz-1;
338     end
339     zzz=zz;
340
341     while qchange(xxx,yyy,zzz) >= threshold
342         qnum(xxx,yyy,zzz)=n;
343         zzz=zzz-1; %move to -zzz
344         if zzz<1
345             zzz=zzz+dim;
346         end
347     end
348     qboundx(end+1)=xxx;
349     qboundy(end+1)=yyy;
350     if zzz==dim
351         qboundz(end+1)=1;
352     else
353         qboundz(end+1)=zzz+1;
354     end
355     zzz=zz;
356     %-----end very little loop-----

```

```

357         yy=yy-1;           %move to -yy direction
358         if yy<1
359             yy=yy+dim;
360         end
361     end
362     qboundx (end+1)=xx;
363     if yy==dim
364         qboundy (end+1)=1;
365     else
366         qboundy (end+1)=yy+1;
367     end
368     qboundz (end+1)=zz;
369     yy=yloc;
370
371     while qchange(xx,yy,zz) >= threshold
372         qnum(xx,yy,zz)=n;
373         %-----very little loope-----
374         while qchange(xxx,yyy,zzz) >= threshold
375             qnum(xxx,yyy,zzz)=n;
376             yyy=yyy+1; %move to +yyy direction
377             if yyy>dim
378                 yyy=yyy-dim;
379             end
380         end
381         qboundx (end+1)=xxx;
382         if yyy==1;
383             qboundy (end+1)=dim;
384         else
385             qboundy (end+1)=yyy-1;
386         end
387         qboundz (end+1)=zzz;

```

```

388         yyy=yy;
389
390         while qchange(xxx,yyy,zzz) >= threshold
391             qnum(xxx,yyy,zzz)=n;
392             yyy=yyy-1; %move to -yyy
393             if yyy<1
394                 yyy=yyy+dim;
395             end
396         end
397         qboundx(end+1)=xxx;
398         if yyy==dim
399             qboundy(end+1)=1;
400         else
401             qboundy(end+1)=yyy+1;
402         end
403         qboundz(end+1)=zzz;
404         yyy=yy;
405         %-----end very little loop-----
406         zz=zz+1; %move to +zz direction
407         if zz>dim
408             zz=zz-dim;
409         end
410     end
411     qboundx(end+1)=xx;
412     qboundy(end+1)=yy;
413     if zz==1
414         qboundz(end+1)=dim;
415     else
416         qboundz(end+1)=zz-1;
417     end
418     zz=zloc;

```

```

419
420     while qchange(xx,yy,zz) >= threshold
421         qnum(xx,yy,zz)=n;
422         %-----very little loope-----
423         while qchange(xxx,yyy,zzz) >= threshold
424             qnum(xxx,yyy,zzz)=n;
425             yyy=yyy+1; %move to +yyy direction
426             if yyy>dim
427                 yyy=yyy-dim;
428             end
429         end
430         qboundx(end+1)=xxx;
431         if yyy==1
432             qboundy(end+1)=dim;
433         else
434             qboundy(end+1)=yyy-1;
435         end
436         qboundz(end+1)=zzz;
437         YYY=YY;
438
439         while qchange(xxx,yyy,zzz) >= threshold
440             qnum(xxx,yyy,zzz)=n;
441             yyy=yyy-1; %move to -yyy
442             if yyy<1
443                 yyy=yyy+dim;
444             end
445         end
446         qboundx(end+1)=xxx;
447         if yyy==dim
448             qboundy(end+1)=1;
449         else

```

```

450         qboundy (end+1)=yyy+1;
451     end
452     qboundz (end+1)=zzz;
453     yyy=yy;
454     %-----end very little loop-----
455     zz=zz-1;           %move to -zz direction
456     if zz<1
457         zz=zz+dim;
458     end
459 end
460 qboundx (end+1)=xx;
461 qboundy (end+1)=yy;
462 if zz==dim
463     qboundz (end+1)=1;
464 else
465     qboundz (end+1)=zz+1;
466 end
467 zz=zloc;
468 %-----end little loop-----
469 xloc=xloc-1;
470 if xloc<1
471     xloc=xloc+dim;
472 end
473 end
474 if xloc==dim;
475     qboundx (end+1)=1;
476 else
477     qboundx (end+1)=xloc+1;
478 end
479 qboundy (end+1)=yloc;
480 qboundz (end+1)=zloc;

```

```

481     xloc=x;                                     ...
        %reset xloc to original x (where max q exists)
482     %-----end large ...
        loop-----
483
484     %-----large ...
        loop-----
485
486     while qchange(xloc,yloc,zloc) >= threshold    ...
        %move to +y direction
487         qnum(xloc,yloc,zloc)=n;
488         %----litte loop-----
489         while qchange(xx,yy,zz) >= threshold
490             qnum(xx,yy,zz)=n;
491             %-----very little loope-----
492             while qchange(xxx,yyy,zzz) >= threshold
493                 qnum(xxx,yyy,zzz)=n;
494                 zzz=zzz+1; %move to +zzz direction
495                 if zzz>dim
496                     zzz=zzz-dim;
497                 end
498             end
499             qboundx(end+1)=xxx;
500             qboundy(end+1)=yyy;
501             if zzz==1
502                 qboundz(end+1)=dim;
503             else
504                 qboundz(end+1)=zzz-1;
505             end
506             zzz=zz;
507

```

```

508         while qchange(xxx,yyy,zzz) >= threshold
509             qnum(xxx,yyy,zzz)=n;
510             zzz=zzz-1; %move to -zzz
511             if zzz<1
512                 zzz=zzz+dim;
513             end
514         end
515         qboundx(end+1)=xxx;
516         qboundy(end+1)=yyy;
517         if zzz==dim
518             qboundz(end+1)=1;
519         else
520             qboundz(end+1)=zzz+1;
521         end
522         zzz=zz;
523         %-----end very little loop-----
524         xx=xx+1; %move to +xx direction
525         if xx>dim
526             xx=xx-dim;
527         end
528     end
529     if xx==1
530         qboundx(end+1)=dim;
531     else
532         qboundx(end+1)=xx-1;
533     end
534     qboundy(end+1)=yy;
535     qboundz(end+1)=zz;
536     xx=xloc;
537
538     while qchange(xx,yy,zz) >= threshold

```

```

539     qnum(xx,yy,zz)=n;
540     %-----very little loope-----
541     while qchange(xxx,yyy,zzz) >= threshold
542         qnum(xxx,yyy,zzz)=n;
543         zzz=zzz+1; %move to +zzz direction
544         if zzz>dim
545             zzz=zzz-dim;
546         end
547     end
548     qboundx(end+1)=xxx;
549     qboundy(end+1)=yyy;
550     if zzz==1
551         qboundz(end+1)=dim;
552     else
553         qboundz(end+1)=zzz-1;
554     end
555     zzz=zz;
556
557     while qchange(xxx,yyy,zzz) >= threshold
558         qnum(xxx,yyy,zzz)=n;
559         zzz=zzz-1; %move to -zzz
560         if zzz<1
561             zzz=zzz+dim;
562         end
563     end
564     qboundx(end+1)=xxx;
565     qboundy(end+1)=yyy;
566     if zzz==dim
567         qboundz(end+1)=1;
568     else
569         qboundz(end+1)=zzz+1;

```

```

570         end
571         zzz=zz;
572         %-----end very little loop-----
573         xx=xx-1;           %move to -xx direction
574         if xx<1
575             xx=xx+dim;
576         end
577     end
578     if xx==dim
579         qboundx(end+1)=1;
580     else
581         qboundx(end+1)=xx+1;
582     end
583     qboundy(end+1)=yy;
584     qboundz(end+1)=zz;
585     xx=xloc;
586
587     while qchange(xx,yy,zz) >= threshold
588         qnum(xx,yy,zz)=n;
589         %-----very little loope-----
590         while qchange(xxx,yyy,zzz) >= threshold
591             qnum(xxx,yyy,zzz)=n;
592             xxx=xxx+1; %move to +xxx direction
593             if xxx>dim
594                 xxx=xxx-dim;
595             end
596         end
597         if xxx==1
598             qboundx(end+1)=dim;
599         else
600             qboundx(end+1)=xxx-1;

```

```

601         end
602         qboundy (end+1)=yyy;
603         qboundz (end+1)=zzz;
604         xxx=xx;
605
606         while qchange(xxx,yyy,zzz) >= threshold
607             qnum(xxx,yyy,zzz)=n;
608             xxx=xxx-1; %move to -xxx
609             if xxx<1
610                 xxx=xxx+dim;
611             end
612         end
613         if xxx==dim
614             qboundx (end+1)=1;
615         else
616             qboundx (end+1)=xxx+1;
617         end
618         qboundy (end+1)=yyy;
619         qboundz (end+1)=zzz;
620         xxx=xx;
621         %-----end very little loop-----
622         zz=zz+1; %move to +zz direction
623         if zz>dim
624             zz=zz-dim;
625         end
626     end
627     qboundx (end+1)=xx;
628     qboundy (end+1)=yy;
629     if zz==1
630         qboundz (end+1)=dim;
631     else

```

```

632     qboundz (end+1)=zz-1;
633     end
634     zz=zloc;
635
636     while qchange(xx,yy,zz) >= threshold
637         qnum(xx,yy,zz)=n;
638         %-----very little loope-----
639         while qchange(xxx,yyy,zzz) >= threshold
640             qnum(xxx,yyy,zzz)=n;
641             xxx=xxx+1; %move to +xxx direction
642             if xxx>dim
643                 xxx=xxx-dim;
644             end
645         end
646         if xxx==1
647             qboundx (end+1)=dim;
648         else
649             qboundx (end+1)=xxx-1;
650         end
651         qboundy (end+1)=yyy;
652         qboundz (end+1)=zzz;
653         xxx=xx;
654
655         while qchange(xxx,yyy,zzz) >= threshold
656             qnum(xxx,yyy,zzz)=n;
657             xxx=xxx-1; %move to -xxx
658             if xxx<1
659                 xxx=xxx+dim;
660             end
661         end
662         if xxx==dim

```

```

663         qboundx (end+1) =1;
664     else
665         qboundx (end+1) =xxx+1;
666     end
667     qboundy (end+1) =yyy;
668     qboundz (end+1) =zzz;
669     xxx=xx;
670     %-----end very little loop-----
671     zz=zz-1;           %move to -zz direction
672     if zz<1
673         zz=zz+dim;
674     end
675 end
676 qboundx (end+1) =xx;
677 qboundy (end+1) =yy;
678 if zz==dim
679     qboundz (end+1) =1;
680 else
681     qboundz (end+1) =zz+1;
682 end
683 zz=zloc;
684 %-----end little loop-----
685 yloc=yloc+1;
686 if yloc>dim
687     yloc=yloc-dim;
688 end
689 end
690 qboundx (end+1) =xloc;
691 if yloc==1
692     qboundy (end+1) =dim;
693 else

```

```

694     qboundy(end+1)=yloc-1;
695     end
696     qboundz(end+1)=zloc;
697     yloc=y;                                     ...
        %reset yloc to original y (where max q exists)
698     %-----end large ...
        loop-----
699
700     %-----large ...
        loop-----
701
702     while qchange(xloc,yloc,zloc) >= threshold    ...
        %move to -y direction
703         qnum(xloc,yloc,zloc)=n;
704         %----litte loop-----
705         while qchange(xx,yy,zz) >= threshold
706             qnum(xx,yy,zz)=n;
707             %-----very little loope-----
708             while qchange(xxx,yyy,zzz) >= threshold
709                 qnum(xxx,yyy,zzz)=n;
710                 zzz=zzz+1; %move to +zzz direction
711                 if zzz>dim
712                     zzz=zzz-dim;
713                 end
714             end
715         qboundx(end+1)=xxx;
716         qboundy(end+1)=yyy;
717         if zzz==1
718             qboundz(end+1)=dim;
719         else
720             qboundz(end+1)=zzz-1;

```

```

721         end
722         zzz=zz;
723
724         while qchange(xxx,yyy,zzz) >= threshold
725             qnum(xxx,yyy,zzz)=n;
726             zzz=zzz-1; %move to -zzz
727             if zzz<1
728                 zzz=zzz+dim;
729             end
730         end
731         qboundx(end+1)=xxx;
732         qboundy(end+1)=yyy;
733         if zzz==dim
734             qboundz(end+1)=1;
735         else
736             qboundz(end+1)=zzz+1;
737         end
738         zzz=zz;
739         %-----end very little loop-----
740         xx=xx+1; %move to +xx direction
741         if xx>dim
742             xx=xx-dim;
743         end
744     end
745     if xx==1
746         qboundx(end+1)=dim;
747     else
748         qboundx(end+1)=xx-1;
749     end
750     qboundy(end+1)=yy;
751     qboundz(end+1)=zz;

```

```

752     xx=xloc;
753
754     while qchange(xx,yy,zz) >= threshold
755         qnum(xx,yy,zz)=n;
756         %-----very little loope-----
757         while qchange(xxx,yyy,zzz) >= threshold
758             qnum(xxx,yyy,zzz)=n;
759             zzz=zzz+1; %move to +zzz direction
760             if zzz>dim
761                 zzz=zzz-dim;
762             end
763         end
764         qboundx(end+1)=xxx;
765         qboundy(end+1)=yyy;
766         if zzz==1
767             qboundz(end+1)=dim;
768         else
769             qboundz(end+1)=zzz-1;
770         end
771         zzz=zz;
772
773         while qchange(xxx,yyy,zzz) >= threshold
774             qnum(xxx,yyy,zzz)=n;
775             zzz=zzz-1; %move to -zzz
776             if zzz<1
777                 zzz=zzz+dim;
778             end
779         end
780         qboundx(end+1)=xxx;
781         qboundy(end+1)=yyy;
782         if zzz==dim

```

```

783         qboundz (end+1) =1;
784     else
785         qboundz (end+1) =zzz+1;
786     end
787     zzz=zz;
788     %-----end very little loop-----
789     xx=xx-1;           %move to -xx direction
790     if xx<1
791         xx=xx+dim;
792     end
793 end
794 if xx==dim
795     qboundx (end+1) =1;
796 else
797     qboundx (end+1) =xx+1;
798 end
799     qboundy (end+1) =yy;
800     qboundz (end+1) =zz;
801     xx=xloc;
802
803 while qchange (xx,yy,zz) >= threshold
804     qnum (xx,yy,zz) =n;
805     %-----very little loope-----
806     while qchange (xxx,yyy,zzz) >= threshold
807         qnum (xxx,yyy,zzz) =n;
808         xxx=xxx+1;   %move to +xxx direction
809         if xxx>dim
810             xxx=xxx-dim;
811         end
812     end
813     if xxx==1

```

```

814         qboundx (end+1) =dim;
815     else
816         qboundx (end+1) =xxx-1;
817     end
818     qboundy (end+1) =yyy;
819     qboundz (end+1) =zzz;
820     xxx=xx;
821
822     while qchange (xxx,yyy,zzz) >= threshold
823         qnum (xxx,yyy,zzz) =n;
824         xxx=xxx-1; %move to -xxx
825         if xxx<1
826             xxx=xxx+dim;
827         end
828     end
829     if xxx==dim
830         qboundx (end+1) =1;
831     else
832         qboundx (end+1) =xxx+1;
833     end
834     qboundy (end+1) =yyy;
835     qboundz (end+1) =zzz;
836     xxx=xx;
837     %-----end very little loop-----
838     zz=zz+1; %move to +zz direction
839     if zz>dim
840         zz=zz-dim;
841     end
842 end
843 qboundx (end+1) =xx;
844 qboundy (end+1) =yy;

```

```

845         if zz==1
846             qboundz (end+1)=dim;
847         else
848             qboundz (end+1)=zz-1;
849         end
850         zz=zloc;
851
852         while qchange(xx,yy,zz) >= threshold
853             qnum(xx,yy,zz)=n;
854             %-----very little loope-----
855             while qchange(xxx,yyy,zzz) >= threshold
856                 qnum(xxx,yyy,zzz)=n;
857                 xxx=xxx+1; %move to +xxx direction
858                 if xxx>dim
859                     xxx=xxx-dim;
860                 end
861             end
862             if xxx==1
863                 qboundx (end+1)=dim;
864             else
865                 qboundx (end+1)=xxx-1;
866             end
867             qboundy (end+1)=yyy;
868             qboundz (end+1)=zzz;
869             xxx=xx;
870
871             while qchange(xxx,yyy,zzz) >= threshold
872                 qnum(xxx,yyy,zzz)=n;
873                 xxx=xxx-1; %move to -xxx
874                 if xxx<1
875                     xxx=xxx+dim;

```

```

876         end
877     end
878     if xxx==dim
879         qboundx(end+1)=1;
880     else
881         qboundx(end+1)=xxx+1;
882     end
883     qboundy(end+1)=yyy;
884     qboundz(end+1)=zzz;
885     xxx=xx;
886     %-----end very little loop-----
887     zz=zz-1;           %move to -zz direction
888     if zz<1
889         zz=zz+dim;
890     end
891 end
892 qboundx(end+1)=xx;
893 qboundy(end+1)=yy;
894 if zz==dim
895     qboundz(end+1)=1;
896 else
897     qboundz(end+1)=zz+1;
898 end
899 zz=zloc;
900 %-----end little loop-----
901 yloc=yloc-1;
902 if yloc<1
903     yloc=yloc+dim;
904 end
905 end
906 qboundx(end+1)=xloc;

```

```

907     if yloc==dim
908         qboundary(end+1)=1;
909     else
910         qboundary(end+1)=yloc+1;
911     end
912     qboundz(end+1)=zloc;
913     yloc=y;                                     ...
          %reset yloc to original (where max q exists)
914     %-----end large ...
          loop-----
915
916     %-----large ...
          loop-----
917
918     while qchange(xloc,yloc,zloc) >= threshold    ...
          %move to +z direction
919         qnum(xloc,yloc,zloc)=n;
920         %----litte loop-----
921         while qchange(xx,yy,zz) >= threshold
922             qnum(xx,yy,zz)=n;
923             %-----very little loope-----
924             while qchange(xxx,yyy,zzz) >= threshold
925                 qnum(xxx,yyy,zzz)=n;
926                 yyy=yyy+1; %move to +yyy direction
927                 if yyy>dim
928                     yyy=yyy-dim;
929                 end
930             end
931         qboundx(end+1)=xxx;
932         if yyy==1
933             qboundary(end+1)=dim;

```

```

934         else
935             qboundy (end+1)=yyy-1;
936         end
937         qboundz (end+1)=zzz;
938         YYY=YY;
939
940         while qchange (xxx,yyy,zzz) >= threshold
941             qnum (xxx,yyy,zzz)=n;
942             yyy=yyy-1; %move to -yyy
943             if yyy<1
944                 yyy=yyy+dim;
945             end
946         end
947         qboundx (end+1)=xxx;
948         if yyy==dim
949             qboundy (end+1)=1;
950         else
951             qboundy (end+1)=yyy+1;
952         end
953         qboundz (end+1)=zzz;
954         YYY=YY;
955         %-----end very little loop-----
956         xx=xx+1; %move to +xx direction
957         if xx>dim
958             xx=xx-dim;
959         end
960     end
961     if xx==1
962         qboundx (end+1)=dim;
963     else
964         qboundx (end+1)=xx-1;

```

```

965     end
966     qboundy (end+1)=yy;
967     qboundz (end+1)=zz;
968     xx=xloc;
969
970     while qchange (xx,yy,zz) >= threshold
971         qnum (xx,yy,zz)=n;
972         %-----very little loope-----
973         while qchange (xxx,yyy,zzz) >= threshold
974             qnum (xxx,yyy,zzz)=n;
975             yyy=yyy+1; %move to +yyy direction
976             if yyy>dim
977                 yyy=yyy-dim;
978             end
979         end
980         qboundx (end+1)=xxx;
981         if yyy==1
982             qboundy (end+1)=dim;
983         else
984             qboundy (end+1)=yyy-1;
985         end
986         qboundz (end+1)=zzz;
987         YYY=yy;
988
989         while qchange (xxx,yyy,zzz) >= threshold
990             qnum (xxx,yyy,zzz)=n;
991             yyy=yyy-1; %move to -yyy
992             if yyy<1
993                 yyy=yyy+dim;
994             end
995         end

```

```

996         qboundx (end+1) =xxx;
997         if yyy==dim;
998             qboundy (end+1) =1;
999         else
1000             qboundy (end+1) =yyy+1;
1001         end
1002         qboundz (end+1) =zzz;
1003         YYY=yy;
1004         %-----end very little loop-----
1005         xx=xx-1;           %move to -xx direction
1006         if xx<1
1007             xx=xx+dim;
1008         end
1009     end
1010     if xx==dim
1011         qboundx (end+1) =1;
1012     else
1013         qboundx (end+1) =xx+1;
1014     end
1015     qboundy (end+1) =yy;
1016     qboundz (end+1) =zz;
1017     xx=xloc;
1018
1019     while qchange (xx,yy,zz) >= threshold
1020         qnum (xx,yy,zz) =n;
1021         %-----very little loope-----
1022         while qchange (xxx,yyy,zzz) >= threshold
1023             qnum (xxx,yyy,zzz) =n;
1024             xxx=xxx+1; %move to +xxx direction
1025             if xxx>dim
1026                 xxx=xxx-dim;

```

```

1027         end
1028     end
1029     if xxx==1
1030         qboundx(end+1)=dim;
1031     else
1032         qboundx(end+1)=xxx-1;
1033     end
1034     qboundy(end+1)=yyy;
1035     qboundz(end+1)=zzz;
1036     xxx=xx;
1037
1038     while qchange(xxx,yyy,zzz) >= threshold
1039         qnum(xxx,yyy,zzz)=n;
1040         xxx=xxx-1; %move to -xxx
1041         if xxx<1
1042             xxx=xxx+dim;
1043         end
1044     end
1045     if xxx==dim
1046         qboundx(end+1)=1;
1047     else
1048         qboundx(end+1)=xxx+1;
1049     end
1050     qboundy(end+1)=yyy;
1051     qboundz(end+1)=zzz;
1052     xxx=xx;
1053     %-----end very little loop-----
1054     yy=yy+1; %move to +yy direction
1055     if yy>dim
1056         yy=yy-dim;
1057     end

```

```

1058     end
1059     qboundx (end+1)=xx;
1060     if yy==1
1061         qboundy (end+1)=dim;
1062     else
1063         qboundy (end+1)=yy-1;
1064     end
1065     qboundz (end+1)=zz;
1066     yy=yloc;

1067
1068     while qchange(xx,yy,zz) >= threshold
1069         qnum(xx,yy,zz)=n;
1070         %-----very little loope-----
1071         while qchange(xxx,yyy,zzz) >= threshold
1072             qnum(xxx,yyy,zzz)=n;
1073             xxx=xxx+1; %move to +xxx direction
1074             if xxx>dim
1075                 xxx=xxx-dim;
1076             end
1077         end
1078         if xxx==1
1079             qboundx (end+1)=dim;
1080         else
1081             qboundx (end+1)=xxx-1;
1082         end
1083         qboundy (end+1)=yyy;
1084         qboundz (end+1)=zzz;
1085         xxx=xx;
1086
1087         while qchange(xxx,yyy,zzz) >= threshold
1088             qnum(xxx,yyy,zzz)=n;

```

```

1089         xxx=xxx-1; %move to -xxx
1090         if xxx<1
1091             xxx=xxx+dim;
1092         end
1093     end
1094     if xxx==dim
1095         qboundx(end+1)=1;
1096     else
1097         qboundx(end+1)=xxx+1;
1098     end
1099     qboundy(end+1)=yyy;
1100     qboundz(end+1)=zzz;
1101     xxx=xx;
1102     %-----end very little loop-----
1103     yy=yy-1; %move to -yy direction
1104     if yy<1
1105         yy=yy+dim;
1106     end
1107 end
1108 qboundx(end+1)=xx;
1109 if yy==dim
1110     qboundy(end+1)=1;
1111 else
1112     qboundy(end+1)=yy+1;
1113 end
1114 qboundz(end+1)=zz;
1115 yy=yloc;
1116 %-----end little loop-----
1117 zloc=zloc+1;
1118 if zloc>dim
1119     zloc=zloc-dim;

```

```

1120         end
1121     end
1122     qboundx(end+1)=xloc;
1123     qboundy(end+1)=yloc;
1124     if zloc==1
1125         qboundz(end+1)=dim;
1126     else
1127         qboundz(end+1)=zloc-1;
1128     end
1129     zloc=z;
1130     %reset zloc to original z (where max q exists)
1131     %-----end large ...
1132     loop-----
1133
1134     %-----large ...
1135     loop-----
1136
1137     while qchange(xloc,yloc,zloc) >= threshold ...
1138         %move to -z direction
1139         qnum(xloc,yloc,zloc)=n;
1140         %-----litte loop-----
1141         while qchange(xx,yy,zz) >= threshold
1142             qnum(xx,yy,zz)=n;
1143             %-----very little loope-----
1144             while qchange(xxx,yyy,zzz) >= threshold
1145                 qnum(xxx,yyy,zzz)=n;
1146                 yyy=yyy+1; %move to +yyy direction
1147                 if yyy>dim
1148                     yyy=yyy-dim;
1149                 end
1150             end
1151         end
1152     end

```

```

1147         qboundx (end+1) =xxx;
1148         if yyy==1
1149             qboundy (end+1) =dim;
1150         else
1151             qboundy (end+1) =yyy-1;
1152         end
1153         qboundz (end+1) =zzz;
1154         YYY=yy;
1155
1156         while qchange (xxx,yyy,zzz) >= threshold
1157             qnum (xxx,yyy,zzz) =n;
1158             yyy=yyy-1; %move to -yyy
1159             if yyy<1
1160                 yyy=yyy+dim;
1161             end
1162         end
1163         qboundx (end+1) =xxx;
1164         if yyy==dim
1165             qboundy (end+1) =1;
1166         else
1167             qboundy (end+1) =yyy+1;
1168         end
1169         qboundz (end+1) =zzz;
1170         YYY=yy;
1171         %-----end very little loop-----
1172         xx=xx+1; %move to +xx direction
1173         if xx>dim
1174             xx=xx-dim;
1175         end
1176     end
1177     if xx==1

```

```

1178         qboundx(end+1)=dim;
1179     else
1180         qboundx(end+1)=xx-1;
1181     end
1182     qboundy(end+1)=yy;
1183     qboundz(end+1)=zz;
1184     xx=xloc;
1185
1186     while qchange(xx,yy,zz) >= threshold
1187         qnum(xx,yy,zz)=n;
1188         %-----very little loope-----
1189         while qchange(xxx,yyy,zzz) >= threshold
1190             qnum(xxx,yyy,zzz)=n;
1191             yyy=yyy+1; %move to +yyy direction
1192             if yyy>dim
1193                 yyy=yyy-dim;
1194             end
1195         end
1196         qboundx(end+1)=xxx;
1197         if yyy==1
1198             qboundy(end+1)=dim;
1199         else
1200             qboundy(end+1)=yyy-1;
1201         end
1202         qboundz(end+1)=zzz;
1203         YYY=yy;
1204
1205         while qchange(xxx,yyy,zzz) >= threshold
1206             qnum(xxx,yyy,zzz)=n;
1207             yyy=yyy-1; %move to -yyy
1208             if yyy<1

```

```

1209             yyy=yyy+dim;
1210         end
1211     end
1212
1213     qboundx(end+1)=xxx;
1214     if yyy==dim
1215         qboundy(end+1)=1;
1216     else
1217         qboundy(end+1)=yyy+1;
1218     end
1219     qboundz(end+1)=zzz;
1220     YYY=yy;
1221     %-----end very little loop-----
1222     xx=xx-1;           %move to -xx direction
1223     if xx<1
1224         xx=xx+dim;
1225     end
1226 end
1227 if xx==dim
1228     qboundx(end+1)=1;
1229 else
1230     qboundx(end+1)=xx+1;
1231 end
1232 qboundy(end+1)=yy;
1233 qboundz(end+1)=zz;
1234 xx=xloc;
1235
1236 while qchange(xx,yy,zz) >= threshold
1237     qnum(xx,yy,zz)=n;
1238     %-----very little loope-----
1239     while qchange(xxx,yyy,zzz) >= threshold

```

```

1240         qnum(xxx,yyy,zzz)=n;
1241         xxx=xxx+1; %move to +xxx direction
1242         if xxx>dim
1243             xxx=xxx-dim;
1244         end
1245     end
1246     if xxx==1
1247         qboundx(end+1)=dim;
1248     else
1249         qboundx(end+1)=xxx-1;
1250     end
1251     qboundy(end+1)=yyy;
1252     qboundz(end+1)=zzz;
1253     xxx=xx;
1254
1255     while qchange(xxx,yyy,zzz) >= threshold
1256         qnum(xxx,yyy,zzz)=n;
1257         xxx=xxx-1; %move to -xxx
1258         if xxx<1
1259             xxx=xxx+dim;
1260         end
1261     end
1262     if xxx==dim
1263         qboundx(end+1)=1;
1264     else
1265         qboundx(end+1)=xxx+1;
1266     end
1267     qboundy(end+1)=yyy;
1268     qboundz(end+1)=zzz;
1269     xxx=xx;
1270     %-----end very little loop-----

```

```

1271         yy=yy+1;           %move to +yy direction
1272         if yy>dim
1273             yy=yy-dim;
1274         end
1275     end
1276     qboundx (end+1)=xx;
1277     if yy==1
1278         qboundy (end+1)=dim;
1279     else
1280         qboundy (end+1)=yy-1;
1281     end
1282     qboundz (end+1)=zz;
1283     yy=yloc;
1284
1285     while qchange(xx,yy,zz) >= threshold
1286         qnum(xx,yy,zz)=n;
1287         %-----very little loope-----
1288         while qchange(xxx,yyy,zzz) >= threshold
1289             qnum(xxx,yyy,zzz)=n;
1290             xxx=xxx+1; %move to +xxx direction
1291             if xxx>dim
1292                 xxx=xxx-dim;
1293             end
1294         end
1295         if xxx==1
1296             qboundx (end+1)=dim;
1297         else
1298             qboundx (end+1)=xxx-1;
1299         end
1300         qboundy (end+1)=yyy;
1301         qboundz (end+1)=zzz;

```

```

1302         xxx=xx;
1303
1304         while qchange(xxx,yyy,zzz) >= threshold
1305             qnum(xxx,yyy,zzz)=n;
1306             xxx=xxx-1; %move to -xxx
1307             if xxx<1
1308                 xxx=xxx+dim;
1309             end
1310         end
1311         if xxx==dim
1312             qboundx(end+1)=1;
1313         else
1314             qboundx(end+1)=xxx+1;
1315         end
1316         qboundy(end+1)=yyy;
1317         qboundz(end+1)=zzz;
1318         xxx=xx;
1319         %-----end very little loop-----
1320         yy=yy-1; %move to -yy direction
1321         if yy<1
1322             yy=yy+dim;
1323         end
1324     end
1325     qboundx(end+1)=xx;
1326     if yy==dim
1327         qboundy(end+1)=1;
1328     else
1329         qboundy(end+1)=yy+1;
1330     end
1331     qboundz(end+1)=zz;
1332     yy=yloc;

```

```

1333         %-----end little loop-----
1334         zloc=zloc-1;
1335         if zloc<1
1336             zloc=zloc+dim;
1337         end
1338     end
1339     qboundx(end+1)=xloc;
1340     qboundy(end+1)=yloc;
1341     if zloc==dim
1342         qboundz(end+1)=1;
1343     else
1344         qboundz(end+1)=zloc+1;
1345     end
1346     zloc=z;                                     ...
1347     %reset zloc to original z (where max q exists)
1348     %-----end large ...
1349     loop-----
1350
1351     %-----till now, part of boundry points ...
1352     are found and recorded, and are marked as 'nth' ...
1353     in a new matrix ('nth' vortex)
1354 else
1355     thismaxpoint=false;
1356 end
1357 if thismaxpoint == true
1358     repeatboundlocs(1,1)=0;
1359     repeatboundlocs(:)=[];
1360 repeatboundlocs(1:length(qboundx), :) ...
1361     =[qboundx(:), qboundy(:), qboundz(:)];
1362 boundlocs(1,1)=0;
1363 boundlocs(:)=[];

```

```

1360 boundlocs=unique(repeatboundlocs,'rows');
1361 [row, colum]=size(boundlocs);
1362
1363 tempqboundx(1)=0;
1364 tempqboundx(:)=[];
1365 tempqboundy(1)=0;
1366 tempqboundy(:)=[];
1367 tempqboundz(1)=0;
1368 tempqboundz(:)=[];
1369 tempqboundx(1:length(boundlocs(:,1))) ...
1370     =boundlocs(:,1);
1371 tempqboundy(1:length(boundlocs(:,2))) ...
1372     =boundlocs(:,2);
1373 tempqboundz(1:length(boundlocs(:,3))) ...
1374     =boundlocs(:,3);
1375 tempvolume1=-1;
1376 tempvolume2=-2;
1377 %-----start with found boundary points-----
1378 while tempvolume1~=tempvolume2
1379     repeatboundlocs(1:length(qboundx), :) ...
1380     =[qboundx(:), qboundy(:), qboundz(:)];
1381     boundlocs=unique(repeatboundlocs,'rows');
1382     tempqboundx(1:length(boundlocs(:,1)))=boundlocs(:,1);
1383     tempqboundy(1:length(boundlocs(:,2)))=boundlocs(:,2);
1384     tempqboundz(1:length(boundlocs(:,3)))=boundlocs(:,3);
1385     tempvolume1=tempvolume2;
1386     for boundnums=1:length(tempqboundx)
1387         xloc=tempqboundx(boundnums);
1388         yloc=tempqboundy(boundnums);
1389         zloc=tempqboundz(boundnums);
1390         if qchange(xloc,yloc,zloc)>= threshold

```

```

1391 %-----large ...
      loop-----
1392 while qchange(xloc,yloc,zloc) >= threshold ...
      %move to +x direction
1393 qnum(xloc,yloc,zloc)=n; %marked ...
      this point in "nth" vortex
1394 xx=xloc; %point ...
      (xloc,yloc,zloc) is regarded as a temporary ...
      origin
1395 yy=yloc;
1396 zz=zloc;
1397 %----litte loop-----
1398 while qchange(xx,yy,zz) >= threshold
1399 qnum(xx,yy,zz)=n;
1400 xxx=xx;
1401 yyy=yy;
1402 zzz=zz;
1403 %-----very little loope-----
1404 while qchange(xxx,yyy,zzz) >= threshold
1405 qnum(xxx,yyy,zzz)=n;
1406 zzz=zzz+1; %move to +zzz direction
1407 if zzz>dim
1408 zzz=zzz-dim;
1409 end
1410 end
1411 qboundx(end+1)=xxx;
1412 qboundy(end+1)=yyy;
1413 if zzz==1
1414 qboundz(end+1)=dim;
1415 else
1416

```

```

1417         qboundz (end+1)=zzz-1;
1418     end
1419     zzz=zz;
1420
1421     while qchange(xxx,yyy,zzz) >= threshold
1422         qnum(xxx,yyy,zzz)=n;
1423         zzz=zzz-1; %move to -zzz
1424         if zzz<1
1425             zzz=zzz+dim;
1426         end
1427     end
1428     qboundx (end+1)=xxx;
1429     qboundy (end+1)=yyy;
1430     if zzz==dim
1431         qboundz (end+1)=1;
1432     else
1433         qboundz (end+1)=zzz+1;
1434     end
1435     zzz=zz;
1436     %-----end very little loop-----
1437
1438     yy=yy+1; %move to +yy direction
1439     if yy>dim
1440         yy=yy-dim;
1441     end
1442 end
1443 qboundx (end+1)=xx;
1444 if yy==1
1445     qboundy (end+1)=dim;
1446 else
1447     qboundy (end+1)=yy-1;

```

```

1448     end
1449     qboundz (end+1)=zz;
1450     yy=yloc;
1451
1452     while qchange(xx,yy,zz) >= threshold
1453         qnum(xx,yy,zz)=n;
1454         %-----very little loope-----
1455         while qchange(xxx,yyy,zzz) >= threshold
1456             qnum(xxx,yyy,zzz)=n;
1457             zzz=zzz+1; %move to +zzz direction
1458             if zzz>dim
1459                 zzz=zzz-dim;
1460             end
1461         end
1462         qboundx (end+1)=xxx;
1463         qboundy (end+1)=yyy;
1464         if zzz==1
1465             qboundz (end+1)=dim;
1466         else
1467             qboundz (end+1)=zzz-1;
1468         end
1469         zzz=zz;
1470
1471         while qchange(xxx,yyy,zzz) >= threshold
1472             qnum(xxx,yyy,zzz)=n;
1473             zzz=zzz-1; %move to -zzz
1474             if zzz<1
1475                 zzz=zzz+dim;
1476             end
1477         end
1478         qboundx (end+1)=xxx;

```

```

1479         qboundy (end+1)=yyy;
1480         if zzz==dim
1481             qboundz (end+1)=1;
1482         else
1483             qboundz (end+1)=zzz+1;
1484         end
1485         zzz=zz;
1486         %-----end very little loop-----
1487         yy=yy-1;           %move to -yy direction
1488         if yy<1
1489             yy=yy+dim;
1490         end
1491     end
1492     qboundx (end+1)=xx;
1493     if yy==dim
1494         qboundy (end+1)=1;
1495     else
1496         qboundy (end+1)=yy+1;
1497     end
1498     qboundz (end+1)=zz;
1499     yy=yloc;
1500
1501     while qchange(xx,yy,zz) >= threshold
1502         qnum(xx,yy,zz)=n;
1503         %-----very little loope-----
1504         while qchange(xxx,yyy,zzz) >= threshold
1505             qnum(xxx,yyy,zzz)=n;
1506             yyy=yyy+1; %move to +yyy direction
1507             if yyy>dim
1508                 yyy=yyy-dim;
1509             end

```

```

1510         end
1511         qboundx (end+1)=xxx;
1512         if yyy==1
1513             qboundy (end+1)=dim;
1514         else
1515             qboundy (end+1)=yyy-1;
1516         end
1517         qboundz (end+1)=zzz;
1518         YYY=YY;
1519
1520         while qchange(xxx,yyy,zzz) >= threshold
1521             qnum(xxx,yyy,zzz)=n;
1522             yyy=yyy-1; %move to -yyy
1523             if yyy<1
1524                 yyy=yyy+dim;
1525             end
1526         end
1527         qboundx (end+1)=xxx;
1528         if yyy==dim
1529             qboundy (end+1)=1;
1530         else
1531             qboundy (end+1)=yyy+1;
1532         end
1533         qboundz (end+1)=zzz;
1534         YYY=YY;
1535         %-----end very little loop-----
1536         zz=zz+1; %move to +zz direction
1537         if zz>dim
1538             zz=zz-dim;
1539         end
1540     end

```

```

1541     qboundx (end+1)=xx;
1542     qboundy (end+1)=yy;
1543     if zz==1
1544         qboundz (end+1)=dim;
1545     else
1546     qboundz (end+1)=zz-1;
1547     end
1548     zz=zloc;
1549
1550     while qchange (xx,yy,zz) >= threshold
1551         qnum (xx,yy,zz)=n;
1552         %-----very little loope-----
1553         while qchange (xxx,yyy,zzz) >= threshold
1554             qnum (xxx,yyy,zzz)=n;
1555             yyy=yyy+1; %move to +yyy direction
1556             if yyy>dim
1557                 yyy=yyy-dim;
1558             end
1559         end
1560         qboundx (end+1)=xxx;
1561         if yyy==1
1562             qboundy (end+1)=dim;
1563         else
1564             qboundy (end+1)=yyy-1;
1565         end
1566         qboundz (end+1)=zzz;
1567         yyy=yy;
1568
1569         while qchange (xxx,yyy,zzz) >= threshold
1570             qnum (xxx,yyy,zzz)=n;
1571             yyy=yyy-1; %move to -yyy

```

```

1572         if yyy<1
1573             yyy=yyy+dim;
1574         end
1575     end
1576     qboundx (end+1)=xxx;
1577     if yyy==dim
1578         qboundy (end+1)=1;
1579     else
1580         qboundy (end+1)=yyy+1;
1581     end
1582     qboundz (end+1)=zzz;
1583     YYY=yy;
1584     %-----end very little loop-----
1585     zz=zz-1;           %move to -zz direction
1586     if zz<1
1587         zz=zz+dim;
1588     end
1589 end
1590 qboundx (end+1)=xx;
1591 qboundy (end+1)=yy;
1592 if zz==dim
1593     qboundz (end+1)=1;
1594 else
1595     qboundz (end+1)=zz+1;
1596 end
1597 zz=zloc;
1598 %-----end little loop-----
1599 xloc=xloc+1;
1600 if xloc>dim
1601     xloc=xloc-dim;
1602 end

```

```

1603     end
1604     if xloc==1
1605         qboundx(end+1)=dim;
1606     else
1607         qboundx(end+1)=xloc-1;
1608     end
1609     qboundy(end+1)=yloc;
1610     qboundz(end+1)=zloc;
1611     xloc=tempqboundx(boundnums); ...
                                     %reset xloc to ...
                                     original x (boundary point)
1612     %-----end large ...
                                     loop-----
1613
1614     %-----large ...
                                     loop-----
1615     while qchange(xloc,yloc,zloc) >= threshold    ...
                                     %move to -x direction
1616         qnum(xloc,yloc,zloc)=n;
1617         %----litte loop-----
1618         while qchange(xx,yy,zz) >= threshold
1619             qnum(xx,yy,zz)=n;
1620             %-----very little loope-----
1621             while qchange(xxx,yyy,zzz) >= threshold
1622                 qnum(xxx,yyy,zzz)=n;
1623                 zzz=zzz+1; %move to +zzz direction
1624                 if zzz>dim
1625                     zzz=zzz-dim;
1626                 end
1627             end
1628         qboundx(end+1)=xxx;

```

```

1629         qboundy (end+1) =yyy;
1630         if zzz==1
1631             qboundz (end+1) =dim;
1632         else
1633             qboundz (end+1) =zzz-1;
1634         end
1635         zzz=zz;
1636
1637         while qchange (xxx,yyy,zzz) >= threshold
1638             qnum (xxx,yyy,zzz) =n;
1639             zzz=zzz-1; %move to -zzz
1640             if zzz<1
1641                 zzz=zzz+dim;
1642             end
1643         end
1644         qboundx (end+1) =xxx;
1645         qboundy (end+1) =yyy;
1646         if zzz==dim
1647             qboundz (end+1) =1;
1648         else
1649             qboundz (end+1) =zzz+1;
1650         end
1651         zzz=zz;
1652         %-----end very little loop-----
1653         yy=yy+1; %move to +yy direction
1654         if yy>dim
1655             yy=yy-dim;
1656         end
1657     end
1658     qboundx (end+1) =xx;
1659     if yy==1

```

```

1660         qboundy (end+1)=dim;
1661     else
1662         qboundy (end+1)=yy-1;
1663     end
1664     qboundz (end+1)=zz;
1665     yy=yloc;

1666
1667     while qchange(xx,yy,zz) >= threshold
1668         qnum(xx,yy,zz)=n;
1669         %-----very little loope-----
1670         while qchange(xxx,yyy,zzz) >= threshold
1671             qnum(xxx,yyy,zzz)=n;
1672             zzz=zzz+1; %move to +zzz direction
1673             if zzz>dim
1674                 zzz=zzz-dim;
1675             end
1676         end
1677         qboundx (end+1)=xxx;
1678         qboundy (end+1)=yyy;
1679         if zzz==1
1680             qboundz (end+1)=dim;
1681         else
1682             qboundz (end+1)=zzz-1;
1683         end
1684         zzz=zz;

1685
1686         while qchange(xxx,yyy,zzz) >= threshold
1687             qnum(xxx,yyy,zzz)=n;
1688             zzz=zzz-1; %move to -zzz
1689             if zzz<1
1690                 zzz=zzz+dim;

```

```

1691         end
1692     end
1693     qboundx (end+1)=xxx;
1694     qboundy (end+1)=yyy;
1695     if zzz==dim
1696         qboundz (end+1)=1;
1697     else
1698         qboundz (end+1)=zzz+1;
1699     end
1700     zzz=zz;
1701     %-----end very little loop-----
1702     yy=yy-1;           %move to -yy direction
1703     if yy<1
1704         yy=yy+dim;
1705     end
1706 end
1707 qboundx (end+1)=xx;
1708 if yy==dim
1709     qboundy (end+1)=1;
1710 else
1711     qboundy (end+1)=yy+1;
1712 end
1713 qboundz (end+1)=zz;
1714 yy=yloc;
1715
1716 while qchange (xx,yy,zz) >= threshold
1717     qnum (xx,yy,zz)=n;
1718     %-----very little loope-----
1719     while qchange (xxx,yyy,zzz) >= threshold
1720         qnum (xxx,yyy,zzz)=n;
1721         yyy=yyy+1;   %move to +yyy direction

```

```

1722         if yyy>dim
1723             yyy=yyy-dim;
1724         end
1725     end
1726     qboundx(end+1)=xxx;
1727     if yyy==1
1728         qboundy(end+1)=dim;
1729     else
1730         qboundy(end+1)=yyy-1;
1731     end
1732     qboundz(end+1)=zzz;
1733     YYY=yy;
1734
1735     while qchange(xxx,yyy,zzz) >= threshold
1736         qnum(xxx,yyy,zzz)=n;
1737         yyy=yyy-1; %move to -yyy
1738         if yyy<1
1739             yyy=yyy+dim;
1740         end
1741     end
1742     qboundx(end+1)=xxx;
1743     if yyy==dim
1744         qboundy(end+1)=1;
1745     else
1746         qboundy(end+1)=yyy+1;
1747     end
1748     qboundz(end+1)=zzz;
1749     YYY=yy;
1750     %-----end very little loop-----
1751     zz=zz+1; %move to +zz direction
1752     if zz>dim

```

```

1753         zz=zz-dim;
1754     end
1755 end
1756 qboundx (end+1)=xx;
1757 qboundy (end+1)=yy;
1758 if zz==1
1759     qboundz (end+1)=dim;
1760 else
1761     qboundz (end+1)=zz-1;
1762 end
1763 zz=zloc;
1764
1765 while qchange(xx,yy,zz) >= threshold
1766     qnum(xx,yy,zz)=n;
1767     %-----very little loope-----
1768     while qchange(xxx,yyy,zzz) >= threshold
1769         qnum(xxx,yyy,zzz)=n;
1770         yyy=yyy+1; %move to +yyy direction
1771         if yyy>dim
1772             yyy=yyy-dim;
1773         end
1774     end
1775     qboundx (end+1)=xxx;
1776     if yyy==1
1777         qboundy (end+1)=dim;
1778     else
1779         qboundy (end+1)=yyy-1;
1780     end
1781     qboundz (end+1)=zzz;
1782     yyy=yy;
1783

```

```

1784         while qchange(xxx,yyy,zzz) >= threshold
1785             qnum(xxx,yyy,zzz)=n;
1786             yyy=yyy-1; %move to -yyy
1787             if yyy<1
1788                 yyy=yyy+dim;
1789             end
1790         end
1791         qboundx(end+1)=xxx;
1792         if yyy==dim
1793             qboundy(end+1)=1;
1794         else
1795             qboundy(end+1)=yyy+1;
1796         end
1797         qboundz(end+1)=zzz;
1798         YYY=YY;
1799         %-----end very little loop-----
1800         zz=zz-1; %move to -zz direction
1801         if zz<1
1802             zz=zz+dim;
1803         end
1804     end
1805     qboundx(end+1)=xx;
1806     qboundy(end+1)=yy;
1807     if zz==dim
1808         qboundz(end+1)=1;
1809     else
1810         qboundz(end+1)=zz+1;
1811     end
1812     zz=zloc;
1813     %-----end little loop-----
1814     xloc=xloc-1;

```

```

1815         if xloc<1
1816             xloc=xloc+dim;
1817         end
1818     end
1819     if xloc==dim
1820         qboundx(end+1)=1;
1821     else
1822         qboundx(end+1)=xloc+1;
1823     end
1824     qboundy(end+1)=yloc;
1825     qboundz(end+1)=zloc;
1826     xloc=tempqboundx(boundnums); ...
                                                    %reset ...
        xloc to original x (where boundry point)
1827 %-----end large ...
        loop-----
1828
1829 %-----large ...
        loop-----
1830
1831 while qchange(xloc,yloc,zloc) >= threshold ...
        %move to +y direction
1832     qnum(xloc,yloc,zloc)=n;
1833     %----litte loop-----
1834     while qchange(xx,yy,zz) >= threshold
1835         qnum(xx,yy,zz)=n;
1836         %-----very little loope-----
1837         while qchange(xxx,yyy,zzz) >= threshold
1838             qnum(xxx,yyy,zzz)=n;
1839             zzz=zzz+1; %move to +zzz direction
1840             if zzz>dim

```

```

1841         zzz=zzz-dim;
1842     end
1843 end
1844 qboundx (end+1)=xxx;
1845 qboundy (end+1)=yyy;
1846 if zzz==1
1847     qboundz (end+1)=dim;
1848 else
1849     qboundz (end+1)=zzz-1;
1850 end
1851 zzz=zz;
1852
1853 while qchange(xxx,yyy,zzz) >= threshold
1854     qnum(xxx,yyy,zzz)=n;
1855     zzz=zzz-1; %move to -zzz
1856     if zzz<1
1857         zzz=zzz+dim;
1858     end
1859 end
1860 qboundx (end+1)=xxx;
1861 qboundy (end+1)=yyy;
1862 if zzz==dim
1863     qboundz (end+1)=1;
1864 else
1865     qboundz (end+1)=zzz+1;
1866 end
1867 zzz=zz;
1868 %-----end very little loop-----
1869 xx=xx+1; %move to +xx direction
1870 if xx>dim
1871     xx=xx-dim;

```

```

1872         end
1873     end
1874     if xx==1
1875         qboundx(end+1)=dim;
1876     else
1877         qboundx(end+1)=xx-1;
1878     end
1879     qboundy(end+1)=yy;
1880     qboundz(end+1)=zz;
1881     xx=xloc;
1882
1883     while qchange(xx,yy,zz) >= threshold
1884         qnum(xx,yy,zz)=n;
1885         %-----very little loope-----
1886         while qchange(xxx,yyy,zzz) >= threshold
1887             qnum(xxx,yyy,zzz)=n;
1888             zzz=zzz+1; %move to +zzz direction
1889             if zzz>dim
1890                 zzz=zzz-dim;
1891             end
1892         end
1893         qboundx(end+1)=xxx;
1894         qboundy(end+1)=yyy;
1895         if zzz==1
1896             qboundz(end+1)=dim;
1897         else
1898             qboundz(end+1)=zzz-1;
1899         end
1900         zzz=zz;
1901
1902     while qchange(xxx,yyy,zzz) >= threshold

```

```

1903         qnum(xxx,yyy,zzz)=n;
1904         zzz=zzz-1; %move to -zzz
1905         if zzz<1
1906             zzz=zzz+dim;
1907         end
1908     end
1909     qboundx(end+1)=xxx;
1910     qboundy(end+1)=yyy;
1911     if zzz==dim
1912         qboundz(end+1)=1;
1913     else
1914         qboundz(end+1)=zzz+1;
1915     end
1916     zzz=zz;
1917     %-----end very little loop-----
1918     xx=xx-1; %move to -xx direction
1919     if xx<1
1920         xx=xx+dim;
1921     end
1922 end
1923 if xx==dim
1924     qboundx(end+1)=1;
1925 else
1926     qboundx(end+1)=xx+1;
1927 end
1928     qboundy(end+1)=yy;
1929     qboundz(end+1)=zz;
1930     xx=xloc;
1931
1932 while qchange(xx,yy,zz) >= threshold
1933     qnum(xx,yy,zz)=n;

```

```

1934 %-----very little loope-----
1935 while qchange(xxx,yyy,zzz) >= threshold
1936     qnum(xxx,yyy,zzz)=n;
1937     xxx=xxx+1; %move to +xxx direction
1938     if xxx>dim
1939         xxx=xxx-dim;
1940     end
1941 end
1942 if xxx==1
1943     qboundx(end+1)=dim;
1944 else
1945     qboundx(end+1)=xxx-1;
1946 end
1947 qboundy(end+1)=yyy;
1948 qboundz(end+1)=zzz;
1949 xxx=xx;
1950
1951 while qchange(xxx,yyy,zzz) >= threshold
1952     qnum(xxx,yyy,zzz)=n;
1953     xxx=xxx-1; %move to -xxx
1954     if xxx<1
1955         xxx=xxx+dim;
1956     end
1957 end
1958 if xxx==dim
1959     qboundx(end+1)=1;
1960 else
1961     qboundx(end+1)=xxx+1;
1962 end
1963 qboundy(end+1)=yyy;
1964 qboundz(end+1)=zzz;

```

```

1965         xxx=xx;
1966         %-----end very little loop-----
1967         zz=zz+1;           %move to +zz direction
1968         if zz>dim
1969             zz=zz-dim;
1970         end
1971     end
1972     qboundx(end+1)=xx;
1973     qboundy(end+1)=yy;
1974     if zz==1
1975         qboundz(end+1)=dim;
1976     else
1977         qboundz(end+1)=zz-1;
1978     end
1979     zz=zloc;
1980
1981     while qchange(xx,yy,zz) >= threshold
1982         qnum(xx,yy,zz)=n;
1983         %-----very little loope-----
1984         while qchange(xxx,yyy,zzz) >= threshold
1985             qnum(xxx,yyy,zzz)=n;
1986             xxx=xxx+1; %move to +xxx direction
1987             if xxx>dim
1988                 xxx=xxx-dim;
1989             end
1990         end
1991         if xxx==1
1992             qboundx(end+1)=dim;
1993         else
1994             qboundx(end+1)=xxx-1;
1995         end

```

```

1996         qboundy (end+1)=yyy;
1997         qboundz (end+1)=zzz;
1998         xxx=xx;
1999
2000         while qchange(xxx,yyy,zzz) >= threshold
2001             qnum(xxx,yyy,zzz)=n;
2002             xxx=xxx-1; %move to -xxx
2003             if xxx<1
2004                 xxx=xxx+dim;
2005             end
2006         end
2007         if xxx==dim
2008             qboundx (end+1)=1;
2009         else
2010             qboundx (end+1)=xxx+1;
2011         end
2012         qboundy (end+1)=yyy;
2013         qboundz (end+1)=zzz;
2014         xxx=xx;
2015         %-----end very little loop-----
2016         zz=zz-1; %move to -zz direction
2017         if zz<1
2018             zz=zz+dim;
2019         end
2020     end
2021     qboundx (end+1)=xx;
2022     qboundy (end+1)=yy;
2023     if zz==dim
2024         qboundz (end+1)=1;
2025     else
2026         qboundz (end+1)=zz+1;

```

```

2027         end
2028         zz=zloc;
2029         %-----end little loop-----
2030         yloc=yloc+1;
2031         if yloc>dim
2032             yloc=yloc-dim;
2033         end
2034     end
2035     qboundx(end+1)=xloc;
2036     if yloc==1
2037         qboundy(end+1)=dim;
2038     else
2039         qboundy(end+1)=yloc-1;
2040     end
2041     qboundz(end+1)=zloc;
2042     yloc=tempqboundy(boundnums); ...
                                                    %reset ...
        yloc to original y (where max q exists)
2043     %-----end large ...
        loop-----
2044
2045     %-----large ...
        loop-----
2046
2047     while qchange(xloc,yloc,zloc) >= threshold    ...
        %move to -y direction
2048         qnum(xloc,yloc,zloc)=n;
2049         %----litte loop-----
2050         while qchange(xx,yy,zz) >= threshold
2051             qnum(xx,yy,zz)=n;
2052         %-----very little loope-----

```

```

2053     while qchange(xxx,yyy,zzz) >= threshold
2054         qnum(xxx,yyy,zzz)=n;
2055         zzz=zzz+1; %move to +zzz direction
2056         if zzz>dim
2057             zzz=zzz-dim;
2058         end
2059     end
2060     qboundx(end+1)=xxx;
2061     qboundy(end+1)=yyy;
2062     if zzz==1
2063         qboundz(end+1)=dim;
2064     else
2065         qboundz(end+1)=zzz-1;
2066     end
2067     zzz=zz;
2068
2069     while qchange(xxx,yyy,zzz) >= threshold
2070         qnum(xxx,yyy,zzz)=n;
2071         zzz=zzz-1; %move to -zzz
2072         if zzz<1
2073             zzz=zzz+dim;
2074         end
2075     end
2076     qboundx(end+1)=xxx;
2077     qboundy(end+1)=yyy;
2078     if zzz==dim
2079         qboundz(end+1)=1;
2080     else
2081         qboundz(end+1)=zzz+1;
2082     end
2083     zzz=zz;

```

```

2084         %-----end very little loop-----
2085         xx=xx+1;           %move to +xx direction
2086         if xx>dim
2087             xx=xx-dim;
2088         end
2089     end
2090     if xx==1
2091         qboundx(end+1)=dim;
2092     else
2093         qboundx(end+1)=xx-1;
2094     end
2095     qboundy(end+1)=yy;
2096     qboundz(end+1)=zz;
2097     xx=xloc;
2098
2099     while qchange(xx,yy,zz) >= threshold
2100         qnum(xx,yy,zz)=n;
2101         %-----very little loope-----
2102         while qchange(xxx,yyy,zzz) >= threshold
2103             qnum(xxx,yyy,zzz)=n;
2104             zzz=zzz+1; %move to +zzz direction
2105             if zzz>dim
2106                 zzz=zzz-dim;
2107             end
2108         end
2109         qboundx(end+1)=xxx;
2110         qboundy(end+1)=yyy;
2111         if zzz==1
2112             qboundz(end+1)=dim;
2113         else
2114             qboundz(end+1)=zzz-1;

```

```

2115         end
2116         zzz=zz;
2117
2118         while qchange(xxx,yyy,zzz) >= threshold
2119             qnum(xxx,yyy,zzz)=n;
2120             zzz=zzz-1; %move to -zzz
2121             if zzz<1
2122                 zzz=zzz+dim;
2123             end
2124         end
2125         qboundx(end+1)=xxx;
2126         qboundy(end+1)=yyy;
2127         if zzz==dim
2128             qboundz(end+1)=1;
2129         else
2130             qboundz(end+1)=zzz+1;
2131         end
2132         zzz=zz;
2133         %-----end very little loop-----
2134         xx=xx-1; %move to -xx direction
2135         if xx<1
2136             xx=xx+dim;
2137         end
2138     end
2139     if xx==dim
2140         qboundx(end+1)=1;
2141     else
2142         qboundx(end+1)=xx+1;
2143     end
2144     qboundy(end+1)=yy;
2145     qboundz(end+1)=zz;

```

```

2146     xx=xloc;
2147
2148     while qchange(xx,yy,zz) >= threshold
2149         qnum(xx,yy,zz)=n;
2150         %-----very little loope-----
2151         while qchange(xxx,yyy,zzz) >= threshold
2152             qnum(xxx,yyy,zzz)=n;
2153             xxx=xxx+1; %move to +xxx direction
2154             if xxx>dim
2155                 xxx=xxx-dim;
2156             end
2157         end
2158         if xxx==1
2159             qboundx(end+1)=dim;
2160         else
2161             qboundx(end+1)=xxx-1;
2162         end
2163         qboundy(end+1)=yyy;
2164         qboundz(end+1)=zzz;
2165         xxx=xx;
2166
2167         while qchange(xxx,yyy,zzz) >= threshold
2168             qnum(xxx,yyy,zzz)=n;
2169             xxx=xxx-1; %move to -xxx
2170             if xxx<1
2171                 xxx=xxx+dim;
2172             end
2173         end
2174         if xxx==dim
2175             qboundx(end+1)=1;
2176         else

```

```

2177         qboundx (end+1) =xxx+1;
2178     end
2179     qboundy (end+1) =yyy;
2180     qboundz (end+1) =zzz;
2181     xxx=xx;
2182     %-----end very little loop-----
2183     zz=zz+1;           %move to +zz direction
2184     if zz>dim
2185         zz=zz-dim;
2186     end
2187 end
2188 qboundx (end+1) =xx;
2189 qboundy (end+1) =yy;
2190 if zz==1
2191     qboundz (end+1) =dim;
2192 else
2193     qboundz (end+1) =zz-1;
2194 end
2195 zz=zloc;
2196
2197 while qchange (xx,yy,zz) >= threshold
2198     qnum (xx,yy,zz) =n;
2199     %-----very little loope-----
2200     while qchange (xxx,yyy,zzz) >= threshold
2201         qnum (xxx,yyy,zzz) =n;
2202         xxx=xxx+1;   %move to +xxx direction
2203         if xxx>dim
2204             xxx=xxx-dim;
2205         end
2206     end
2207     if xxx==1

```

```

2208         qboundx (end+1)=dim;
2209     else
2210         qboundx (end+1)=xxx-1;
2211     end
2212     qboundy (end+1)=yyy;
2213     qboundz (end+1)=zzz;
2214     xxx=xx;
2215
2216     while qchange(xxx,yyy,zzz) >= threshold
2217         qnum(xxx,yyy,zzz)=n;
2218         xxx=xxx-1; %move to -xxx
2219         if xxx<1
2220             xxx=xxx+dim;
2221         end
2222     end
2223     if xxx==dim
2224         qboundx (end+1)=1;
2225     else
2226         qboundx (end+1)=xxx+1;
2227     end
2228     qboundy (end+1)=yyy;
2229     qboundz (end+1)=zzz;
2230     xxx=xx;
2231     %-----end very little loop-----
2232     zz=zz-1; %move to -zz direction
2233     if zz<1
2234         zz=zz+dim;
2235     end
2236 end
2237 qboundx (end+1)=xx;
2238 qboundy (end+1)=yy;

```

```

2239         if zz==dim
2240             qboundz (end+1)=1;
2241         else
2242             qboundz (end+1)=zz+1;
2243         end
2244         zz=zloc;
2245         %-----end little loop-----
2246         yloc=yloc-1;
2247         if yloc<1
2248             yloc=yloc+dim;
2249         end
2250     end
2251     qboundx (end+1)=xloc;
2252     if yloc==dim
2253         qboundy (end+1)=1;
2254     else
2255         qboundy (end+1)=yloc+1;
2256     end
2257     qboundz (end+1)=zloc;
2258     yloc=tempqboundy (boundnums); ...
                                                    %reset ...
        yloc to original (where max q exists)
2259     %-----end large ...
        loop-----
2260
2261     %-----large ...
        loop-----
2262
2263     while qchange(xloc,yloc,zloc) >= threshold ...
        %move to +z direction
2264         qnum(xloc,yloc,zloc)=n;

```

```

2265 %-----litte loop-----
2266 while qchange(xx,yy,zz) >= threshold
2267     qnum(xx,yy,zz)=n;
2268 %-----very little loope-----
2269 while qchange(xxx,yyy,zzz) >= threshold
2270     qnum(xxx,yyy,zzz)=n;
2271     yyy=yyy+1; %move to +yyy direction
2272     if yyy>dim
2273         yyy=yyy-dim;
2274     end
2275 end
2276 qboundx(end+1)=xxx;
2277 if yyy==1
2278     qboundy(end+1)=dim;
2279 else
2280     qboundy(end+1)=yyy-1;
2281 end
2282 qboundz(end+1)=zzz;
2283 YYY=yy;
2284
2285 while qchange(xxx,yyy,zzz) >= threshold
2286     qnum(xxx,yyy,zzz)=n;
2287     yyy=yyy-1; %move to -yyy
2288     if yyy<1
2289         yyy=yyy+dim;
2290     end
2291 end
2292 qboundx(end+1)=xxx;
2293 if yyy==dim
2294     qboundy(end+1)=1;
2295 else

```

```

2296         qboundy (end+1) =yyy+1;
2297     end
2298     qboundz (end+1) =zzz;
2299     yyy=yy;
2300     %-----end very little loop-----
2301     xx=xx+1;           %move to +xx direction
2302     if xx>dim
2303         xx=xx-dim;
2304     end
2305 end
2306 if xx==1
2307     qboundx (end+1) =dim;
2308 else
2309     qboundx (end+1) =xx-1;
2310 end
2311 qboundy (end+1) =yy;
2312 qboundz (end+1) =zz;
2313 xx=xloc;
2314
2315 while qchange (xx,yy,zz) >= threshold
2316     qnum (xx,yy,zz) =n;
2317     %-----very little loope-----
2318     while qchange (xxx,yyy,zzz) >= threshold
2319         qnum (xxx,yyy,zzz) =n;
2320         yyy=yyy+1; %move to +yyy direction
2321         if yyy>dim
2322             yyy=yyy-dim;
2323         end
2324     end
2325     qboundx (end+1) =xxx;
2326     if yyy==1

```

```

2327         qboundy (end+1) =dim;
2328     else
2329         qboundy (end+1) =yyy-1;
2330     end
2331     qboundz (end+1) =zzz;
2332     YYY=YY;
2333
2334     while qchange (xxx,yyy,zzz) >= threshold
2335         qnum (xxx,yyy,zzz) =n;
2336         yyy=yyy-1; %move to -yyy
2337         if yyy<1
2338             yyy=yyy+dim;
2339         end
2340     end
2341     qboundx (end+1) =xxx;
2342     if yyy==dim
2343         qboundy (end+1) =1;
2344     else
2345         qboundy (end+1) =yyy+1;
2346     end
2347     qboundz (end+1) =zzz;
2348     YYY=YY;
2349     %-----end very little loop-----
2350     xx=xx-1; %move to -xx direction
2351     if xx<1
2352         xx=xx+dim;
2353     end
2354 end
2355 if xx==dim
2356     qboundx (end+1) =1;
2357 else

```

```

2358     qboundx (end+1)=xx+1;
2359     end
2360     qboundy (end+1)=yy;
2361     qboundz (end+1)=zz;
2362     xx=xloc;
2363
2364     while qchange (xx,yy,zz) >= threshold
2365         qnum (xx,yy,zz)=n;
2366         %-----very little loope-----
2367         while qchange (xxx,yyy,zzz) >= threshold
2368             qnum (xxx,yyy,zzz)=n;
2369             xxx=xxx+1; %move to +xxx direction
2370             if xxx>dim
2371                 xxx=xxx-dim;
2372             end
2373         end
2374         if xxx==1
2375             qboundx (end+1)=dim;
2376         else
2377             qboundx (end+1)=xxx-1;
2378         end
2379         qboundy (end+1)=yyy;
2380         qboundz (end+1)=zzz;
2381         xxx=xx;
2382
2383         while qchange (xxx,yyy,zzz) >= threshold
2384             qnum (xxx,yyy,zzz)=n;
2385             xxx=xxx-1; %move to -xxx
2386             if xxx<1
2387                 xxx=xxx+dim;
2388             end

```

```

2389         end
2390         if xxx==dim
2391             qboundx(end+1)=1;
2392         else
2393             qboundx(end+1)=xxx+1;
2394         end
2395         qboundy(end+1)=yyy;
2396         qboundz(end+1)=zzz;
2397         xxx=xx;
2398         %-----end very little loop-----
2399         yy=yy+1;           %move to +yy direction
2400         if yy>dim
2401             yy=yy-dim;
2402         end
2403     end
2404     qboundx(end+1)=xx;
2405     if yy==1
2406         qboundy(end+1)=dim;
2407     else
2408         qboundy(end+1)=yy-1;
2409     end
2410     qboundz(end+1)=zz;
2411     yy=yloc;
2412
2413     while qchange(xx,yy,zz) >= threshold
2414         qnum(xx,yy,zz)=n;
2415         %-----very little loope-----
2416         while qchange(xxx,yyy,zzz) >= threshold
2417             qnum(xxx,yyy,zzz)=n;
2418             xxx=xxx+1; %move to +xxx direction
2419             if xxx>dim

```

```

2420         xxx=xxx-dim;
2421     end
2422 end
2423 if xxx==1
2424     qboundx(end+1)=dim;
2425 else
2426     qboundx(end+1)=xxx-1;
2427 end
2428     qboundy(end+1)=yyy;
2429     qboundz(end+1)=zzz;
2430     xxx=xx;
2431
2432     while qchange(xxx,yyy,zzz) >= threshold
2433         qnum(xxx,yyy,zzz)=n;
2434         xxx=xxx-1; %move to -xxx
2435         if xxx<1
2436             xxx=xxx+dim;
2437         end
2438     end
2439     if xxx==dim
2440         qboundx(end+1)=1;
2441     else
2442         qboundx(end+1)=xxx+1;
2443     end
2444     qboundy(end+1)=yyy;
2445     qboundz(end+1)=zzz;
2446     xxx=xx;
2447     %-----end very little loop-----
2448     yy=yy-1; %move to -yy direction
2449     if yy<1
2450         yy=yy+dim;

```

```

2451         end
2452     end
2453     qboundx (end+1)=xx;
2454     if yy==dim
2455         qboundy (end+1)=1;
2456     else
2457         qboundy (end+1)=yy+1;
2458     end
2459     qboundz (end+1)=zz;
2460     yy=yloc;
2461     %-----end little loop-----
2462     zloc=zloc+1;
2463     if zloc>dim
2464         zloc=zloc-dim;
2465     end
2466 end
2467 qboundx (end+1)=xloc;
2468 qboundy (end+1)=yloc;
2469 if zloc==1
2470     qboundz (end+1)=1;
2471 else
2472     qboundz (end+1)=zloc-1;
2473 end
2474 zloc=tempqboundz (boundnums); ...
                                     %reset ...
                                     zloc to original z (where max q exists)
2475 %-----end large ...
                                     loop-----
2476
2477 %-----large ...
                                     loop-----

```

```

2478
2479     while qchange(xloc,yloc,zloc) >= threshold     ...
           %move to -z direction
2480     qnum(xloc,yloc,zloc)=n;
2481     %-----litte loop-----
2482     while qchange(xx,yy,zz) >= threshold
2483         qnum(xx,yy,zz)=n;
2484         %-----very little loope-----
2485         while qchange(xxx,yyy,zzz) >= threshold
2486             qnum(xxx,yyy,zzz)=n;
2487             yyy=yyy+1; %move to +yyy direction
2488             if yyy>dim
2489                 yyy=yyy-dim;
2490             end
2491         end
2492         qboundx(end+1)=xxx;
2493         if yyy==1
2494             qboundy(end+1)=dim;
2495         else
2496             qboundy(end+1)=yyy-1;
2497         end
2498         qboundz(end+1)=zzz;
2499         YYY=yy;
2500
2501     while qchange(xxx,yyy,zzz) >= threshold
2502         qnum(xxx,yyy,zzz)=n;
2503         yyy=yyy-1; %move to -yyy
2504         if yyy<1
2505             yyy=yyy+dim;
2506         end
2507     end

```

```

2508         qboundx (end+1) =xxx;
2509         if yyy==dim
2510             qboundy (end+1) =1;
2511         else
2512             qboundy (end+1) =yyy+1;
2513         end
2514         qboundz (end+1) =zzz;
2515         YYY=yy;
2516         %-----end very little loop-----
2517         xx=xx+1;           %move to +xx direction
2518         if xx>dim
2519             xx=xx-dim;
2520         end
2521     end
2522     if xx==1
2523         qboundx (end+1) =dim;
2524     else
2525         qboundx (end+1) =xx-1;
2526     end
2527     qboundy (end+1) =yy;
2528     qboundz (end+1) =zz;
2529     xx=xloc;
2530
2531     while qchange (xx,yy,zz) >= threshold
2532         qnum (xx,yy,zz) =n;
2533         %-----very little loope-----
2534         while qchange (xxx,yyy,zzz) >= threshold
2535             qnum (xxx,yyy,zzz) =n;
2536             yyy=yyy+1; %move to +yyy direction
2537             if yyy>dim
2538                 yyy=yyy-dim;

```

```

2539         end
2540     end
2541     qboundx(end+1)=xxx;
2542     if yyy==1
2543         qboundy(end+1)=dim;
2544     else
2545         qboundy(end+1)=yyy-1;
2546     end
2547     qboundz(end+1)=zzz;
2548     yyy=yy;
2549
2550     while qchange(xxx,yyy,zzz) >= threshold
2551         qnum(xxx,yyy,zzz)=n;
2552         yyy=yyy-1; %move to -yyy
2553         if yyy<1
2554             yyy=yyy+dim;
2555         end
2556     end
2557     qboundx(end+1)=xxx;
2558     if yyy==dim
2559         qboundy(end+1)=1;
2560     else
2561         qboundy(end+1)=yyy+1;
2562     end
2563     qboundz(end+1)=zzz;
2564     YYY=YY;
2565     %-----end very little loop-----
2566     xx=xx-1; %move to -xx direction
2567     if xx<1
2568         xx=xx+dim;
2569     end

```

```

2570         end
2571         if xx==dim
2572             qboundx(end+1)=1;
2573         else
2574             qboundx(end+1)=xx+1;
2575         end
2576         qboundy(end+1)=yy;
2577         qboundz(end+1)=zz;
2578         xx=xloc;
2579
2580         while qchange(xx,yy,zz) >= threshold
2581             qnum(xx,yy,zz)=n;
2582             %-----very little loope-----
2583             while qchange(xxx,yyy,zzz) >= threshold
2584                 qnum(xxx,yyy,zzz)=n;
2585                 xxx=xxx+1; %move to +xxx direction
2586                 if xxx>dim
2587                     xxx=xxx-dim;
2588                 end
2589             end
2590             if xxx==1
2591                 qboundx(end+1)=dim;
2592             else
2593                 qboundx(end+1)=xxx-1;
2594             end
2595             qboundy(end+1)=yyy;
2596             qboundz(end+1)=zzz;
2597             xxx=xx;
2598
2599             while qchange(xxx,yyy,zzz) >= threshold
2600                 qnum(xxx,yyy,zzz)=n;

```

```

2601         xxx=xxx-1; %move to -xxx
2602         if xxx<1
2603             xxx=xxx+dim;
2604         end
2605     end
2606     if xxx==dim
2607         qboundx(end+1)=1;
2608     else
2609         qboundx(end+1)=xxx+1;
2610     end
2611     qboundy(end+1)=yyy;
2612     qboundz(end+1)=zzz;
2613     xxx=xx;
2614     %-----end very little loop-----
2615     yy=yy+1; %move to +yy direction
2616     if yy>dim
2617         yy=yy-dim;
2618     end
2619     end
2620     qboundx(end+1)=xx;
2621     if yy==1
2622         qboundy(end+1)=dim;
2623     else
2624         qboundy(end+1)=yy-1;
2625     end
2626     qboundz(end+1)=zz;
2627     yy=yloc;
2628
2629     while qchange(xx,yy,zz) >= threshold
2630         qnum(xx,yy,zz)=n;
2631         %-----very little loope-----

```

```

2632     while qchange(xxx,yyy,zzz) >= threshold
2633         qnum(xxx,yyy,zzz)=n;
2634         xxx=xxx+1; %move to +xxx direction
2635         if xxx>dim
2636             xxx=xxx-dim;
2637         end
2638     end
2639     if xxx==1
2640         qboundx(end+1)=dim;
2641     else
2642
2643         qboundx(end+1)=xxx-1;
2644     end
2645     qboundy(end+1)=yyy;
2646     qboundz(end+1)=zzz;
2647     xxx=xx;
2648
2649     while qchange(xxx,yyy,zzz) >= threshold
2650         qnum(xxx,yyy,zzz)=n;
2651         xxx=xxx-1; %move to -xxx
2652         if xxx<1
2653             xxx=xxx+dim;
2654         end
2655     end
2656     if xxx==dim
2657         qboundx(end+1)=1;
2658     else
2659
2660         qboundx(end+1)=xxx+1;
2661     end
2662     qboundy(end+1)=yyy;

```

```

2663         qboundz (end+1)=zzz;
2664         xxx=xx;
2665         %-----end very little loop-----
2666         yy=yy-1;           %move to -yy direction
2667         if yy<1
2668             yy=yy+dim;
2669         end
2670     end
2671     qboundx (end+1)=xx;
2672     if yy==dim
2673         qboundy (end+1)=1;
2674     else
2675         qboundy (end+1)=yy+1;
2676     end
2677     qboundz (end+1)=zz;
2678     yy=yloc;
2679     %-----end little loop-----
2680     zloc=zloc-1;
2681     if zloc<1
2682         zloc=zloc+dim;
2683     end
2684 end
2685 qboundx (end+1)=xloc;
2686 qboundy (end+1)=yloc;
2687 if zloc==dim
2688     qboundz (end+1)=1;
2689 else
2690     qboundz (end+1)=zloc+1;
2691 end
2692 zloc=tempqboundz (boundnums); ...

```

%reset ...

```

                zloc to original z (where max q exists)
2693      %-----end large ...
                loop-----
2694
2695      end
2696      end
2697      tempvolume2=sum(qnum(:)==n);
2698      end
2699
2700      if tempvolume2 >= cutoffvolume
2701          disp(['The volume of ',num2str(n),' th vortex is ...
                ',num2str(tempvolume2)])
2702      [x1,y1,z1]=ind2sub(size(qnum),find(qnum==n));
2703          for positions=1:length(x1)
2704              qfinal(x1(positions),y1(positions),z1(positions)) ...
2705                  =q(x1(positions),y1(positions),z1(positions));
2706              qchange(x1(positions),y1(positions),z1(positions))=0;
2707          end
2708      else
2709          [x1,y1,z1]=ind2sub(size(qnum),find(qnum==n));
2710          for positions=1:length(x1)
2711              qnum(x1(positions),y1(positions),z1(positions))=0;
2712              qchange(x1(positions),y1(positions),z1(positions))=0;
2713          end
2714          n=n-1;
2715      end
2716      n=n+1;
2717      end
2718      qboundx(:)=[];
2719      qboundy(:)=[];
2720      qboundz(:)=[];

```

```
2721     end
2722     qmax=max(max(max(qchange)));
2723 end
2724 saveqnum=reshape(qnum,[dim^3,1]);
2725
2726 fid = fopen([filepath2,'qnum',num2str(t,'%04i'),'.dat'],'w');
2727     fprintf(fid, '%8.1f\n', saveqnum);
2728     fclose(fid);
2729 hintnumber=((t-aal)/interv+1)/((aa2-aal)/interv+1);
2730 hints=[num2str(hintnumber*100),'% is finished'];
2731 waitbar(hintnumber,hh,hints)
2732 % filename=[filepath2,'qnum',num2str(t,'%04i'),'.dat'];
2733 % save(filename,'saveqnum','-ascii')
2734 end
2735 toc
2736 close(hh)
```